PhD in Electronic and Computer Engineering
University of Cagliari

Topology matters:

Characteristics of functional brain networks in healthy subjects and patients with Epilepsy, Diabetes, or Amyotrophic Lateral Sclerosis during a resting-state paradigm.

Matteo Demuru

Curriculum: ING-INF/05
Advisor: Matteo Fraschini
Director of the PhD Program: prof. Fabio Roli

Cycle XXVII
2013-2014
April 27th, 2015

Abstract

The brain can be seen as a complex structural and functional network. Cognitive functioning strongly depends on the organization of functional brain networks. EEG/MEG resting-state functional connectivity and functional brain networks studies attempt to characterize normal brain organization as well as deviation from it due to brain diseases. Despite the impact on the understanding of brain functioning that these tools provided, there are still methodological hurdles that might compromise the quality of the results. The main aim of this thesis was to gain an understanding of the role of functional connectivity and network topology on brain functioning by: (i) addressing the methodological issues intrinsic in the analysis that can bias the results; (ii) quantifying functional connectivity differences possibly induced by brain impairments; (iii) detecting and quantifying how network topology changes, due to brain impairments.
In order to achieve these objectives, functional connectivity and functional brain networks obtained by empirical recordings were reconstructed. Recordings were acquired with different modalities (EEG or MEG) and under different pathologies: epilepsy, diabetes and amyotrophic lateral sclerosis. Specifically three research questions were addressed:

- Do functional brain network architectures obtained from pharmaco-resistant epileptic patients responding to vagal nerve stimulation (VNS) change compared to patients not responding to VNS?
- Are functional connectivity alterations related to cognitive performance and clinical status in type I diabetes mellitus patients?
- Is functional network topology related to disease duration in amyotrophic lateral sclerosis patients?

In order to answer these questions, avoiding possible biases which may affect the results, two key choices were made: first, the selection of the phase lag index [1] as functional connectivity estimator because it is less sensible to common sources problem; second, the application of minimum spanning tree (MST) [2] approach to overcome the problem of network comparison and characterize network topology reliably.
In summary, this thesis confirms that alterations of functional connectivity and functional brain networks in disease may be used as potential biomarkers for more objective diagnosis and the choice of effective treatment options. Specifically, in epileptic patients implanted with VNS the relation between network measures and clinical benefit suggest that these measures can be used as a marker in monitoring the efficacy of the treatment; in amyotrophic lateral sclerosis the relation between disease duration and whole brain network disruption suggests diagnostic relevance of network measures in evaluating and monitoring the disease; and finally in type 1 diabetic mellitus patients functional connectivity measures can be complementary to cognitive tests and may help to monitor the effect of T1DM on brain functions.

Funding
Matteo Demuru gratefully acknowledges Prof. Francesco Marrosu for partly supports his PhD with Assegno di Ricerca related to D.R. 832/2012 University of Cagliari and the Fondazione Banco di Sardegna for his financial support by (Prat.2013.1237)

1 General Introduction

1.1 Introduction

The brain can be considered as one of the most complex systems known to man; and this is true whatever the level of resolution we are looking at, from the microscopic (i.e. where single neurons are analyzed) to macroscopic levels (i.e. ensembles of neurons or areas of the brain). Deciphering how interactions, both at microscopic and macroscopic levels, are related to higher-order cognitive processes (e.g. language comprehension, memory recall, visual representation etc. etc.) and how neurological diseases result in failure of such interactions are active neuroscientific topics.[3], [4].

Microscopically signal transmission takes places at the neuron synapses through release of neurotransmitters, this lead to excitatory and inhibitory post-synaptic potentials (EPSP and IPSP). Temporal and spatial summations of EPSPs and IPSPs in assemblies of neurons give rise to a measurable signal at scalp level. Electro-encephalography (EEG) and magneto-encephalography (MEG) can pick up such signals. These non-invasive recordings allow exploring brain interactions through signal-processing techniques. One way to define interaction between different areas is through synchronization of the recorded signals, which are represented as time-series. Statistical interdependency between time-series is thought to reflect interactions between brain areas from which those time-series are recorded [5], and is generally referred to *functional connectivity*. The term *effective connectivity* is used when the directionally is also considered (how a brain area directly influence another one)[6], [7].

Historically individual brain regions have been associated with specific cognitive functions (segregation or specialization), an example is given by Broca's area to which the capacity of speech is thought to be linked. This area was called Broca's area after the French surgeon Pierre Paul Broca who first observed that the incapacity to speak was related to an injury to the posterior inferior frontal gyrus [8]. However recently it has been shown that speech production required a collaboration of different areas (such as motor areas in order to articulate muscles to produce the word) and Broca's area plays a role in mediating information across large-scale cortical networks involved in speech [9]. Therefore each brain area needs to communicate with other areas and to integrate information (integration) from other areas in order to implement higher-order cognitive functions. These two properties, segregation and integration, coexist in the brain to form a complex communication network.

This complex communication network is referred to as a functional network, however it relies on and exploits the structural network that is formed by the neuronal fibres connecting neurons in different areas. A useful analogy to the brain structural and functional networks is the transport infrastructure of a country (high-ways connecting cities), where the traffic on the roads reflects the functional network. Using this analogy it is possible to pinpoint at least two concepts: firstly, that structure and function, even if they are indeed intrinsically related, can be studied independently. Secondly, that the abstraction of imagining streets as axonal bundles and cities as brain areas suggests that brain networks as well as transport networks can be analysed in general terms exploiting the extensive knowledge from other scientific fields that already dealt with complex systems, such as the social sciences [10], using modern network theory.

Modern network theory originated from at least three older and established disciplines: graph theory, statistical mechanics of networks and dynamical system theory [4]. Graph theory is an old branch of mathematics which birth is attributed to Euler who was the first using abstract

concepts of nodes and edges to solve the problem of the seven bridges of Königsberg [11]. Nodes are elements used to represent entities of the system under study while the presence/absence of an edge between nodes represents the existence of a relationship between those entities (nodes). Statistical mechanics extended the concepts of graph theory adding the capacity to deal with larger networks and providing models to describe the characteristic of the networks. Examples of such models are random graphs [12], small-world [13], scale-free [14], hierarchical and modular [15] network models. Furthermore dynamical system theory supplies the theoretical knowledge to study the processes occurring on the network [16]. Modern network theory therefore provides the tools for the investigation of complex brain networks [4].

1.2 Methodological issues

During the last fifteen years a wealth of EEG/MEG studies focusing on the investigation of functional connectivity and functional brain networks were published. These studies attempted to characterize normal brain organization [7] as well as deviation from it due to brain diseases [3]. Despite the impact on the understanding of brain functioning that these tools provided there are still critical issues arising from the pipeline of analysis, due to the assumptions and choices that are made, that can compromise the results obtained through these analysis [17]-[19]. The reasons lie on the assumptions and choices made during the analysis steps. The typical pipeline of analysis consists of three main steps: i) acquisition of brain signals, ii) estimation of functional connectivity between all pairs of recorded signals and iii) functional brain networks construction and assessment using the framework of modern network theory.

Acquisition of brain activity depends on technical details and choices related to the instruments (EEG or MEG) and their settings. For example during EEG recordings technical choices such as electrode montage, sampling frequency, impedance, etc., should be specified carefully, bearing in mind that they will affect the following analysis steps. Furthermore, the assessment of the quality of the recordings should be performed, thereby discarding recordings perturbed by activity that it is clearly not originated in the brain (artefacts). Example of such contaminations include those arising from myogenic activity or external electromagnetic activity such as cell phones, power line etc. .

Once brain signals are stored as time-series their off-line manipulation enable extraction of information on their statistical relationship. In this context the choice of a functional connectivity measure should be defined. Nowadays there is a plethora of mathematical indices for the estimation of functional connectivity: linear, non-linear, information-based techniques [20]. Every measure has its own assumptions and tries to highlight a different aspect of interaction between two signals (e.g. amplitude relations, phase relations, spectral properties).
The estimation of functional connectivity can be affected by a series of problems related to the lack of a straightforward relation between active brain sources and time-series obtained by scalp recordings (EEG or MEG). Dealing with these problems is a compulsory prerequisite in order to avoid spurious estimates of functional connectivity. In literature these problems are often referred as volume conduction, however at least three different phenomena can be recognized: volume conduction, field spread and linear mixing.
A brain source typically generates a primary current which EEG can detect (i.e. the summation of EPSP and IPSP), however this primary current induces a secondary current in the

surrounding tissues which together with conductive properties of the tissues distort the signal propagation resulting in a blurred signal at the scalp level: this effect is what correctly should be called volume conduction [21].
Field spread is the phenomenon consisting of the projection of a single brain source to multiple EEG/MEG sensors [22]. Moreover since at each time there can be more than one active brain source, because of field spread, the contribution of multiple sources may be present in the signal recorded from each EEG/MEG sensor as a weighted summation of the active sources (linear mixing).
It is clear that these problems together may affect the estimation of synchronization between two recorded brain signals. The main problem is the detection of spurious correlation between time-series of different EEG/MEG sensors: there is a high probability to pick up the same activity from two time-series recorded by nearby EEG/MEG sensors, therefore (uncorrected) synchronization measures will display high values between the two time-series.
In the rest of the thesis the term common sources will be used to indicate phenomena that are due to volume conduction, field spread or linear mixing and an appropriate selection of functional connectivity measures will be done in order to be less sensitive to these phenomena. A similar problem specific to EEG that can be added to the category of common sources is due to the use of a so-called active reference electrode. It arises because every signal in EEG is not an absolute measurement but is computed as a difference in voltage potential with respect to a reference electrode (placed in the scalp therefore active), which influences with similar components the other recording electrodes.

The final steps in the analysis pipeline are the construction of a functional brain networks from functionally connectivity values and the topological assessment of this network.
Estimating the functional connectivity between every pair of signals related to every pair recording locations (electrodes/sensors) leads to a definition of the functional connectivity matrix. Supposing to have Nrecording locations we obtain a $N \times N$ matrix in which every entry of this matrix expresses the degree of interaction between any pair of brain areas under the recording locations. Every node in the functional network represents a recording location and every functional connectivity value is used as the weight of the edge connecting a pair of nodes. This weighted matrix is the starting point to construct the functional brain network. It can be directly used to form a fully connected weighted network or can be transformed into a binary matrix to create an unweighted network. Such an unweighted network is obtained by setting a threshold on the weights to keep only the most important weights whilst discarding weak connections (low weight values) that are potentially due to noise. The choice of a threshold is arbitrary and at the same time critical because it influences the resulting network topology and its topological assessment [23]. The selection of a threshold affects the network density (i.e. number of connections in a network) which is directly related to the network comparison problem [23]. It was shown [23] that even when the full weighted matrix is used the results can be biased.
Comparing networks is the essence of many studies on functional brain networks. Networks are typically compared across different subject populations (i.e. patients versus healthy controls) or between different conditions or tasks. One of the goals of network analysis is to discriminate between these conditions in terms of topological differences of the associated networks. Topological differences rely on the computation of network metrics [24] allowing to infer properties of the organization of the network under study. However such metrics depend on network size (i.e. number of nodes), network density (i.e. number of edge), and on other network parameters: if these parameters change the network metrics values can change even if the topology remains the same.

The alteration of the network density is a typical outcome of the threshold choice. Applying the same threshold to two different networks may result in two different network densities therefore biasing the network topology comparison.
A straightforward and unbiased method to compare functional brain networks is still missing although there are strategies that overcome this problem [25], [26].

This brief overview of the analysis pipeline highlights the main and critical issues that should be addressed and tackled during functional brain network analysis study.

1.3 Aims and Research Questions

The main aim of this thesis was to gain an understanding of the role of functional connectivity and network topology on brain functioning by:

- addressing the methodological issues intrinsic in the analysis that can bias the results;
- quantifying functional connectivity differences possibly induced by brain impairments;
- detecting and quantifying how network topology changes, due to brain impairments.

In order to achieve these objectives, functional connectivity and functional brain networks obtained by empirical recordings were reconstructed. Recordings were acquired with different modalities (EEG or MEG) and different pathologies ranging: epilepsy, diabetes and amyotrophic lateral sclerosis.
The leitmotif shared by all these different investigations is the methodological choices that are used in order to deal with typical problems arising from the pipeline of analysis. The inference connectivity and functional brain networks based on empirical data poses a series of inevitable assumptions that affect the interpretation of the results. Therefore the aim of the thesis was twofold, on the one hand investigate new clinical and neuroscientific questions exploiting network theory and on the other hand enhance the reliability and interpretability of the results using bias-free methodological choices to address brain network analysis problems.

In this thesis the following research questions were addressed:

1. Do functional brain network architectures obtained from pharmaco-resistant epileptic patients responding to vagal nerve stimulation (VNS) change compared to patients not responding to VNS?
2. Are functional connectivity alterations related to cognitive performance and clinical status in type I diabetes mellitus patients?
3. Is functional network topology related to disease duration in amyotrophic lateral sclerosis patients?

The thesis is divided in two parts; the first part starts with an introduction of the basic concepts regarding the field of brain network analysis. The second part contains the application of the aforementioned unbiased methodology to analyze experimental data for each of the former three questions. In the last section we draw general conclusions after summarizing the key results from this thesis, and describe future research directions, both from a neurophysiological and methodological point of view.

2 Concepts and Methodological pipeline

Introduction

The invention of electroencephalography is due to Hans Berger, a German psychiatrist, who from the mid-1920 recorded the first human EEG. In his pioneering paper of 1929 he described the 'alpha-rhythm', the first oscillatory activity observed through recordings of the voltage changes at scalp level during an eye-closed condition, where the subject was in an awake and calm state without performing any kind of task. From that time on neuroscientists have been engaged in the fascinating endeavour of unravelling this dynamic behaviour of the brain. These efforts are directed to understanding these oscillatory patterns of activity: from where they originate to their relationship with cognitive functions and pathology.

Nowadays the EEG is used as routine exam for neurologists, especially for pathology such as epilepsy, where the recorded spontaneous on-going activity helps in the diagnosis. However its usage spans over other clinical disciplines from EEG monitoring during anaesthesia, during sleep, in operative and post-operative intensive care units [27]. Furthermore the EEG is exploited to understand cognitive processes and can be considered a window on the brain for a discipline such as neuroscience.

EEG is just one of the neuroimaging techniques available to study the brain. Together with MEG and functional magnetic resonance (fMRI), they are the most employed techniques used to study the functional aspect (dynamics of neuronal activity) of our brain. Generally, the term neuroimaging also includes even the techniques such as magnetic resonance imaging (MRI), computed axial tomography (CAT) and positron emission tomography (PET) that provide information about the structure and metabolic demands of our brain.

In the following chapter a brief overview of the basic concepts necessary to understand the analysis and results of the experimental part will be given.

2.1 Basic concepts

2.1.1 Origin of EEG/MEG oscillatory signals

The electrical signal EEG measures as potential difference between two electrodes at scalp level, as well as the associated magnetic field that MEG can detect, both are originated by the summation of post-synaptic potentials.

Neurons are cells that have the special properties of sending 'messages' between each other. Three main parts essentially compose a neuron: a cell body, dendrites and an axon. Dendrites can be considered as the input filaments of the cell through which it receive the input 'messages' from other neurons while the axon is the output filament from which the neuron sends its own 'messages' to the receiver neurons (terminal neurons). A synapse is basically a contact between the axon of a neuron and the cell body or dendrite of another neuron. Neurotransmitters open ion channels; ions flow in/out altering membrane potential and current flows. This membrane potential alteration is called excitatory (EPSP) or inhibitory (IPSP) post-synaptic potentials depending on the how the membrane deviates from its baseline potential.

A neuron integrates all the EPSP and IPSP arriving from the other neurons to which it is connected and these can affect the internal state of the neuron that is triggered to fire an action potential (spike), which is a rapid discharge through the axon caused by a sudden rise

and fall of the membrane potential. Spikes propagate through the axon to the dendrites of terminal neurons.

The electric signal that EEG/MEG can pick up at scalp level is not given by this rapid discharge, however it consists of the addition of EPSP and IPSP from a patch of neighbour neurons. In fact usually only a small number of neurons fires spikes at the same time, while EPSPs and IPSPs allow for a temporal integration generating an electromagnetic signal that reveals the activities of a set interacting neurons. The structural arrangement of cortical neurons, which are aligned in columns, allow for spatial summation and facilitates the propagation of this signal till the scalp where it is measured as a wavelike potential fluctuation. This wavelike activity has been classified and the analysis of its properties is usually referred as the study of brain rhythms or brain oscillations.

2.1.2 MEG and EEG

The basic principles of EEG technique have essentially been the same from that time on even though technological developments, better electronics and software, improved the quality and accuracy of recordings. EEG traces consists of the quantification of the electric potential differences between pairs of electrodes glued to the scalp [28]. The position and number of electrodes in the clinical settings are defined by standards [27]. Typically 19 electrodes covering homogeneously the scalp surface are enough for clinical assessment. However in a research setting the number of electrodes ranges from 64 to 512 and usually they are embedded in an elastic cap to allow an easier positioning.

Independently of the number of electrodes two different kinds of set-ups for EEG recording are used:

- Bi-polar montage, in which electrodes are organized in pairs and the signals arise as electric voltage potential differences between each pair.
- Mono-polar montage, where each electrode is associated to a unique reference electrode and voltage potential differences are computed relatively to this reference.

The material employed in the manufacturing of the EEG electrodes is typically silver chloride because of its low impedance (from 1 to 20 KΩ) and its wide frequency response (KHz). EEG recordings are characterized by fast sampling rate (up to 5KHz) enabling millisecond precision and multimodal compatibility, in fact EEG can be used simultaneously with fMRI or MEG [29].
Figure 1 showed the primary electric current (red arrow) originated from the integration of EPSPs and IPSPs at microscopic level that can be measured at scalp level as a voltage potential difference (yellow lines). As it can be seen from Figure 1 electric generator (red line) induces a second current (yellow lines), which propagates through different brain tissues till the scalp, where can be picked up by a pair of electrodes. As we already discuss this phenomenon is called volume conduction and affects the quality of the signal recorded at the scalp level.

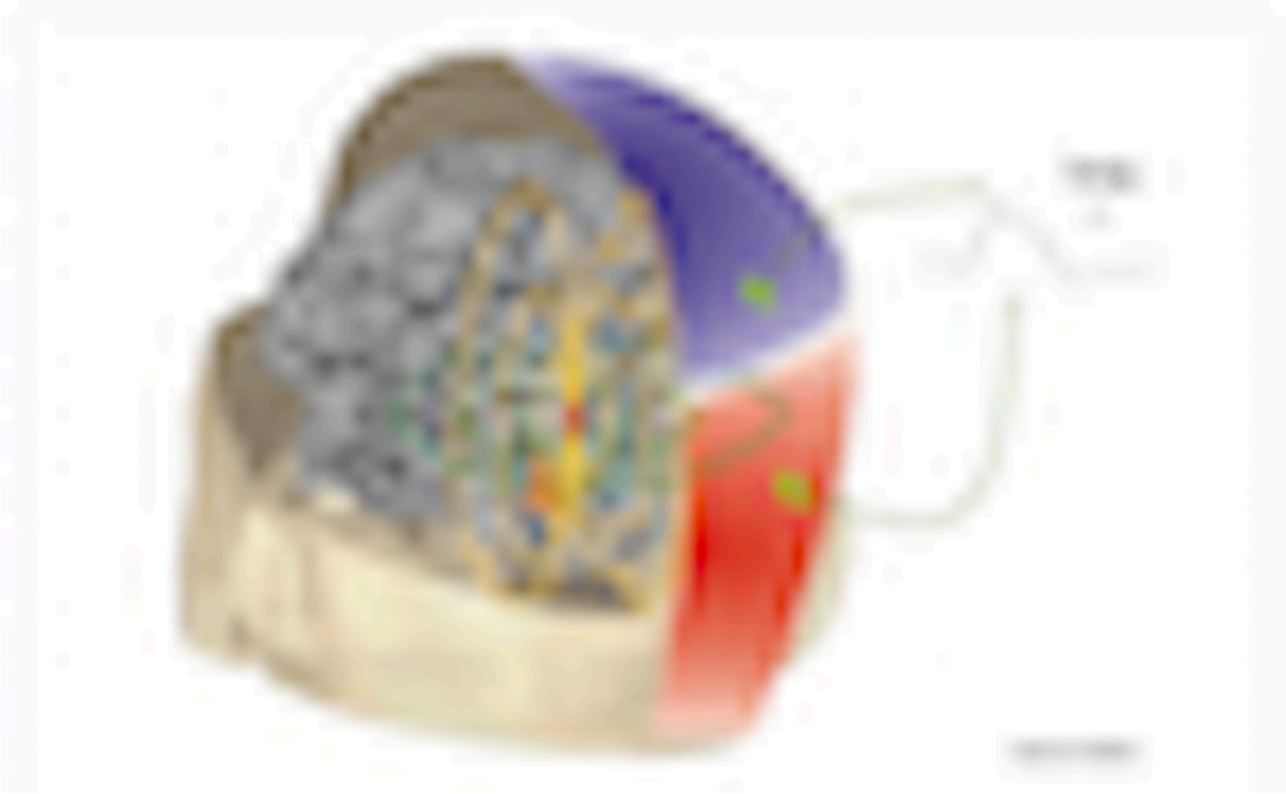

Figure 1 EEG and MEG signal origin. EPSP and IPSP add up locally and generate a primary current (shown in red). This induced secondary currents (shown in yellow) that travel through the head tissues where can be detected using EEG. Magnetic fields (in green) related to the primary current are less distorted than current flows and they can be captured using MEG. The picture was adapted from [29].

Among the different analysis approaches two common ways of exploring EEG data are the study of so called 'stimulus-locked' activity (or 'evoked activity') and 'induced' activity [27]. The former relies on the averaging of EEG traces related to multiple presentation of a sensory stimulus (i.e. auditory or visual stimulus) or the performance of a task (e.g. movements) in order to improve the signal to noise ratio and disclose pattern of activity related to presented stimulus or executed task. This analysis implies that the all the activity that cancels out in the averaging process is considered as background noise while the brain activity related to the stimulus is stationary [30]. This hypothesis in general does not hold, inspiring the investigation of the 'background noise' and encouraging the analysis of unaveraged EEG data ('induced activity') [31].

As Hans Berger discloses alpha rhythm for EEG, the first MEG recordings showing alpha oscillatory activity is due by David Cohen [32] in 1968. After the invention of Superconductive Quantum Interference Device (SQUID) by Zimmerman and colleagues it was possible to obtain and record oscillatory activity with quality comparable to EEG [28]. MEG signals originate from the same electrical activity caused by EPSPs and IPSPs, but rather than the potential differences MEG picks up the magnetic field (green lines Figure 1) induced by the primary electric current (red arrow Figure 1).
Describing the details of MEG technology is beyond the scope this thesis however in the following lines a brief overview of commonalities, advantages and disadvantages of MEG compared to the EEG will be given, an extensive description of MEG methods and applications can be found in [27], [33].

First of all, EEG and MEG (see Figure 2) are both non-invasive techniques, provide a direct measure of neural activity and share the temporal resolution: their recordings of brain activity have a millisecond precision.
MEG compared to EEG is an expensive instruments requiring ad-hoc solutions (shielded room, superconducting sensing technology working at -269 C°, cooling system based on liquid to maintaining the system at that working temperatures, etc. etc.) in order to pick up the brain magnetic field which is very small: of the order of femto Tesla (compared to, for example, the earth magnetic field: ~30 μTesla).
An important advantage of MEG measurements is related to higher spatial discrimination of brain activity due to the fact that the magnetic field is less sensible to the conductivity of head tissue (volume conduction). As we will see later (paragraph 2.1.6) this will help in the source modelling: the attempt to localize assemblies of neurons responsible of the activity recorded at scalp level. Another benefit of MEG is that differently from the EEG, measurements are absolute and do depend on the reference choice. Finally it worth to note that EEG and MEG are sensitive to different kinds of brain source generator: EEG picks up currents with directions that are both radial and tangential with respect to the head surface while MEG records magnetic flux associated to currents with tangential directions [34]. The information about the brain activity both techniques brought can be considered orthogonal and they should be seen as complementary techniques.

MEG

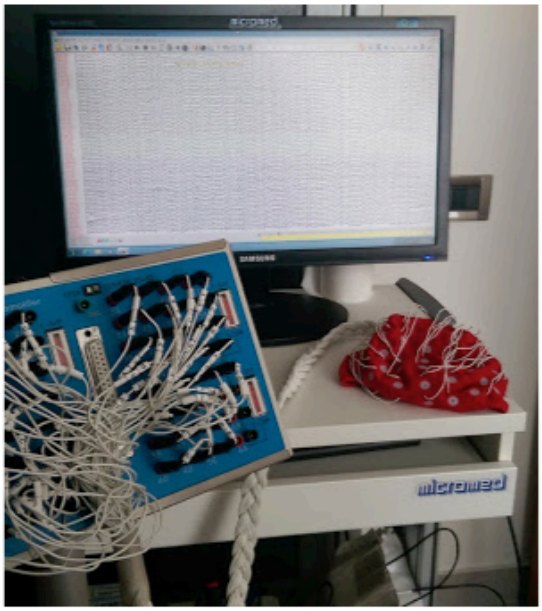

EEG

Figure 2 MEG and EEG. Electroencephalographic (EEG) with 64 channels EEG system (Brain QuickSystem, Micromed, Mogliano-Veneto, Italy). MEG system in a magnetically shielded room (VacuumSchmelze GmbH, Hanua, Germany) with a 306-channel whole-head neuromagnetometer (Elekta Neuromag Oy, Helsinki, Finland).

2.1.3 Brain Rhythms

Communication is one of the most essential operation our brain performs and understanding how this happens, what are the mechanisms that allow information to flow and how information is coded are perhaps the most challenging and hard problems researcher are trying to solve. Brain oscillations represent one of the topics that neuroscientists have investigated the most because they are considered the framework through which neuronal communication is implemented[35].

Two key features of brain computations: local-global communications and persistent activity are thought to exploit brain oscillations to be accomplished. Local communications refers to computations of nearby assembly of neurons, while global communications allude to integration of information between distant assemblies of neurons. Persistent activity is the property of the brain to sustain the effect of a perturbation of the current 'state' caused for example by a stimulus [36].

One of the reasons why brain oscillations have such an important role lies on the observation that they are preserved across different species with different size of brains: from mice, rats and cats to monkey and humans. This remark highlights the role of brain rhythms as a foundational and basic mechanism to allow communication [36].

Furthermore brain oscillatory activity has been found to correlate with different cognitive processes and behaviour [37]. Examples of such correlations are briefly described in the following lines with the attempt to introduce some of the most investigated rhythms (both in animal and human studies), which are usually divided into frequency bands because it is thought that every band conveys different information. These bands are typically: delta band (from 0.5 to 4 Hz), theta band (from 4 to 8 Hz), alpha band (from 8 to 13 Hz), beta band (from 13 to 30 Hz) and gamma band (from 30 to 90 Hz). This of course is a extreme generalization and it should be noted that usually band boundaries are not strict and not only animal studies differed from human studies, but quite often even within human studies boundary can have slight differences.

2.1.3.1 Delta rhythm

Oscillation in delta frequency band were first reported to be associated to brain tumours, Walters [38] was the first who coined the term 'delta waves'. More recent studies related delta activity to sleep and anaesthesia [39], [40]. Furthermore delta rhythm is supposed to play a key role in consolidating memories created during the wakeful state [41].

2.1.3.2 Theta rhythm

Oscillatory activity in the theta band has been historically studied in animals from which through invasive recording the role of hippocampus as primary generator of such rhythms has been disclosed [42]. Behavioural correlates of this rhythm consist of different aspect of movements: from preparation of movements and spatial navigation [43] to the encoding and retrieval of spatial information [44].
In humans, invasive recording from depth electrodes placed in the hippocampus of epileptic patients reported the involvement of theta rhythm in different behavioural conditions: from writing to sitting or walking [45]. Other invasive experiments described the presence of theta activity even in cortical areas, during a navigation task in a virtual maze [46] or during more complex virtual scenarios in which both learning of fixed locations and navigation were involved [47]. Furthermore recent non-invasive works performed with EEG and MEG

corroborate existing knowledge on the role theta as movement related-rhythm and broaden its role to support learning and memory processing of spatial features [48]-[50].

2.1.3.3 Alpha rhythm

Alpha rhythm is one of the rhythms with the strongest amplitude/power and it was usually referred as 'idling rhythm' [51] because of its presence (detectable even by naked eye) in paradigms where the subject has the eyes-closed and is not engaged in a particular task. Nowadays experimental evidence challenged the 'idling' hypothesis and suggested the important functional role that alpha rhythm plays in information processing [52]. Furthermore alpha activity has been reported in association with different cognitive processes such as working memory [53] and attention [54]; a comprehensive survey of alpha rhythm functional correlates was written by Basar [55].
Alpha activity was successfully investigated with a modelling perspective trying to understand its origin and dynamics from simple abstractions of the underlining physiological neuronal mechanism. Neural mass model is the name under which such modelling is usually indicated [56]-[59] and the basic idea is to study with a mean-field approach, in which the mean activity of cortical neuronal macro-columns is summarized, the dynamics of a whole neuronal population.

2.1.3.4 Beta rhythm

The functional role of beta band activity is still poorly understood even if classical findings associated beta rhythm to motor activity. Engel and Fries [60], in a recent review, suggested that beta band activity is exploited to maintain and signal the current motor set. They pointed out how beta activity is expressed more strongly during steady muscular contractions and it is reduced when a change of motor status is engaged: for example starting a voluntary movement, to be eventually restored when continuation of such movement holds. Experimental evidence for the contribution of beta rhythm in motor functions is given by two recent papers [61], [62] in which a perturbation of beta activity is obtained through transcranial alternating current stimulation (tACS). Feurra and colleagues showed how cortical stimulation at 20 Hz enhanced the muscular response measured in the hand as a motor-evoked potential (MEP) induced by transcranial magnetic stimulation. However Pogosyan and colleagues using the same stimulation technique revealed that 20 Hz tACS is detrimental, leading to a slowing down of movements. Davis et al. [63] in their work suggested an interpretation with the attempt to reconcile these two contrasting results. They claimed that stimulation and enhancement of beta activity improve the excitability of the whole motor cortex but in an indiscriminate way; so that a physiologically increase of beta activity (hence the positive outcome recorded with MEP) is not followed by functional better performance (slowing down of movements).
Strong confirmation of the role of beta activity in motor functions is also given by Parkinson disease, the 'movement disorder' par excellence, of which Kuhn and colleagues [64] reported an exaggerate beta activity and they attempted to restore its 'normal' amount with deep brain stimulation showing the beneficial effect of such restoration for the movement execution [64]. Moreover beta-activity is typically exploited to train and drive brain computer interfaces [65], [66].

2.1.3.5 Gamma rhythm

Gamma oscillatory activity in recent years became one of the most investigated bands because of its omnipresence in a variety of experimental conditions. It seems related to a broad spectrum of processes including: feature integrations and object recognition (binding problem) [67], multi-sensory integration [68], attention and memory [69], [70]. Furthermore gamma band power (both increase and decrease) has also been related to cognitive impairments [71].

2.1.3.6 Evoked and Induced activity

Oscillations in the brain arise either spontaneously (without external stimuli, see resting-state in 2.1.7) or linked to the processing of stimuli. Usually brain oscillatory activity in response to external stimuli is further divided in two types of activity: 'evoked' and 'induced'. Evoked oscillations are related to the activity occurring with the same latency and phase-locked to different repetition of the stimulus, while induced oscillation vary either on latency or phase with respect to the stimulus. Evoked activity gives rise to so called evoked potentials by aligning and averaging recorded signals after the stimulus, while to reveal induced activity a different approach should be taken (i.e. the independent analysis of every single response) because non phase-locked activity tends to average out [72].
For what concern the EEG and MEG such estimations rely on the analysis of the time-series consisting of signals recorded at the scalp level. The usual technique exploited to inspect signal properties is spectral analysis (i.e. Fourier or Wavelet analysis) through which studying power variations as a function of frequency. Thanks to this approach oscillatory components of the signal can be disclose and the local activation of a particular brain area can be defined as increase or decrease in power, for a specific frequency band, of the signal recorded from the electrode placed above that area. A common example of such technique is called event-related synchronization (ERS) and event-related desynchronization (ERD) [31] through which it is possible to explore stimulus induced activity as a ratio of power between a baseline period (before stimulus occurrence) and an active period (after stimulus occurrence).

This brief description of cognitive correlates in different frequency bands is far from exhaustive and should not be taken as a suggestion of the existence of a unique relation between a specific frequency band and a single cognitive process. Similarly, it seems that single cognitive functions are implemented through the complementary action of different rhythms [73]-[75]. A unifying theory is still missing but there is nowadays agreement regarding the fact that oscillations at different frequencies together are related to changes in the functional brain state.

2.1.4 Structural, Functional and Effective connectivity

At macroscopic level, connectivity is usually the term employed to represent the interrelationship existing between two or more brain areas. This term is usually preceded by an adjective describing the nature of the relationship: structural, functional or effective [7], [76].
Structural connectivity, also known as connectomics [77], refers to the study of anatomical connections, efferent or afferent tracts of white matter fibres between different brain areas, or correlation between cortical thickness of grey matter areas. Functional connectivity refers to statistical interdependences computed between recordings of the activity of different brain areas. Recordings of such activity can be acquired either directly through EEG (or MEG), measuring the differences of electrical voltage potential (or the magnetic field) at scalp level which are representative of neuronal population activity under the recording electrodes (sensors); or indirectly analysing the metabolic activity measured as a function of blood oxygenation through fMRI. This latter is considered an indirect measure because it is based on the assumption that the metabolic demand is related to the level of activity of the neuronal population.

Functional and effective connectivity shared the type of data used to investigate functional interactions, but if on the one hand functional connectivity has a descriptive aim, on the other hand effective connectivity look into the causal relationship of the functional interactions [7].

The birth of modern study of brain connectivity coincides with a shift of interest from the concepts of functional segregation and local activation to functional integration. Functional segregation implies that anatomically defined areas of the brain are specialized to implements defined brain functions, such as perceptual or motor functions, and therefore it is possible to localize and trace the execution of a function in a well-defined area of the brain (local activation). However functional integration reflects the distributed processing of information among different segregated areas in order to realize brain functions.

During the early days of functional investigations, functional segregation and local activation were the hypotheses that moved the research of brain activity. This was due by the influence of earlier studies based on the 'lesion method' [78] which gave evidence of a strong relation between the damage of precise brain areas and the resulting cognitive impairment [8], [79]-[82]. The prototypical way neuroscientists investigated cognitive, emotional, perceptual, motor or any mental processes, was by correlating these processes induced by an appropriate experimental paradigm to the alterations of local brain activity estimated in some way depending on the modality (e.g. through EEG, MEG or fMRI).

What the early analysis of brain activity based on the functional segregation assumption shared is the oversimplified attempt to reduce neural information processing to two dimensions: space and local activation [83]. The idea of the existence of a simple one-to-one relation between mental processes and a precise brain area turns out to be to naïve and experimentally unsustainable because some mental process can activate more than one areas or different mental processes can activate the same brain areas. What began to be clear was that higher mental processes are implemented with a balanced collaboration of different and distant brain areas communicating and working together (functional integration).

Typically to obtain information about local activation a univariate approach, in which each signal is analysed independently from the others, is enough. However to have an insight on the communication and interactions between two or more brain areas a multivariate

approach is required. This latter exploits the assessment of interdependences between two or more signals to gain information on the functioning of the brain generating them.

Bivariate time-series analysis (investigating relationship between two signals) is a common way to enhance the univariate analysis and to explore the communication other than the local activation. In this context the concept of synchronization [84] between two signals is the mathematical mean through which to unveil and quantify communication and interactions between two brain areas.

Two categories of time-series analysis techniques to detect synchronization can be defined: linear and non-linear[1]. Linear measures focus on the study of linear relationship between two signals. One of the most important linear measure used in neurophysiological studies is coherence, which describes the linear correlation between two signals as a function of frequency. Non-linear measures were developed and used because of the observation that neurophysiological data contains non-linear properties derived from the intrinsic non-linear behaviour of neuronal activity [85]. An extensive review of linear and non-linear measures with a brief description of their usefulness and examples of their application to neurophysiological recordings is given by Pereda [20].

Furthermore in the framework of non-linear synchronization two relevant concepts are generalized and phase synchronization, which determine how measures of the synchronization are constructed. The intuition of the former is that the synchronization between two dynamical systems (i.e. two recorded signals from two brain areas) X and Y exists if the state of a system Y can be written as a function of the state of the system X and the synchronization can be reconstructed from time-series representing the dynamics of the attractors [86]. A popular example of a non-linear measure based on the concept of generalized synchronization is synchronization likelihood [87].
However phase synchronization principle [88] implies that synchronization can be estimated by quantifying the consistency of phase differences between the two signals recorded from two brain areas. This latter approach led to the definition of the measure of functional connectivity used in the experimental part of this thesis to estimate synchronization between brain areas. This measure is called phase lag index (PLI) [1] and will be the topic of the next chapter.

[1] Strictly speaking synchronization in physics is a term born in non-linear dynamical system theory to describe weak coupling between two or more oscillatory objects which interact modifying accordingly their phases and frequency, therefore amplitude adjustment are not compulsory to have synchronization. However typically in neurophysiological literature the synchronization is often used with a more broad meaning as 'statistical dependecy' between time-series.

2.1.5 Phase Lag Index

There are typically two approaches in order to correct for the problem of common sources. The first one is called source reconstruction technique and the main idea is to project the activity recorded at scalp level back to the generating sources inside the brain ('source space') in order to obtain more reliable information on the activity of each source, so that estimation of functional connectivity should reflect real interactions [28]. The second approach works directly on the time-series recorded at the scalp level ('signal space') detecting interactions unlikely produced by common sources.

Phase lag index (PLI) [1] is a measure of statistical interdependence between two time-series that estimates their synchronization examining their phase relationship and at the same time handling the common sources problem.

The definition of phase synchronization PLI exploits is the weak phase synchronization, [88] which states that there exists phase-locking between two time-series if their phase difference remains bounded. This is a relaxed definition of the stricter concept of phase synchronization in which phase difference between the time-series is required to be constant.

The intuition of PLI measure is that the activity related to common sources is present in both time-series with a zero phase lag (i.e. its contribution in both signals is instantaneous) therefore quantifying consistent non-zero phase lags it is possible to discard common source influence and disclose real interaction if present.

Consistent non-zero phase lags can be detected studying the distribution of instantaneous phase differences between the two time-series. An asymmetry in the distribution of phase differences centred at zero phase lag ($0\ mod\ \pi$) represents the presence of synchronization not ascribable to common sources while a flat or symmetric distribution indicate no synchronization.

In order to compute and evaluate the distribution of instantaneous phase differences first of all the instantaneous phase of each time-series should be computed. Hilbert transform represent a common way to extract instantaneous phase from a signal:

$$z(t) = x(t) + i\tilde{x}(t) = A(t)e^{i\phi(t)} \tag{1}$$

Where $z(t)$ is the complex valued analytical signal, $x(t)$ is the real time-series, $\tilde{x}(t)$ its Hilbert transform as function of time t. From equation (1) both instantaneous amplitude $A(t)$ and instantaneous phase $\phi(t)$ for a signal can be determined as

$$A(t) = \sqrt[2]{[x(t)]^2 + [\tilde{x}(t)]^2} \tag{2}$$

$$\phi(t) = arctan\frac{\tilde{x}(t)}{x(t)} \tag{3}$$

Using equation (3) the instantaneous phase differences between two time-series can be computed as $\Delta\phi(t) = \phi_1(t) - \phi_2(t)$ where $\phi_1(t)$ and $\phi_2(t)$ are the instantaneous phase of the two time-series at time t.

The time-series of the instantaneous phase difference $\Delta\phi(t)$ is the basis for the construction of the PLI, which is given by:

$$PLI = | < sign\left(\sin\left(\Delta\phi(t_k)\right)\right) > | \quad (4)$$

Where t_k represents the time in divided discrete steps $k = 1..N$, with N the total number of samples considered, $<..>$ is the average across these time steps and $|..|$ is the absolute operator. Averaging the sign of phase differences at each time step (t_k) and taking the absolute value of this quantity gives a measure of the asymmetry of the instantaneous phase distribution. PLI values range from $0 \leq PLI \leq 1$; with 0 indicating no synchronization at all and phase differences centred around 0 $mod\ \pi$ (possibly influenced by common source). PLI greater than 0 quantify the level of synchronization in term of asymmetry of the phase difference distribution: the more asymmetric the distribution is the more the PLI will be high.

2.1.6 Source Analysis

MEG and EEG data at level of the scalp offer the possibility to explore the dynamics of brain activity with high temporal resolution. However understanding from which anatomical brain area this activity originates could be crucial not only for interpretation issues but at the same time can improve the estimation of the activity per se: as already explained scalp data are affected by linear mixing (common sources) and blurring effects which are related to both distance sensors from the electrical sources and volume conduction influences.

The problem to detect which neural sources are responsible for the signals at scalp level is typically referred as 'inverse modelling problem' and it is a problem not confined to neuroimaging discipline [89].
In general terms the framework to study a physical systems (e.g. the Earth, a quantum particle, the brain) can be divided into at least three steps: i) define a set of parameters which completely characterize the system (model parameters); ii) define the physical laws allowing, for known values of model parameters, to predict measurements of some observable parameters (forward modelling problem); iii) infer the actual model parameters from measurements of observable parameters (inverse modelling problem) [89].

In the context of brain functional imaging the model parameters are represented by two categories: head model parameters (geometry of the head, conductivity of tissues, recording locations outside the head) and source model parameters (the parameters that describe neuronal currents such as their location, orientation and amplitude). The observable parameters are represented by the measurements of the electrical (magnetic) signals outside the head. The 'forward modelling problem' represents the prediction of the electromagnetic field and potential at the level of the scalp for known model parameters, while the 'inverse modelling problem' is the estimation of unknown sources corresponding to measured EEG/MEG signals.

A fundamental issue is that whereas the 'forward problem' has a unique solution (once defined the model parameters), the EEG/MEG 'inverse problem' non-unique, it admits infinite solutions [90] making it by definition ''ill-posed'' [91]. There is a copious and ever growing literature about brain source reconstruction techniques, which attempt to reduce the multiples solutions and transform the ill-posed problem in a well-defined and tractable problem. These techniques basically differ in the assumptions that are used to reduce the non-uniqueness of the problem. An overview with technical details of different approaches can be found in [28], whilst here we briefly introduce the beamformer approach [92] which will be adopted in the experimental part.

2.1.6.1 Beamformer analysis in MEG

Beamformer techniques are basically spatial filters, where the main idea is to estimate activity at each location of the brain volume blocking the contribution of possible electromagnetic neuronal sources located elsewhere. The assumption behind beamformer analysis is that there are no any two macro-neuronal sources (order of mm^2) with activity that is correlated over long time scale [92]. The estimation of activity is obtained by selectively weighting the contribution of MEG sensor data on the neuronal source at a location of interest.

The MEG signals recorded at scalp level (B) at any time instant is related to the neuronal activity by the equation:

$$B = LQ \tag{5}$$

Where Q is a $N\times1$ vector representing the strength of neuronal activity, L is a $M\times N$ matrix also called lead field matrix with M the number of sensors and N the number of element in the predefined source space.
The lead field is entirely determined by head model parameters and source parameters (supposing the MEG signal to be produced by unitary strength and optimizing the orientation of the sources [92]).

Based on the scalp level measurements over time (B), the aim is to define the locations and strength of the neuronal activity. The following equation shows how the neuronal activity at source level can be estimated at any latency where C_j represents the source covariance matrix and C_b the data covariance matrix.

$$Q = C_j L^T C_b^{-1} B \tag{6}$$

Given the beamformer assumption of uncorrelated sources it is possible to estimate C_j as a diagonal matrix where every entry corresponding to a location θ is related to the scalp recording with the following equation:

$$\sigma_\theta^2 = \left(L_\theta^T C_b^{-1} L_\theta\right)^{-1} \tag{7}$$

Combinations of equations (5), (6), and (7) allow the estimation of the beamformer weights W and beamformer output Q at θ location [92].

$$Q_\theta = \left(L_\theta^T C_b^{-1} L_\theta\right)^{-1} L^T C_b^{-1} B = W^T B \tag{8}$$

The weights specify the spatial filtering characteristics and allow reducing the contribution of sources at locations different from the source location of interest. Beamformer output is computed at any time latency generating a source time-series for location of interest [93]. Computing time-series at all the source locations of interest results in a multivariate data set that can enter the typical signal processing and functional connectivity pipeline.

2.1.7 Resting-state paradigm and resting-state networks

Resting-state paradigm consists of a condition in which an awake subject is recorded while he is asked to relax and not perform any physical or mental task. During the last fifteen years the investigation of such a condition of 'rest' has received considerable attention because it is thought that can help to disclose the intrinsic activity of the brain, which can increase our understanding of how different brain areas communicate [94]-[96].
Although recordings with such a paradigm were commonly adopted in EEG research experiments (the birth of EEG began with a resting-state experiment) the renewed interest in this paradigm is related to important discoveries in fMRI [97], [98] which revealed the existence of pattern of interactions between brain regions while a subject was not performing any task. Since then, many studies have established distinct sets of brain regions, so called resting-state networks (RSNs), which exhibit robust temporal correlations in spontaneous brain activity under resting condition [96], [97], [99]-[102].
Changes in RSN connectivity patterns have been related to cognitive performance: either too much or too little RSN activity in various pathologies (Alzheimer, schizophrenia and epilepsy)

has been correlated with cognitive deficits [103], whereas increased RSN activity after resective surgery for glioma correlated with improved cognitive performance [104]. Furthermore clinical investigations have also shown that RSN activity can distinguish patients from healthy subjects and it can correlate with disease severity [105].

The analysis in a resting-state paradigm was not only confined to the study of RSNs, however MEG and EEG connectivity and functional brain network studies benefit of such paradigm. These studies have provided evidence on the alterations on connectivity patterns and abnormal networks organization in disease [3], [4].

Figure 3 Resting-state networks. Spatial maps representing the resting-state networks: 1 default mode network, 2 sensorimotor network, 3 executive control network, 4 visual network, 5 and 6 fronto-parietal left and right networks 7 auditory network, 8 temporo-parietal network. Maps display high level of correlated blood oxygen level depend (BOLD) signal activity. Figure adapted from [105]

2.2 Network Analysis

2.2.1 General introduction

Modern network science is a combination of at least three different disciplines: graph theory, statistical mechanics and dynamical system theory. The main aim of modern network theory is to provide the ability to investigate complex systems and phenomena with simple but powerful and effective mathematical tools.

It inherits from graph theory the possibility to abstract and summarize the relationships between entities of a complex system in terms of nodes and edges. Nodes represent entities of the system under study, while edges represent interactions between entities. Together nodes and edges compose the network, which is the abstraction of the whole system. This simple conceptualization comes with a generalization property allowing to study very different systems. For example, nodes could be individuals and edges can describe social relationships of different kinds: so-called social networks arise. Nodes can embody computers, while edges stand for physical or logical connections between them: we construct a description of Internet or the World Wide Web. Furthermore we can have biological networks (e.g. genetic, metabolic), transport network, electrical network and so on [106]. It is clear how these two concepts are extremely practical and helpful to represent heterogeneous systems providing at the same time very simple approximations of such systems.

Statistical mechanics provides modern network theory with the capability to model large-scale networks and through the investigation of their topologies it points out unifying principles of real networks. One of the first examples of such modelling can be considered the work of Erdos and Renyi [12] which represents a transition from the study of small and deterministic graphs (ordered graph such as lattices) to the investigation of large and not deterministic graphs (random graphs).
Two seminal papers that influenced and foster the growth of network science are the Watt and Strogatz study [13] on *small-world* networks and the study of Barabasi and Albert on origin of *scale-free* networks [14]. Both works had an enormous impact because the described models can mimic properties present in most real life empirical networks.
Small-world networks are characterized by a topology in between regular (i.e. lattice) networks and random networks. They take advantage of two properties from both networks: the local connectedness from regular networks and short path-length between any two nodes from random networks. Local connectedness implies that neighbour nodes are highly connected among each other, while short path-lengths reflect the fact that the number of edges separating any pair of randomly chosen nodes is small. *Small-world* networks take the name from the known *small-world* phenomenon observed by Milgram [10] in his famous experiment. He described that social networks have the so-called 'six-degree of separation' property meaning that, surprisingly, the estimated number of edges in a chain of acquaintances is almost six. Watts and Strogatz described how this property was also present in other networks from different contexts such as the neural network of the worm Caenorhabditis Elegans, the electrical power grid of United States and the collaboration network of film actors [13], reflecting somehow that the *small-world* architecture is a very general one. Furthermore they provide a model to build networks with this property and explain how the right balance between local connectedness and short path lengths give rise to *small-world* networks.
Scale-free network is one of the first models dealing with not homogenous networks. Homogenous in this context means that the nodes typically are topologically equivalent: the number of edges each node possesses (i.e. the degree of a node) is similar. This holds true for

regular lattice and random networks, however many real world networks have very heterogeneous degree distribution: there exists nodes with extraordinary high number of edges (hubs) and other nodes with few edges. Barabasi and Albert suggested an algorithm in order to explain the appearance of hubs. They proposed a growing algorithm for the construction of a network with a preferential attaching rule. New nodes connect to existing ones accordingly to their degree: a new node has higher probability to be connected to an existing node with a higher degree than to connect to low degree node. This growing procedure affects the degree distribution of the network producing a highly skewed power law degree distribution explaining the appearance of hubs. Examples of such networks are Internet and the World Wide Web.

Dynamical system theory supports modern network science with the means and concepts to study processes taking place on networks. Specifically investigating how the topology structure affects the emergence of dynamical processes. Of particular interest is the inclination of a network to synchronize. Synchronization on a network is a phenomenon relevant in different situations spanning from brain diseases like epilepsy, where an abnormal synchronization of large neural population occurred, to sociological context with the emergence of social collective behaviours (i.e. emergence of strikes, new fashion, spread of a gossip). In both cases it is possible to understand the mechanism underlying the genesis of the process in terms of synchronization and its interplay with the network topology [106].

Topology, as the title of this thesis stated, is the main issue in here. Characterizing the topology of a network reveals important information regarding the complex system or phenomenon under study: from the topology depends the system function.

2.2.2 Brain networks

The brain can be considered a complex system both structurally and functionally: its intricate structural organization underlies and shapes its complex neural functional dynamics. Therefore a network perspective can provide the right tools to gain an understanding on how normal brain function arises and how its breakdown is caused by diseases [3], [4], [76].

Brain networks studies can be divided mostly in two categories: the study of structural networks and the study of functional networks.

Structural brain networks are based on the mapping of structural connections through different modalities and at different resolution scales. At the micro-scale, synapse connections between neurons are investigated with the use of electron microscopy. At the meso-scale the reconstruction axonal projections through histological dissection and staining studies [107] is performed to give a description of whole-brain white matter connectivity. Due to the invasiveness of the techniques these studies are conduct on animals or in post-mortem human brain. At the macro-scale level, thanks to non-invasive neuroimaging techniques [108], the whole-brain anatomy in live humans can be explored. Magnetic resonance imaging (MRI) and diffusion-weighted MRI are nowadays the most used non-invasive techniques to investigate macroscopically structural connectivity.
As well as structural techniques, physiological methods investigate brain activity from brain cells to brain regions [109]. It is beyond the scope of this thesis to describe all the techniques at different resolution scales to estimate brain activity. However, we are mainly interested in the macroscopically non-invasive techniques allowing the construction of functional brain networks. Nowadays the three most employed modalities permitting a whole-brain estimation of brain activity are EEG, MEG and fMRI. The first two give a direct estimation of

the electromagnetic activity of large neuronal populations, while fMRI estimates brain activity looking at the metabolic demand. In particular, it measures the blood flow related to energy consumption of brain areas which is related to neural activity.

2.2.3 Construction of structural and functional brain networks

The construction of structural and functional brain networks requires different steps [110] .

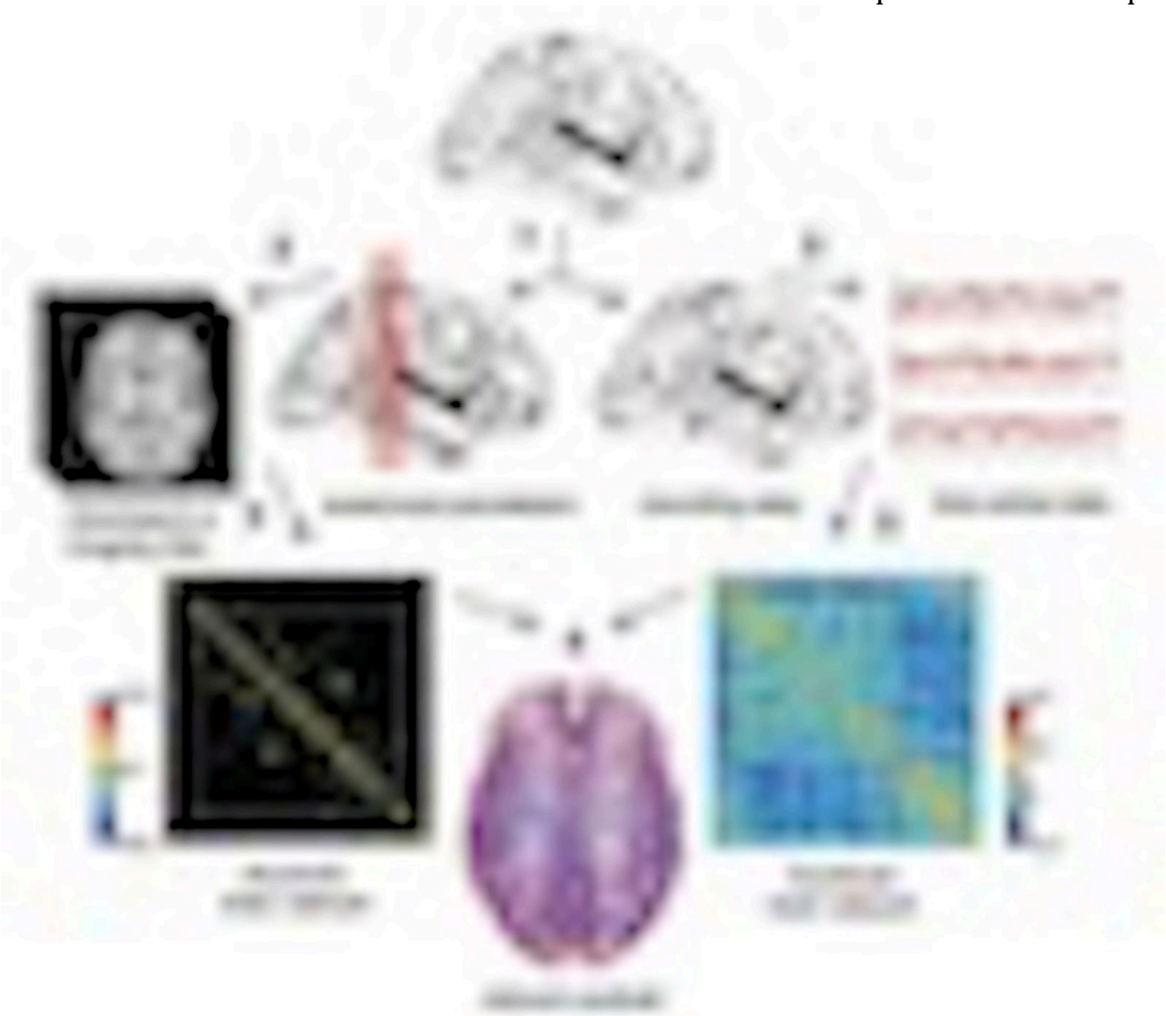

Figure 4 Brain networks construction from empirical data. On the left structural brain network are constructed. Nodes are defined by parcellating the brain into regions of interest (ROIs) based on structural features (2). The connections between these nodes are derived by MRI (estimation of cortical thickness) or diffusion MRI (estimation of white matter tracts) and used to build the structural connectivity matrix (3) from which the structural brain network is obtained. On the right node assignment is based on the EEG or MEG recording sites (2), functional interaction between each pair of the recorded signals is estimated with a functional connectivity measure and form the functional connectivity matrix (3) from which functional brain network is obtained. Figure from [77]

First, nodes of the network should be defined. For what concern structural studies typically a parcellation of the brain into coherent regions of interest (ROI) is performed. This parcellation can be done using different criteria, which can be based on previous anatomical atlas [111] or by defining homogeneously regions taking into account size and shape [112]. The definition of nodes in functional studies depends on the modality of analysis. In EEG/MEG scalp level studies, typically the nodes are represented by sensors of recordings, while in fMRI studies can be used strategies similar to the structural node definition (i.e. atlas based). Furthermore in EEG/MEG studies atlas-based approaches can be adopted thanks to source reconstruction techniques [93].

Once the nodes are defined, their relationships should be estimated. For structural brain networks the relationship between two brain areas (two nodes) can be computed looking at the estimation of neuronal fibres connecting the two areas. Such estimations can be obtained with diffusion-weighted MRI, which provides information about the spatial orientation of the neuronal fibres. The subsequent application of reconstruction algorithms exploiting spatial orientation information allow for the whole anatomical tract approximation which connects the two areas [113]. Alternatively, the correlation between thickness or grey matter volume of two cortical areas (estimated with MRI) can be used as a prediction of presence of anatomical connections between two areas [114]. The pair-wise computation of all structural relations between any pair of areas produces a structural connectivity matrix representing the structural brain network.
In functional brain networks the relationship between two brain areas is computed with functional connectivity 2.1.4, which corresponds to the strength of temporal correlations in activity between the two brain areas. As already stated the functional connectivity is computed between the signals recorded in those areas. The pair-wise estimation of functional connectivity between any pair of signals results in the functional connectivity matrix corresponding to the functional brain network.
A generic entry *(i, j)* of the structural or functional connectivity matrix represents existence or absence of an edge between node *i* to node *j*. If the value in the entry *(i, j)* is greater than zero an edge labelled with the value exists between node *i* and node *j* otherwise no edge exists.
Finally, once the structural or functional brain network is obtained, network metrics to assess its topology can be calculated.

2.2.4 Network Measures

Network measures quantify several properties of network elements (nodes and edges) and allow to depict the whole topology of the network. An overview of the most used network measures employed in structural and functional brain network analysis is represented by the work of Rubinov and Sporns [24]. Here, a brief introduction to the most important categories of network measures will be given (in Table 1 some of them are reported, for a more detailed reference see [24]).

It is worth to note that a typical approach before to perform a network analysis is to transform the weighted connectivity matrix into a binary matrix: so, from a weighed network where every edge has a value, an un-weighted network is obtained in which edges have no values associated. The main reason of this manipulation is to limit the potential effect of weak connections (edges with low values) on the overall topology. Weak connections are generally thought to represent spurious connections and may obscure the topology of strong connections, which are considered more reliable. This transformation is done either for structural brain network or functional brain networks and relies on an arbitrary threshold definition on the values of the connectivity matrix. The implications of such operation will be explained in paragraph 2.2.6. What is important to mention here is that the metrics computed for binary networks have their equivalents for weighted networks [24].

Network measures can be divided into different categories reflecting the type of information they convey about the network or its elements. Three main categories can be distinguished: measures of network segregation, measures of network integration and measure of network influence [24]. Measures of segregation investigate the way nodes can be locally connected in separated cliques (cluster or modules). Measures of integration refer to the global property of a network to be interconnected as whole: how nodes can ‘easily’ reach each other. Measures

of influence characterize the importance of individual nodes or edges and the role they play in the organization of the network.

The simplest and most used example of segregation measures is the clustering coefficient, which counts the number of triangles in the networks. Triangles (a complete sub-graphs of three nodes) are important because they reflect the robustness of the network [106]. The reason why triangles, used as building-blocks of the network, provide error tolerance is intuitively easy to understand. Imagine three nodes connected with each other (a triangle), if an edge is removed this small network still remains connected (it is possible from each of the three nodes to reach every other node). Therefore if a network contains a high percentage of triangles a random deletion of edges does not compromise the connectedness of the network. The clustering coefficient represents a nodal measure meaning that it gives an estimate of the number of triangles around an individual node. However it is possible to compute the clustering coefficient of the whole network as the average of all the clustering coefficients of individual nodes [24].

Motifs are another way to investigate local properties around an individual node. A motif is generalization of triangle, a sub-graph of few nodes connected in a particular way (i.e. from square, pentagon and other arrangements) that it is likely to have a functional role. In order to obtain an estimation of a particular motif in the network usually the occurrence of such motifs are counted and compared to the results obtained with random-networks [115].

More advanced measures of segregation describe the presence of modules in the network. Modules define a partitioning of the network into sub-networks satisfying a particular criterion. Typically a module consists of number of nodes in the network that are more strongly connected to each other (i.e., within the module) than with other nodes outside their own module [116].

Measures of integration in a network are based on the concept of path. A path between two nodes A and B consists of a sequence of distinct nodes and edges that should be traversed from node A to reach node B. The length of a path in binary network is given by the number of edges that should be traversed while in weighted network a weighted path length is equal to the total sum of individual edged weights. There could be many paths between node A and node B, however the shortest path length reflects how easily node A can communicate with node B therefore represents an estimate of how they can integrate information. The average shortest path between all pairs of nodes in the network reflects the integration properties of the whole network and it is the simplest and most used measure of integration [24]. Diameter is another measures of whole network integration; it consists of the longest shortest path between any pair of nodes in the network. It is a global measure representing how the network is more ‘stretched’ or ‘compact’.

Both average path length and average clustering coefficient are the most network measures employed to provide global information of the network and are commonly used to describe the brain network topology. As already explained, a short average shortest path length and a high average clustering coefficient characterize *small-world* topology. In order to detect such an optimal network organization an index of *small-world-ness* was developed based on these two measures [117].

The third category regards measures influence, reflecting the relative role of a node (or edge) in the organization of the network. The simplest measure is the degree of a node, which

represents the number of edges connected to the node. Degree is one of the most common ways to assess the importance of a node and its contribution to the whole network structure.
There are other measures based on the degree of a node. Degree correlation allows to evaluate if nodes are connected according to some rule depending on their degree. For example, it is possible to distinguish between network where high degree nodes tend to be connected to high degree nodes (assortative mixing) or network where high degree nodes have a preference to connect to low degree nodes (dissortative mixing) [118]. Furthermore, it is possible to assess the whole distribution of the degree values in the network that is informative of the overall topology structure. Using the degree distribution it is possible to discriminate between different models of networks (i.e. scale-free vs random network).
The importance of a node is commonly referred as centrality and degree is not the only way to evaluate this parameter. Other measures exploit the concept of path in order to assess the centrality. Betweenness centrality is nodal measure consisting of the ratio between the number of shortest paths traversing a node and all shortest paths in the network. Nodes with high betweenness centrality play an important role on information flow in the network. Betweenness centrality can be also computed for every edge [119].
Eccentricity of a node is another measure based on the paths, and it is computed as the longest shortest path from that node to any other node. The shorter the eccentricity of a node is the more central role it plays in the network because it means that is easily reachable by any other node.

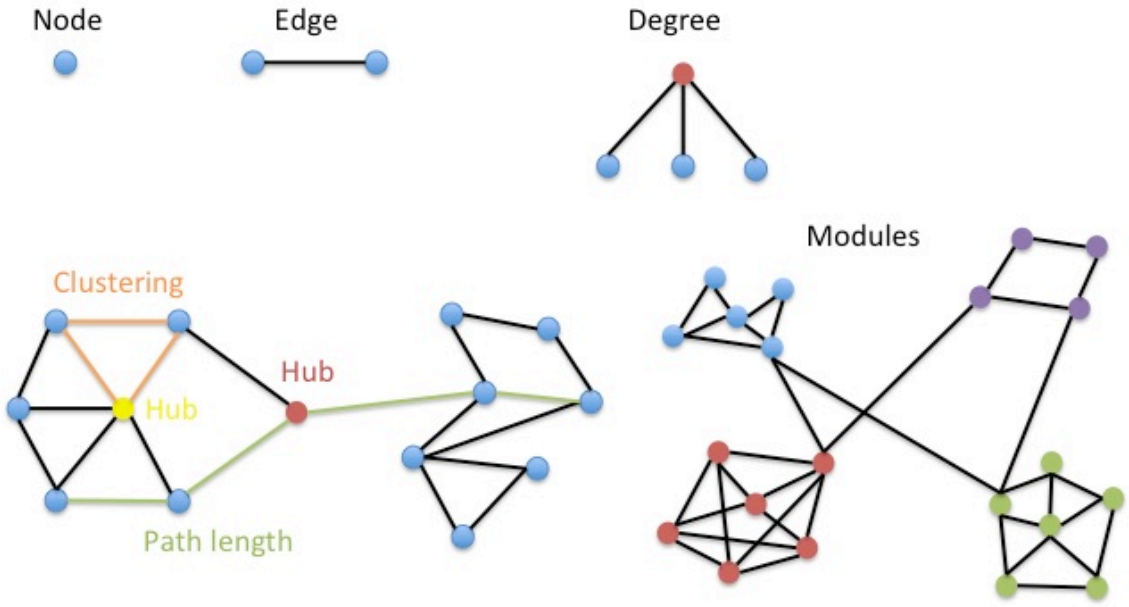

Figure 5 Network measures. Illustration of some of the described network measures for characterizing the network topology. Measures of segregation are based on the number of triangles (orange) or more sophisticated measures can decompose the network in modules (bottom right network). However measures of integration are based on the concept of path length (green). Measures of influence are based on a node degree (purple) which can be used to detect hubs (yellow node on the bottom left network). However hubs can be defined with the number of shortest path passing through a node (high betweenness centrality, red node on the bottom left network).

It is important to note that the number of nodes, the number of edges and the degree distribution of the network influences network measures [23]. Typically the significance of network measures computed on empirical networks (such as structural or functional brain networks) is obtained as comparison with the same measures evaluated in reference networks also referred as null-model networks. These null-model networks are commonly known model of networks, such as random or regular network, but preserving the same number of nodes, density (number of edges), and degree distribution of the empirical network [24].

	Concept	Explanation	Formula
N	Number of nodes		
M	Number of edges		
k	Degree	Number of edges for a given node *i*. a_{ij} is the entry of the connectivity matrix which establish the existence/absence of a connection between node *i* and node *j*	$k_i = \sum_{j \in N} a_{ij}$
C	Clustering coefficient	C it fraction of triangles in the network	$C = \frac{1}{N} \sum_{i \in N} \left(\frac{\sum_{j,h \in N} a_{ij} a_{ih} a_{jh}}{k_i (k_i - 1)} \right)$
C_W	Weighted clustering coefficient	Clustering coefficient for weighted networks. Where w_{ij} is the entry of the weighted connectivity matrix representing the value assigned to the edge connecting node *i* and node *j*	$C_W = \frac{1}{N} \sum_{i \in N} \left(\frac{\sum_{j,h \in N} \left(w_{ij} w_{ih} w_{jh} \right)^{\frac{1}{3}}}{k_i (k_i - 1)} \right)$
L	Path length	Average shortest path length between any two nodes in the network. Where d_{ij} is the distance in terms of number of edges	$L = \frac{1}{N} \sum_{i \in N} \left(\frac{\sum_{j \in N j \neq i} d_{ij}}{N - 1} \right)$
L_W	Weighted path length	Average shortest path length between any two nodes in the network. Where d_{ij}^w is the distance considering the weights assigned to the edges	$L_W = \frac{1}{N} \sum_{i \in N} \left(\frac{\sum_{j \in N j \neq i} d_{ij}^w}{N - 1} \right)$
BC	Betweenness centrality	Fraction of all shortest path that traverse a particular node *i*. Where ρ_{hj} is the number of shortest path between node *h* and node *j* and $\rho_{hj}^{(i)}$ is the number of shortest path between node *h* and node *j* passing through node *i*	$BC_i = \frac{1}{(N-1)(N-2)} \sum_{\substack{h,j \in N \\ h \neq j, h \neq i, j \neq i}} \frac{\rho_{hj}^{(i)}}{\rho_{hj}}$

Table 1 Network measures

2.2.5 Human brain networks in healthy and pathological conditions

Modern network theory has been applied to both structural and functional brain networks in health and disease [3], [4], [110], [120]. In these last fifteen years several results have been revealed for both structural and functional brain networks exploiting network theory:

Brain networks display a *small-world* topology [112], [114], [121] characterized by an high level of clustering and small average shortest path length.

Brain networks revealed a degree distribution close to a *scale-free* degree distribution [122], [123], reflecting the existence of hubs (nodes highly connected). These hubs in structural networks tend to be connected to each other forming a structural core called 'rich-club' [124].

Brain networks exhibit a hierarchical modular structure [125]. Modular structure implies that brain network can be partitioned in homogeneous (i.e. nodes inside a module are highly connected with each other than outside the module) sub-networks, while hierarchical organization reflects the fact that modules can be internally subdivided into sub-modules over several levels. Importantly modules typically are related to functional systems of the brain.

These topological properties of structural and functional brain networks seem to capture aspects of brain organization that have neurobiological relevance. Topology is related to the development of the healthy brain [126], [127] as well as to its aging [128], [129]. Cognitive performance seems to be associated with brain architecture, an example is given by intelligence which seems correlated with shortest average path length [130], [131]. However the relation between brain network topology and the arising of a pathologic condition can be considered the most striking result. It seems that the optimal and efficient *small-world, scale-free* and *hierarchical modular* structure of the healthy brain becomes disrupted in disease. Even the most disparate neurological disorders can be understood as deviation from optimal network topology. Alzheimer, epilepsy, multiple sclerosis, brain tumours, Parkinson and schizophrenia can be related to abnormal network organization and network modifications correlated with disease gravity and cognitive impairments [3], [4].

2.2.6 Example of pipeline of analysis and network comparison problem

Although network measures have enhanced our knowledge on the complexity of the brain's architecture, methodological issues may hinder the interpretation of the results. One of the main methodological problems dealing with brain networks is related to network comparison. Comparing networks is a typical operation performed during a brain network study: network of a patient group are compared with network of healthy subjects with the aim to find differences in network organization. These differences are computed in terms of network measures, which permit to infer different aspect of network topology. However network measures are influenced by: the size (number of nodes) and the density (number of edges) of the network, the distribution of the weights (if a whole connectivity matrix is used to construct the network) or by the use of an arbitrary threshold (used to obtain an un-weighted network).

In order to explain the network comparison problem it is useful to start with an example of the typical pipeline of analysis of a brain network study. It is worth to note that the comparison problem is a general problem arising for both structural and functional brain network. However, since in this thesis the focus is on functional brain networks, the illustrative example will summarize all the basic steps for functional analysis which will be later adopted in the experimental part 3.
For the sake of simplicity a schematic example is shown in Figure 6. Figure 6 (a) shows resting-state recordings that can be obtained by EEG from N electrodes. These recording are typically divided into epochs of a certain length and a number of artefact-free epochs are selected (i.e. removing epochs contaminated by muscle artefact, drowsiness, eye movement etc. etc.), see Figure 6 (b). At this point it is possible to either continue the analysis at level of the scalp (signal space) or perform a source reconstruction analysis and obtain the corresponding signals at source level. However, no matter the choice, the next step is to filter the selected epochs (either signal space or source space) in the frequency bands of interest (delta, theta, alpha, beta and gamma see 2.1.3) and analyze them independently Figure 6 (c).
Supposing we concentrate on a frequency band, the subsequent step is to compute the functional connectivity matrix using a synchronization measure for all selected epochs.
In all the studies presented in the experimental part the measure of functional connectivity is the phase lag index (2.1.5). This results in a $N \times N$ functional connectivity matrix for every selected filtered epoch where each element of the matrix contains the magnitude of the synchronization for a pair of electrodes (or a pair of reconstructed region of interest), see Figure 6 (d). A single average functional connectivity $N \times N$ matrix is obtained averaging over all epochs, as depicted in Figure 6 (e). Now the network analysis can continue in two different ways, Figure 6 (g-h).

The first possibility is to use a threshold T. Nodes in the network correspond to the N EEG electrodes (or N reconstructed sources) and values in the matrix correspond to the pair-wise relationship between the signals recorded in those electrodes (or reconstructed signals). Two nodes i and j are connected in the network if the synchronization value in the functional connectivity matrix in the position (i, j) exceeds the threshold T, otherwise they are not connected. A binary network is constructed, where the edges exist or not exist, and no weight is assigned to the edges.

The alternative is to use the whole functional connectivity matrix to construct a weighted network and then apply network analysis. In this case each edge is assigned with a weight obtained from the synchronization value in the functional connectivity matrix.

The PLI is a measure without direction: the synchronization values between node *i* and node *j* is equal to the one between node *j* and node *i*; therefore the PLI matrix is a symmetrical matrix and the resulted weighed network is undirected. The maximum number of edges *m* is $\frac{N(N-1)}{2}$ because self-connections (the diagonal of the matrix) are not considered. It is worth to remember that network analysis for weighted networks requires modified network measures that take into account the presence of weights [24].

The synchronization values, as in the case of PLI, range from 0 (no synchronization) to 1 (maximum synchronization). Typically in network analysis the importance of an edge is inversely proportional to its assigned value: the smaller the value, the more important the edge is. This is due by the fact that usually the edge values represent a cost to pay for its traversal; so the smaller the cost, the more convenient is to pass through that edge. However in our case the relation between importance of the edge and value is inverted: the most important edges represent the strong connections (higher value of synchronization). Therefore a transformation of the weights should be done in order to comply to the general network analysis assumption and typically all the weights are re-defined as $\frac{1}{synchronization\ value}$ (i.e. $\frac{1}{PLI}$). Let's denote the sum of all transformed weights as W.

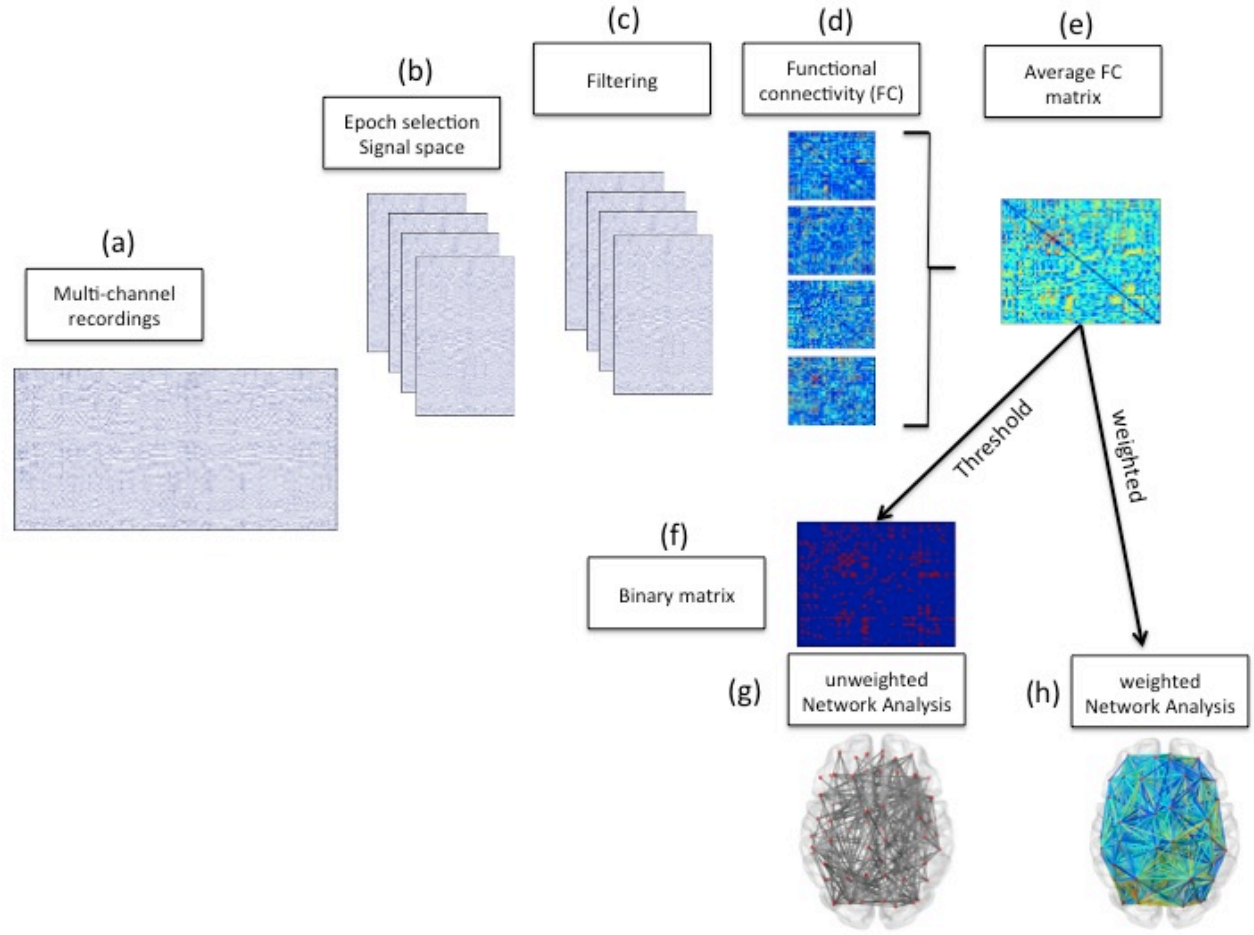

Figure 6 Pipeline of analysis: (a) multi-channel resting-state recordings, (b) selection of artefact-free epochs, (c) filtering in the band of interest delta, theta, alpha, beta and gamma. For each filtered epoch the estimation of functional connectivity (FC) is computed (d), subsequently the average functional connectivity matrix is calculated across epochs (e). The average FC matrix is either thresholded (f) and an unweighted network analysis is performed (g), or the weighted FC matrix is used for weighted network analysis (h).

With this example it was possible to introduce the parameters useful to explain the nature of the comparison problem, these parameter are N, T, m and W [23], [26].
Let's begin with the comparison of two functional un-weighted networks. If G_1 and G_2 are two un-weighted networks with N nodes and where a threshold T was applied, it is likely that they will have a different number of edges (densities) m_1 and m_2. This is because there is no guarantee that the two functional connectivity matrices have the same distribution of values, therefore the application of a common threshold T produce different results. In general a different value of m affect the network measures. For example it is highly probable that the clustering coefficient (C) will increase if the density m get bigger: there is a higher probability to have triangles. However it is likely that the average shortest path length (L) decrease if the density increases: more edges means higher possibility of 'short cuts'. In conclusion it is clear that the comparison between of network measures (like C and L) is biased by different values of densities (m_1 and m_2).
Two approaches are typically proposed in order to solve the problem: fixing network density m or normalizing network measures. Moreover it is worth to note that the choice of a threshold is completely arbitrary and this introduces an additional problem.

The first approach relies on the definition of two different thresholds T_1 and T_2 allowing to fix a common density m for both networks. However this approach is not sufficient to correct the problem [23]. The reason lies on the fact that typically, as already said, the distribution of connectivity values for experimental networks, such as the functional brain networks G_1 and G_2 are different. Supposing that G_1 has a low average connectivity compared to the higher average connectivity of G_2. A fixed value of m could be relatively large for G_1 so that edges with low connectivity values will be inserted in the network even tough they could reflect spurious or noisy connections (i.e. the assumption is that low connectivity value are potentially influenced by noise). Conversely the same m could be small for G_2 and connections that are important (high connectivity values) can be ignored because their inclusion may result in the exceeding the fixed density m. This may affect the topology of G_1 and G_2 biasing the comparison.
The second approach is normalization of network measures. This is achieved constructing an ensemble of reference networks (null-model networks) with the same N, T and m of the original network in order to normalize network measures. These ensembles are typically random networks or are random networks obtained by rewiring the original network while preserving some network characteristic (such as average degree, degree distribution) [132].
Network measures such as clustering coefficient (C_{random}) and shortest path length (L_{random}) are computed for every random network.
Then they are averaged over the ensemble giving an average clustering coefficient $\hat{C}_{random} = < C_{random} >$ and an average path length $\hat{L}_{random} =< L_{random} >$. These values are then used to normalize the network measures $\mathrm{C}_{normalized} = \frac{C}{\hat{C}_{random}}$ and $\mathrm{L}_{normalized} = \frac{L}{\hat{L}_{random}}$. However even the normalization do not solve the problem and leave the arbitrary choice of a proper m to compare the networks [23].

In the case of weighted network constructed using the full connectivity matrix and without applying any threshold there are still problems. As the threshold T affected the network measures the total weight W will affect the corresponding weighted network measures. Weighted network measures, such as weighted clustering coefficient C_w and weighted average shortest path L_w, are computed taking into account the weight on the edges. Therefore a higher value of W is likely to correspond to higher values C_w and L_w. If G_1 and G_2 have different values of W the corresponding weighted network measure will be biased by this difference [23], [26].

As the number of edges affects the comparison between networks also the number of nodes N influences such comparison. Network measures such as clustering coefficient and average shortest path length are influenced by the number of nodes in the network. This bias as well cannot be completely solved with normalization [23].

In conclusion the choice of parameters such as N, T, m and the different distribution of connectivity values resulting from the empirical data (i.e. reflected in differences in W) influences network measures, which are used to make inferences on network topology. The comparison between two network topologies based on biased network measures may be therefore be unreliable. To some extent this may be the reason why studies on network alterations in brain diseases reported contradictory results [133], [134].

In order to avoid methodological biases when comparing networks in the next paragraph it will be explained how the use of the minimum spanning tree (MST) might help to solve this problem.

2.2.7 Minimum spanning tree

In graph theory a tree is an acyclic connected graph (a graph without any loops, even self-loops) where a path between any pair of nodes exists [135]. A tree with N nodes has $m = N - 1$ edges. Given a graph, a spanning tree is a subgraph including all nodes in the original graph. In weighted graphs it is possible to have different spanning trees according to the total sum of the weights included in the spanning tree. The minimum spanning tree (MST) is the spanning tree that minimizes the sum of the weights in the original weighted graph.
Given a weighted graph one way to compute the MST is using the Kruskal's algorithm [2]. Supposing to have a weighted graph with N nodes, the algorithm begins ordering in a list (ordered edge-lists) the edges weights of the original graph, from the edge with the lowest value to the edge with the highest value. Once this edge-list is stored all the edges are removed from the graph leaving N disconnected nodes. Then the construction starts selecting the first edge (edge with lowest weight) in the ordered edge-list and connecting the two nodes that the edge connected in the original graph. Subsequently the edge is removed from the edge-list, the second edge (second lowest weight) is selected and two other nodes will be connected in the growing graph. This process continues selecting the edges from the edge-list and adding them to the growing graph unless a cycle is made, in that case the algorithm stops, remove the edge causing the cycle, discard the edge from the edge-list and continue to the next edge in the list. The algorithm continues until $N - 1$ edges are added to the growing graph obtaining the MST.

An important property of the MST is that if the weights of the original graph are unique the MST is unique. MST approach offers an approach to control for differences in network density. It is possible to compare two MSTs of different weighted networks directly if they have the same number of node N, because they will have the same number $m = N - 1$ of edges. The uniqueness of MST allows avoiding any arbitrary choice of a threshold T or any choice of a density m to compare the networks. Furthermore another advantage of the MST, if compared to the analysis of the full weighted network, is that it considers only the most important subgraph and avoids the problem caused by the differences in the total sum of weights W.

As for traditional networks it is possible to investigate and infer the MST topology using MST metrics. MST is a simpler structure than the original weighted network and this simplification limit the study of some properties of the original weighted network. For example the fact that MST does not contain loops make impossible to compute the clustering coefficient. However this is not truly a serious disadvantage because it has been reported that traditional network metrics are strongly correlated and thus redundant [136]. For example it was shown that clustering coefficient and average shortest path length in the small-world model are highly correlated thus the information loss computing just one of the two can be considered negligible.

Some of the traditional metrics can be used as well to characterize the topology of a tree. For example the degree, the eccentricity and the betweenness centrality of a node are computed in the same way in trees and can be used to assess the centrality of nodes (see Figure 7). Furthermore, measures such as the diameter (longest path in the tree) and the average shortest path can be applied to assess global properties of the tree.
In addition a simple measure that is useful to describe the topology of a tree is the leaf number. A leaf is a node of the tree with a degree equal to one (i.e. it is attached only to one edge), thus leaf number represents the number of leaves in the tree. Another useful measure developed to characterize the hierarchy of a tree is tree hierarchy T_h (see Table 2), which captures how tree is layered.

Tree topology can vary between two extremes: the path-like topology and the star-like topology, see Figure 7. If we have a tree with N nodes a path-like topology consists of a tree where $N-2$ nodes are connected to two other nodes (the degree of each node is 2) while the remaining two nodes are the extreme and each has only one connection. The star-like topology consists of a tree where one node has $N-1$ edges and all the remaining nodes have one edge (i.e. they are leaves). Using the leaf number these two type of topologies can be easily characterized: in fact star-like topology has a leaf number equals to $N-1$, while path-like topology has leaf number equals to 2. Star-like and path-like topologies have their pros and cons. For example a star-like topology can be very efficient in term of communications between nodes: path lengths between any pair of nodes is no more than two edges (other than the node with the highest degree that can reach every node in one step). Therefore we can say that the integration property of the network is maximized. This is not true for path-like topology where the average shortest path length is greater than two. However in a star-like topology the connectedness could be easily compromise by removing the node with the highest degree, while in a path-like configuration the removal of a node results in two connected sub-trees. Between these extreme topologies many types of different topologies exist and network measures can help in assessing their respective properties.

Figure 7 Schematic representation of minimum spanning tree (MST). Examples of star-like and path-like topologies. Blue nodes represent leaves. In the star-like topology the red node is the node with higher betweenness centrality (it is equal to 1) and higher degree (it is equal to 8) and lowest eccentricity (it is equal to 1). All the other nodes in the star-like topology have degree=1, eccentricity=2 and betweenness centrality=0. In the path-like topology red node characteristic are degree=2, betweenness centrality=0.5 and eccentricity=2. Tree characteristic in star-like topology are diameter=2, leaf number=8 and tree hierarchy=0.5. In path-like topology, red node characteristics are: degree = 2, BC = 0.5, and eccentricity = 2. The tree characteristics are leaf number = 2, tree hierarchy = 0.5, and diameter = 4. Adapted from [137].

An important finding is that MST topology is related to the underlying topology of the weighted network from which MST is extracted. Changes in the original network topology are reflected in changes in MST measures. Examples of how different network models, such as small-world and scale-free, affect MST measures are reported in [25]. Therefore MST still captures most of the important topological information in the original network.

An increasing number of studies have revealed the importance of MST for network analysis in resting state EEG and MEG recordings [26], [123], [137]-[139]. These studies have shown that MST topology measures allow to distinguish healthy subjects from patients and that changes in MST topology is related to the severity of the disease. Furthermore, theoretical studies have suggested the importance of the MST. An important finding is that under certain conditions

[119], [140], [141] and interpreting the original network as a transport network, the MST tend to form a critical backbone or 'core' where all the transport of the original graph flows. This may be relevant for the interpretation of the MST of brain networks since information flowing is a fundamental prerogative of the brain.

	Concept	Explanation	Formula
N	Number of nodes		
M	Number of edges		$M = N - 1$
L_f	Leaf fraction	Ratio between number of leaves (nodes with degree=1) and maximum number of possible leaves	$\frac{number\ of\ leaves}{M}$
D	Diameter of the tree	Longest shortest path in the tree. In the MST an upper limit of the diameter is related to the number of leaves as $d_{max} = M - number\ of\ leaves + 2$	
E	Eccentricity	Longest shortest path from a reference node to any other node in the MST.	
T_h	Tree hierarchy	Quantifies the trade-off between overall integration (short path length) and the overload of central nodes. Where BC_{max} is the maximum betweenness centrality of the tree	$T_h = \frac{(number\ of\ leaves)}{2MBC_{max}}$

Table 2 MST measures

3 Experimental part

3.1 Epilepsy and VNS

3.1.1 Introduction

Epilepsy is family of neurological disorders affecting the central nervous, characterized by the occurrence of recurrent and unpredictable seizures. Seizures are sudden and critical events represented by abnormal synchronous activity in the brain [142].
Practically the diagnosis of epilepsy is done by detecting two unprovoked epileptic seizures >24 hours apart. However, in 2005 the international league against epilepsy (ILAE) extends this definition to consider also situation [143] in which the two seizures criteria does not hold.

Nowadays it is estimated that about 1% of world population has epilepsy, such a diagnosis dramatically affects the quality of life [144]. Seizure unpredictability puts in danger even normal activities of everyday life, for example driving is prohibited. Typically a pharmacological approach with anti-seizure medications is the adopted treatment. However in almost 30% of epileptic patients such medications are not sufficient and other alternatives should be pursued. For refractory epilepsy, surgery can be a possible solution, however only a small number of cases can be handled with operations even because their outcomes may compromise cognitive performance [144].
Neuronal stimulation using vagus-nerve stimulation (VNS) is another viable option and can be considered a well-established add-on treatment for patients with pharmaco-resistant epilepsy. Vagus-nerve stimulation is a moderately invasive technique in which an electrode is implanted in the vagus nerve tract nearby the neck. Train of electrical pulses traverse the vagus nerve projecting fibres that finally impinge in various brain structures (thalamus, amygdala and other cortical areas) [145]. These kinds of neuronal stimulations even though are still partially understood [146] seem to induce a reduction in the seizure frequency. The outcome of VNS stimulation sometime is not successful; there are patients who do not show any improvement and undergo the removal of the stimulator device. There is still an open debate on the effectiveness of VNS add-on treatments [147]-[149].

Different and complementary hypotheses have tried to explain the mechanism of action of VNS for epilepsy. The main hypotheses are the synchronization theory, the neurotransmitter theory and cerebral blood flow theory [150]. Synchronization theory postulated that VNS has a desynchronizing effect on the hyper-synchronized activity observed in cortical and thalamo-cortical circuits occurring during seizure [151]. Neurotransmitter theory suggests that the chronic stimulations of VNS affect the modulation of neurotransmitter production, which eventually may lead to seizure suppression [152]. Finally, cerebral blood flow theory proposes that the alteration of blood flow caused by the VNS stimulation may activate inhibitory structures in the brain [153]. None of these theories is exhaustive and the precise mode of action remains not clear.

It has been reported [133], [154], [155] that analysis of functional brain network may reveal mechanism underlying the development of epilepsy. There is nowadays agreement in considering epilepsy a disease affecting the overall brain dynamics, characterized by both functional [156], [157] and structural [19-20] [158], [159] pathological connectivity. Furthermore, it was also observed how the topology of functional brain networks is altered in epileptic patients [160]-[163] and that these alterations are related to seizure vulnerability [164]. Therefore an investigation of possible VNS-induced changes in the topology of functional brain network is not only advantageous but it is required in order to shed light on its mechanism of action.

Previous EEG studies showed that changes in neuronal activity with a reduction in global synchronization are related to VNS therapy [165], [166]. It could be therefore particularly relevant to investigate if these changes extend also to the topology of functional brain networks.

Recent studies on the topological organization of brain networks in epilepsy are in disagreement: some reported a more regular brain architecture, other a more random network arrangement [158], [160], [167]-[170]. However a shift toward a less efficient organization in epileptic patients during the inter-ictal state seems a consistent finding. It could be therefore beneficial to investigate if VNS is related to a re-organization functional network topology.
The fact that discording results have been found suggest that care should be taken during all the analysis steps. As already mentioned bias induced by the network comparison problem or inappropriate choice of functional connectivity measure can invalidate the results.

In this chapter the question whether VNS induces functional network re-organization in those patients showing clinical improvements after implantation will be addressed. To reduce the effects of common sources, PLI will be employed for the estimation of functional connectivity and in order to deal with network comparison the MST analysis will be exploited. The main hypothesis is that as a consequence of VNS therapy, functional brain networks modify its configuration in patients responding to the treatment.

3.1.2 Methods

Ten patients affected by pharmaco-resistant partial epilepsy, who attended the Epilepsy Diagnostic and Treatment Centre of Cagliari (Italy), were retrospectively selected from a group who had a VNS (Cyberonics, Houston, TX) implanted for a duration of 5 years. Informed consent was obtained and the study was approved by the local ethical committee (NP/2013/438).
The main patient selection criteria for inclusion in the study were: (i) a relative stability of clinical features related to inter-ictal EEG activity; (ii) the resistance to classical first- and second-line antiepileptic drugs (AEDs) assessed bi-monthly for optimal therapeutic range; (iii) homogeneity in their pharmacological treatment; (iv) normal findings of neurological and psychiatric evaluations; (v) lack of abnormalities of cerebral structure on a recent MRI scan. The VNS stimulation parameters were set with a standard stimulation cycle of 30 s on and 5 min off and a frequency of 30 Hz. Patient characteristics are summarized in Table 3.
Patients were assigned to two different groups, responders and non-responders, based on the success of VNS therapy as quantified by the Labar index [171], which quantifies the effect of therapy in terms of change in seizure frequency/trimester. A previous analysis, which only studied the effect of VNS on global phase synchronization, has been performed on the same dataset [165].
Electroencephalographic (EEG) signals were recorded according to standard protocol using a 19 channels EEG system (Brain QuickSystem, Micromed, Mogliano-Veneto, Italy), both at least three months before the VNS implantation and five years after the onset treatment. During the EEG recording, patients were instructed to close their eyes, stay awake, and to reduce eye movements. The reference electrode was placed in close approximation of the electrode POz, with the ground electrode on the forehead. The acquired signals were digitized with a sampling frequency of 256Hz and successively band-pass filtered between 0.5 and 70 Hz. For each subject three eyes-closed (excluding periods indicating drowsiness) artifact-free epochs of 2048 samples (8 s) were selected and band-pass filtered in the classical EEG frequency

bands: delta (0.5–4 Hz), theta (4–8 Hz), alpha (8–13 Hz) and beta (13–30 Hz). All the analyses were performed for each band separately.
The phase lag index [1], was used in order to assess the functional connectivity between EEG channels with minimal bias due common source problem. All pair wise combinations of channels results in matrix of 19 × 19 entries, each reporting the corresponding PLI value. From every matrix, the MST was computed by Kruskal's algorithm [and from these MST graphs several measures were successively estimated in order to characterize the topology of the MST: diameter (largest distance between any two nodes), mean eccentricity (where eccentricity represents the longest distance between a node and any other node), normalized leaf number (number of nodes with degree = 1 divided the total number of nodes, where degree represents the number of edges the node has to other nodes) and hierarchy (refers to balance in hub nodes). Since the low spatial resolution of EEG, we decided, except for the eccentricity, to discard any MST nodal measures (i.e., degree and betweenness centrality). Furthermore, degree, eccentricity, and betweenness centrality represent different parameters to evaluate relative nodal importance. All the analyses were performed using the BrainWave software (version 0.9.70, http://home.kpn.nl/stam7883/brainwave.html).
In Table 4 the results of the MST analysis are provided, but please note that before performing the statistical analyses a natural log-transformation was applied to these MST metrics in order to obtain normal distributions. Two-way repeated measure ANOVA was used to test differences in age and seizure frequency. Multivariate analysis of variance (MANOVA) was used to evaluate the effect of group (responders/non-responders), condition (pre/post VNS implantation) and the interaction effect. MST measures were used as dependent variables, group and condition were the independent variables. In case of significant effect, univariate tests (ANOVA) were successively used as post-hoc analysis. Partial η^2 is reported as a proportion of the total variance explained by the independent factor.

3.1.3 Results

Demographic, clinical and network characteristics are listed in Table 3 and Table 4. No significant difference in age was observed between groups in either condition (pre/post VNS implantation). A significant main effect of condition (pre/post VNS implantation) $F(1, 8) = 19.61$, $p = 0.002$ and a significant interaction effect (group × condition) $F(1, 8) = 13.62$, $p = 0.006$ were observed for seizure frequency.
No effects of group (responders/non-responders) and condition (pre/post VNS implantation) were observed in any of the frequency bands. However, a significant interaction effect (group × condition) was obtained, $F(4, 5) = 9.25$, $p = 0.016$, Wilks' lambda = 119, partial $\eta^2 = 0.881$, in the 4–8 Hz theta band.
Successively, post-hoc ANOVA tests revealed that the observed significant interaction effect was caused by MST diameter ($F(1, 8) = 11.97$, $p = 0.009$, partial $\eta^2 = 0.599$) and MST eccentricity ($F(1, 8) = 10.85$, $p = 0.011$, partial $\eta^2 = 0.576$). Results for MST leaf fraction and MST hierarchy were, respectively ($F(1, 8) = 4.98$, $p = 0.056$, partial $\eta^2 = 0.384$) and ($F(1, 8) = 2.69$, $p = 0.14$, partial $\eta^2 = 0.251$). In particular, MST diameter and MST eccentricity decreased in patients responding to VNS add-on treatment after the VNS implantation, whereas these measures increased in non-responders (see Figure 8). Furthermore, even if not statistically significant, increases of MST leaf fraction and MST hierarchy were observed at trend-level in the responder to treatment group in the post VNS implantation, whereas these measures decreased in non-responders (Figure 8). In Figure 9 the schematic representation of the MST for the average connectivity matrix of responder and non responder combined with condition (pre/post implantation) is shown.

Patient	Age	Sex	AEDs	VNS-induced change in seizure frequency	Group
1	45	M	OXC+LMT	0%	non-responder
2	54	F	CBZ+LMT	-3%	non-responder
3	32	M	CBZ+VA	-7%	non-responder
4	57	F	CBZ+LMT	-11%	non-responder
5	33	M	CBZ+TOP	-14%	non-responder
6	36	F	CBZ+LMT	-67%	responder
7	50	M	CBZ+VA	-67%	responder
8	40	F	CBZ+TOP	-70%	responder
9	37	F	CBZ+LMT	-83%	responder
10	51	F	CBZ+LMT	-95%	responder

Table 3 Patient characteristics. AEDs = antiepileptic drugs; VA = valproic acid; CBZ = carbamazepine; LMT = lamotrigine; TOP = topiramate

Subject results

	Non responder		Responder	
	Pre-VNS	Post-VNS	Pre-VNS	Post-VNS
Patients (number)	5	5	5	5
Age (years)	43 ± 7	48 ± 7	44 ± 12	49 ± 12
Gender (M/F)	1/4	1/4	3/2	3/2
Seizure frequency (/trimester)	39 ± 25	35 ± 22	44 ± 17	9 ± 3
MST diameter	0,404 ± 0,023	0,463 ± 0,029	0,433 ± 0,046	0,359 ± 0,045
MST leaf	0,606 ± 0,034	0,544 ± 0,064	0,581 ± 0,081	0,667 ± 0,067
MST hierarchy	0,407 ± 0,030	0,380 ± 0,053	0,396 ± 0,064	0,442 ± 0,036
MST eccentricity	0,328 ± 0,017	0,365 ± 0,027	0,347 ± 0,034	0,293 ± 0,029

Table 4 Group characteristics and MST results. Values are expressed as mean and standard deviation

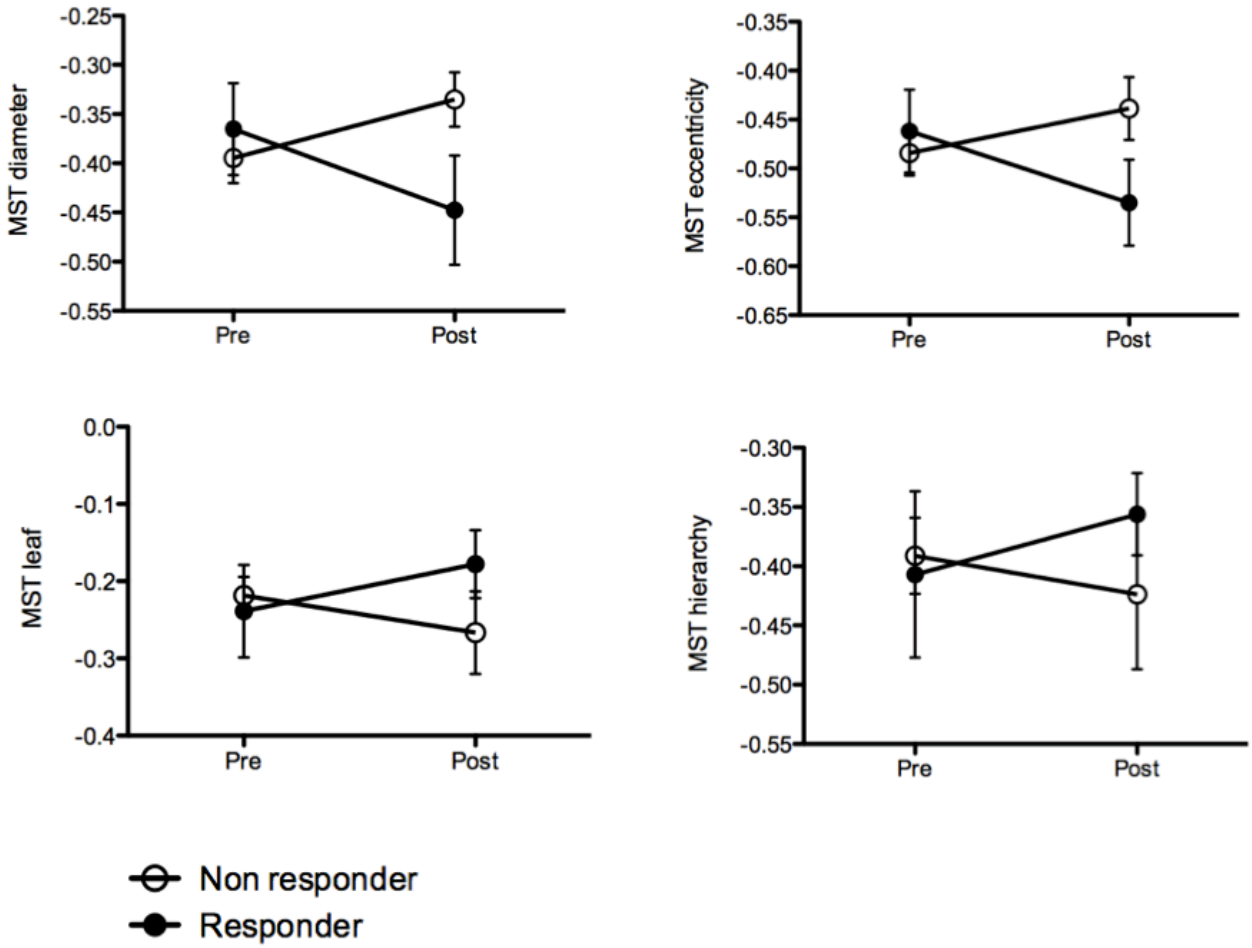

Figure 8 MST parameters for the responders and non-responders, both before and after VNS. Error-bars denote standard deviation.

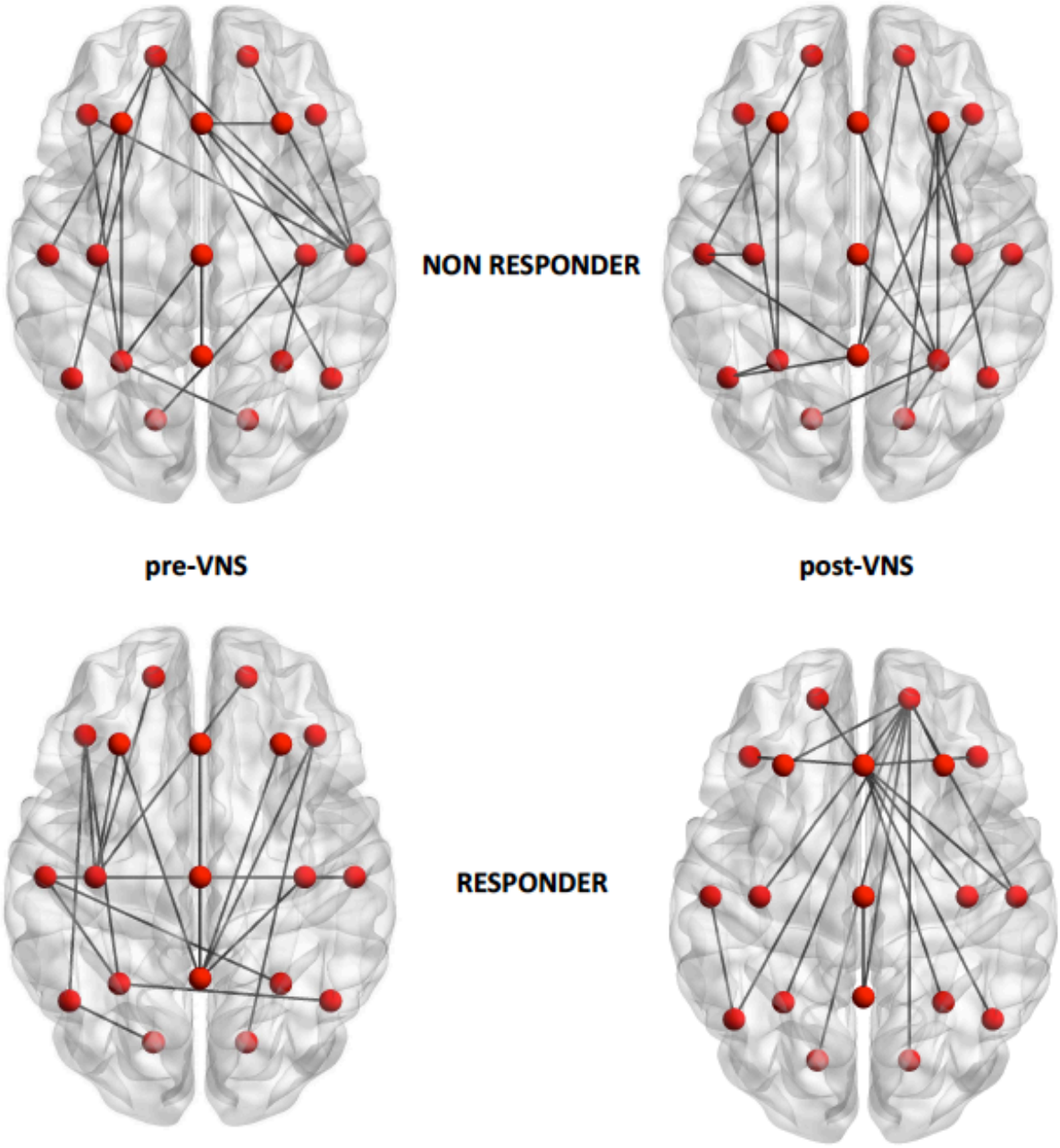

Figure 9 The MST of the average connectivity matrix for non responder (top line) and responder (bottom line) pre (left column) and post (right column) implantation.

3.1.4 Discussion

The main result of the present study was a significant interaction effect between VNS treatment outcome (responder/non-responder) and condition (pre/post VNS implantation) in the theta band. Specifically MST diameter and eccentricity decrease in those patients responding to the therapy while in non-responder there was an increase of these measures. It is worth to note that it was observed an opposite behavior for MST leaf number and hierarchy (i.e. an increase in responder vs decrease in non-responder), even if it was not significant.

Together these results suggest a functional network re-organization in responder, possibly induced by the VNS therapy, consisting of a more integrated (smaller diameter and eccentricity), more balanced (higher hierarchy: no overloading of nodes) and less path-like (higher leaf fraction) architecture. Results are in line with the formulated hypothesis that VNS therapy affects functional brain network organization and the more efficient (i.e. more integrated, more balanced and less path-like) re-organization is related to the clinical benefit in responder. These findings are also in line with the theory that includes epilepsy in the framework of network disorders: an aberrant topology of structural and functional networks promote seizure occurrence [133], [154], [155].

VNS seems to be related to a widespread network re-organization and this may explain why its potential effect is not only confined to epilepsy but it was reported to be beneficial for other pathological conditions such as obesity and depression [150], [172].

Results in theta band agree with other works [161] which suggest a pivotal role of theta functional connectivity and network topology modifications toward a sub-optimal organization in epileptic patients if compared to healthy controls. This alteration in network topology in theta band was also observed in [173] where a disruption of global integration properties in epileptic glioma patients seems to be related to occurrence of seizures. Furthermore, loss of optimal network configuration in theta band has been shown to correlate with seizure frequency, duration of the disease and cognitive decline [161], [162], [164], [170].
This study may be influenced by some limitations:

- the small number of subjects involved in the analysis,
- the small number of EEG electrodes used to infer topological properties,
- no statistical correction for the multiple comparison problem over frequency bands,
- an active common reference can influence the functional connectivity analysis,
- potentially confounding effects due to the different regime medication are considered,
- potential effect of AED on network topology

Therefore caution should be taken in the interpretation of results. However for some of the limitations it is plausible to think that the effect on the overall result should be minimal. For example it is accepted that each frequency band is related to different phenomena, consequently can be treated as independent and no correction is required. Moreover the effect of common reference should be reduced due to the use of PLI as a functional connectivity measure. Furthermore, the very strict inclusion criteria on medication used during the selection of patients and the comparable drug regime across groups should limit this confounding factor. Finally even if it is not possible to discriminate between the independent effect induce by AEDs medications and VNS alone on the topology re-organization, results support the idea that together both are involved in the functional network re-configuration. Future studies should address the question if changes to network

topology induced only by AEDs are different from modifications observed in responder to VNS.

On the contrary the strong points of the present study are the way common source problem and network comparison problem are handled. The use of PLI and MST together permit to overcome problems that typically are neglect in previous connectivity studies leading to biased results.

In conclusion this study support the hypothesis that VNS add-on treatment promote a network re-organization in patients responding to the treatment. It also proposes that functional network properties can be used as a marker in monitoring the efficacy of the treatment.

3.2 Diabetes

3.2.1 Introduction

The incapacity to produce insulin is the deficit characterizing Type 1 diabetes mellitus (T1DM). This impairment is related to destruction of pancreatic beta cell, which are responsible for the insulin production. As a consequence T1DM patients require the assumption of external insulin through extra-cutaneous injections to compensate the failure of insulin secretion.

T1DM patients are vulnerable to dysglycaemia phenomena, hyperglycaemia and hypoglycaemia, that together with cumulative hyperglycaemic exposure can lead to micro-vascular damage such as retinopathy and nephropathy [174].

Although T1DM is not a proper neurological disease, recently the potential effect of dysglycaemia on the central nervous system has been investigated. Structural studies [175], [176] reported modifications of both grey and white matter. Functional studies described alterations of functional connectivity and brain networks of T1DM patients compared to non-diabetes controls [177], [178]. Moreover moderate cognitive impairments affecting speed-related cognitive performance were observed in these patients [179].

Chronic hyperglycaemia is hypothesized to be related to these cerebral functional alterations and cognitive impairments [180], [181]. A marker of cumulative hyperglycaemic exposure is microangiopathy (i.e. retinopathy, neuropathy and microalbuminuria). The retina shares developmental and physiological characteristics with the brain [182], and proliferative retinopathy has been related to cognitive decline in T1DM, and may thus be a marker of the effect of cumulative hyperglycaemia on the brain [183].
Furthermore the importance of proliferative retinopathy was even revealed in EEG/MEG functional connectivity [177], [184] and fMRI resting-state networks (RSNs) [178] studies, which reported a reduction in functional connectivity measure in T1DM patients with proliferative retinopathy, while an increase was observed in T1DM patient without proliferative retinopathy. Moreover this reduction correlated with cognitive performance suggesting that functional connectivity is involved in cognitive functioning [177], [178].

Biases in the analysis approach could affect the results of these studies. In particular the analysis performed at the sensor-level (both EEG/MEG) can be strongly influenced by common source problem. Furthermore the poor temporal resolution of fMRI may neglect the richer brain dynamics.
In this study a RSN functional connectivity analysis was performed with a MEG dataset from a previously described patient cohort with the objective to handle biased from the previous analysis pipeline [177], [178].

In particular:

- A larger cohort is used than in the original MEG study [177] to enhance statistical power;
- Analyses are performed in source-space instead of sensor-space, in order to enhance the interpretability of the results;
- The phase lag index, that is insensitive to spurious interactions [1] is used, instead of the synchronization likelihood[87], [185];
- Although fMRI allows for the spatially accurate reconstruction of RSNs [178] it does not capture the rich temporal dynamics of the neuronal activity that underlies the

Blood Oxygenation Level Dependent (BOLD) signal. Here, using fMRI literature to define meaningful RSNs [105] in combination with the beamforming technique [93], it was possible to reconstruct frequency-specific functional connectivity within these RSNs;
- The focus was not only on functional resting-state sub-networks but also on the special sub-network represented by the minimum spanning tree.

Our aim was to test whether functional connectivity in RSNs differs according to clinical status and correlates with cognition in T1DM patients with and without proliferative retinopathy, using an unbiased approach with high spatio-temporal resolution functional network.

3.2.2 Methods

3.2.2.1 Participants

Forty-two type 1 diabetes mellitus patients with proliferative retinopathy ($T1DM^+$), 41 diabetes mellitus patients without microvascular complications ($T1DM^-$) and 33 healthy control subjects, matched for sex, BMI, and education were recruited in this study. Age range criteria were 18-56 years and participants were excluded if they had a BMI above 35 kg/m^2, use of drugs affecting cerebral functioning, current or history of alcohol (men >21 and women >14 units a week) or current drug use, psychiatric disorders, anaemia, thyroid dysfunction, use of glucocorticoids, hepatitis, stroke, severe head trauma, epilepsy, pregnancy, or poor visual acuity. For T1DM patients a disease duration of at least 10 years was required.
To control for confounding effects of depression on cognitive performance and functional connectivity, depressive symptoms were assessed using the Centre for Epidemiological Studies scale for Depression (CES-D). To prevent confounding due to current blood glucose level differences, these were measured in T1DM patients before the MEG recording. Blood glucose levels between 4 and 15 mmol/l (72-270 mg/dl) were regarded as appropriate. A detailed description of the inclusion/exclusion criteria for patients and control subjects is provided in our previous work [177] where the MEG data from a sub-set of these participants (n=15, 29, and 26 for $T1DM^+$, $T1DM^-$, and healthy controls, respectively) were analysed at sensor-level. The original dataset consisted of 148 subjects, but 32 subjects were discarded either because of bad MEG recordings (n=24) or problems with MRI co-registration (n=8).

3.2.2.2 Neuropsychological assessment

As described in detail in [177] all participants were assessed using a battery of neuropsychological tests to evaluate cognitive performance in six cognitive domains: memory, information processing speed, executive functioning, attention, motor speed and psychomotor speed. For each neuropsychological test z-values were created based on the mean and standard deviation of the controls. These were then grouped to form the cognitive domains (see appendix 5.1). When necessary, z-values were transformed so that higher z-scores represent better performance. In this study 'general cognitive ability' was considered and was obtained by averaging the z-scores over all cognitive domains.

3.2.2.3 MEG

MEG data were recorded using a 151-channel whole-head MEG system (CTF Systems; Port Coquitlam, BC, Canada) while participants were in a supine position in a magnetically shielded room (Vacuumschmelze, Hanau, Germany). A third-order software gradient [186] was used with a recording passband of 0.25–125 Hz and a sample frequency of 625 Hz. Magnetic fields were recorded for 2 minutes in an eyes-open, 5 minutes in an eyes-closed, 10 minutes in a task, and then 3 minutes in an eyes-closed condition.

At the beginning and end of each of these recordings, the head position relative to the coordinate system of the helmet was determined by leading small alternating currents through three head position coils attached to the left and right preauricular points and the nasion. Changes in head position of <0.5 cm during a recording were accepted. Here, only the first (5 minutes) eyes-closed resting-state condition was analyzed, which was divided into 45 trials of 6.55 seconds (4096 samples). Channels and epochs containing artefacts were discarded after careful visual inspection, rejecting on average 3 channels (range: 0-11). A minimum of 25 epochs were selected and considered sufficient for the beamformer analysis [187].

3.2.2.4 Beamforming

A structural T1-weighted MRI-scan was used for co-registration as a first step for beamforming. Only data with an estimated co-registration error < 1.0 cm were accepted for further analysis. MRI-data were then spatially normalised to a template MRI using the SEG toolbox in SPM8 [188], [189], after which anatomical labels were applied [190]. An atlas-based beamformer approach [93] was used to project MEG sensor signals to an anatomical framework consisting of 78 cortical regions (ROIs) [190] identified by means of automated anatomical labelling (AAL) [191]. This resulted in time-series of neuronal activation for all voxels within a ROI, after which a representative voxel was selected (the one with maximum power for a given frequency band [93]. The time-series for the 78 ROIs were filtered in the following frequency bands: delta (0.5–4 Hz), theta (4–8 Hz), lower alpha (8–10 Hz), upper alpha (10–13 Hz), beta (13–30 Hz), and lower gamma bands (30–48 Hz). This resulted in a total of 6 sets (one for each frequency band) of 78 time-series (one for each AAL region). Five artefact-free epochs of 4096 samples (6.55 seconds) were selected from these time-series, based on careful visual inspection to obtain stable results [104], [137]-[139], [192]-[196]. These data were further analysed using Brainwave v0.9.70 [authored by C.S.; available at http://home.kpn.nl/stam7883/brainwave.html].

3.2.2.5 Functional connectivity analysis

Functional connectivity between all 78 reconstructed time-series was estimated using the phase lag index [1] independently for each frequency band. For each subject and epoch, PLI values were computed for each pair of ROIs (i.e. a 78x78 adjacency matrix was obtained) and subsequently the mean PLI values were calculated by averaging over the five selected epochs (i.e. a 78x78 matrix containing average PLI values per subject was obtained). Using the PLI adjacency matrix it was possible to estimate phase coupling within so-called resting-state networks (RSNs) [104], [105], [196]. This was done by averaging the PLI values between the ROIs belonging to a specific resting-state network (see appendix 5.1). Functional connectivity was estimated for the auditory, default-mode (DMN), executive control (ECN), left and right frontoparietal, sensorimotor (SMN), temporoparietal and visual resting-state networks.
In addition, average functional connectivity within the network resulting from a minimum spanning tree (MST) analysis was estimated.. Here, each ROI was considered as a node and (1 divided by) the PLI value for each pair of ROIs was used as the weight for the edge between the nodes.. The MST algorithm acts as a filter on the PLI matrix, keeping only the connections that form part of the critical backbone of the original network (assuming that the strong disorder limit holds) [138], [197], [198].

3.2.2.6 Statistical analysis

Participant characteristics were assessed using one-way ANOVA or Student's t-test for continues variables and chi-square for dichotomous variables.

Group differences for general cognitive ability were evaluated using an ANCOVA, with group and gender as independent variables and age, systolic blood pressure and depressive symptoms as covariates.
For each frequency band independently, a MANCOVA model was used to evaluate differences in functional connectivity between groups. PLI values of resting-state and MST networks were used as dependent variables, with group and gender as independent variables. Functional connectivity values were log-transformed (log10(x/1-x)) to obtain normal distributions to allow the use of parametric statistics. This resulted in 6 MANCOVAs. When the overall F-test was significant, post-hoc MANCOVA was used to determine which networks contributed most to the model. In order to correct for possible confounding factors, age, depression symptoms and systolic blood pressure were used as covariates in all statistical tests.
Finally, for those networks that differed between groups, it was determined the association with general cognitive ability using stepwise regression analyses for each patient group separately. For this analysis, significant RSNs and MST PLI values were used as predictors for 'general cognitive ability' z-scores as dependent variable. In order to correct for possible confounding factors, age, depression symptoms, systolic blood pressure, diabetes duration were entered in the regression. Statistical analyses were performed with SPSS v.19 (IBM-SPSS, Chicago, IL, USA).

3.2.3 Results

3.2.3.1 Subject characteristics

Subject characteristics are summarised in Table 5. There were no differences in gender distribution between groups ($p>0.05$). Groups were significantly different for age ($F(2,113)=6.55$, $p=0.002$), systolic blood pressure ($F(2,113)=4.03$, $p=0.02$), depressive symptoms ($F(2,113)=5.82$, $p=0.004$), diabetes duration ($t(81)=6.14$, $p<0.001$) and diabetes onset age ($t(81)=-3.00$, $p=0.004$). $T1DM^+$ patients were the oldest, had highest systolic blood pressure values and highest scores on the depressive symptoms assessment. The $T1DM^-$ and control groups did not differ on any of these three characteristics.

Table 5 Subject characteristics.

	T1DM+ patients	T1DM- patients	Control subjects	p-values
N	42	41	33	-
Age (years)	44.7±7.15*#	38.39 ±9.18	38.21 ±11.09	**0.002**
Gender (m/f)	19/23	17/24	15/18	0.922
Depressive Symptoms (CES-D)[a]	12.07±10.56	7.00 ±6.61	6.09 ±7.12	**0.004**
Estimated IQ (NART)[b]	110.05±13.69	106.29±11.16	108.66±12.14	0.306
Systolic Blood Pressure (mmHg)	135.42 ±17.41*	128.82 ±13.89	126.34 ±10.78	**0.020**
Diastolic Blood Pressure (mmHg)	77.26±8.62	77.68±9.72	78.92±6.65	0.694
BMI (kg/m^2)	26.04±4.23	25.12±3.62	24.88±3.40	0.365
Hypertension (%)[c]	30 (71.4)	11 (26.8)	-	**<0.001**
Diabetes early onset (%)[D]	13 (31)	6 (14.6)	-	0.077
Diabetes duration (years)	33.78±7.80	21.85±9.78	-	**<0.001**
Diabetes onset age (years)	10.09±7.47	16.53±9.50	-	**0.004**
Lifetime severe hypoglycaemic events[e]	6.09±9.83	6.85±11.15	-	0.576
Peripheral neuropathy (%)[f]	21(50)	-	-	-

Subject characteristics for T1DM with proliferative retinopathy (T1DM+), T1DM without complications (T1DM-) and control participants. Data are given as means with SD or absolute numbers with percentage. * Significantly different from controls ($p<0.05$); # significantly different from T1DM- ($p<0.05$).

a: Depressive symptoms were measured using the Centre for Epidemiological Studies scale for Depression.

b: Estimated IQ was measured using the Dutch version of the National Adult Reading Test.

c: Hypertension was defined as a systolic blood pressure of ≥140 mmHg, a diastolic blood pressure of ≥90 mmHg, or use of antihypertensive drugs.

d: Diabetes early onset was defined as an onset age below the age of 7 years.

e: Severe hypoglycaemic events were self-reported and defined as events for which the patient needs assistance from a third person to recuperate as a result of loss of consciousness or seriously deranged functioning, coma, or seizure owing to low glucose levels.

f: Peripheral neuropathy was based on medical records or, in case they were not available, based on self-report.

3.2.3.2 Neurophysiological assessment

A significant effect of group ($F(2,107)=6.86$, $p=0.002$) for general cognitive ability was found, but no gender effect or interaction effect, was observed. Post-hoc analysis revealed significant poorer performance in T1DM+ patients compared with $T1DM^-$ (mean difference (MD)=-0.301; 95% confidence interval (CI)=[-0.512, -0.090]; $p=0.006$) and controls (MD=-0.409; 95% CI=[-0.636, -0.182]; $p=0.001$).

3.2.3.3 MEG results

The MANCOVA model with log-transformed PLI values for the RSNs and MST network revealed a significant effect of group for the lower alpha band ($F(20,196)=2.06$, $p=0.006$; Wilk's $\Lambda=0.683$, partial $\eta^2=0.174$), while the other frequency bands did not show a significant group effect. Neither a main effect of gender nor an interaction effect was found.
Post-hoc MANCOVA analysis revealed significant differences in DMN ($F(2,107)=3.45$, $p=0.035$, partial $\eta^2=0.061$), ECN ($F(2,107)=5.55$, $p=0.005$, partial $\eta^2=0.094$), SMN ($F(2,107)=4.67$, $p=0.011$, partial $\eta^2=0.080$) and MST ($F(2,107)=3.11$, $p=0.049$, partial $\eta^2=0.055$). Specifically, for every significant sub-network, $T1DM^+$ patients showed the lowest functional connectivity values (Figure 10), while $T1DM^-$ had similar values to, or showed higher functional connectivity values than controls.
$T1DM^+$ patients compared to $T1DM^-$ patients had significantly lower functional connectivity within the DMN (log-transformed MD=-0.072; 95% CI=[-1.136, -0.009]; $p=0.026$), ECN (MD=-0.144; 95% CI=[-0.230, -0.058]; $p=0.001$), SMN (MD=-0.100; 95% CI=[-0.177, -0.023]; $p=0.011$) and MST (MD=-0.061; 95% CI=[-0.109, -0.012]; $p=0.015$). For the SMN a significant difference (MD=-0.117; 95% CI=[-0.199, -0.034]; $p=0.006$) between $T1DM^+$ and control subjects was found, while in DMN a significant difference (MD=0.067; 95% CI=[0.005, 0.128]; p=0.034) was found between $T1DM^-$ and controls, with functional connectivity being higher for the T1DM- group.
Stepwise regression using gender, age, systolic blood pressure, depressive symptoms and diabetes duration as covariates; and the significant MST and RSN values as predictor, showed that DMN functional connectivity was a significant predictor (Adj. $R^2=0.427$, standardized Beta=0.343, p=0.013) for general cognitive ability in $T1DM^+$ patients.

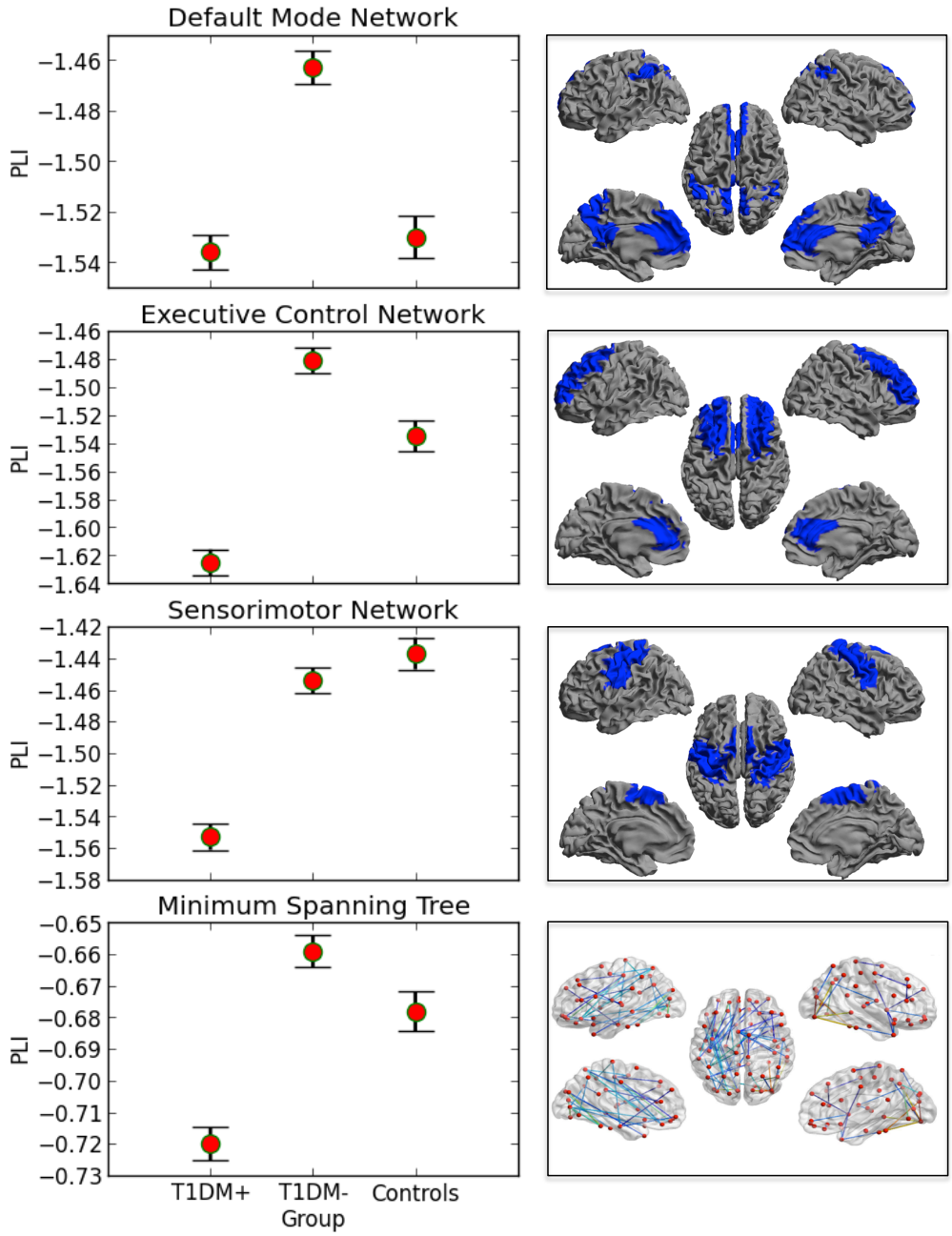

Figure 10: Left panels: Average (and 2 standard errors) connectivity (lower alpha band, log-transformed) within Resting-state Networks and MST networks that showed a significant group effect. Note that for all these networks the functional connectivity was significantly lower for the patient group with microvascular complications (T1DM+) than for the patient group without microvascular complications (T1DM-), as well as in the sensorimotor network (SMN) for the T1DM+ group compared to controls. In the default mode network (DMN), the PLI was significantly higher for the T1DM- group than for the controls. Right panels: shows the areas for the relevant RSN (highlighted in blue) on a template brain (see also Appendix A), and (bottom panel) the MST of the average connectivity matrix for the control group (visualized using BrainNet Viewer [199]). Here, cold colours indicate low PLI, hot colours indicate high PLI.

3.2.4 Discussion

Type 1 diabetes mellitus with microvascular complications ($T1DM^+$) showed a reduction of functional connectivity both for MEG resting-state networks (RSNs) and minimum spanning tree analysis when compared to type 1 diabetes patients without microvascular complications (T1DM-), as well as compared to healthy subjects. Moreover it was observed an increased DMN functional connectivity in T1DM- patients relative to controls. The alteration of functional connectivity was found in the lower alpha band of three resting-state networks (DMN, ECN, SMN) and for the MST sub-network. Finally, in $T1DM^+$ it was observed significant correlation between a diminished cognitive performance (general cognitive ability) and DMN functional connectivity in lower alpha.

Nevertheless methodological differences and/or modalities of previous findings [177], [178], [184] this study confirms and agrees with the main overall result: T1DM influences functional connectivity. Furthermore the results showed in this study benefit from an enhanced methodology consisting of: i) a larger cohort of patients [177]; ii) the use of PLI at source-level which together allow for more reliable estimates of functional interaction and at the same time improve interpretability revealing more precisely anatomical regions involved [177]; iii) the advantageous exploit of source-reconstructed MEG RSNs which allow to investigate directly the rich temporal dynamics of neuronal activity [178]; iv) the MST analysis permit to capture the connectivity of the core functional network.

Methodological differences might explain why Cooray et al. [184] did not find any diabetes-related reduction in PLI functional connectivity or why in [178] similar pattern of connectivity were found but in different RSNs. The former discrepancy in results can be influenced by many factors such as the different acquisition method, different epoch time lengths, different resting-protocol and no reconstructed signals at source level. Whereas the different RSNs compared to [178] may lay in the different modality of investigation, in fact the exact relationship between functional connectivity estimated through hemodynamic correlations, and the functional connectivity based on electrophysiological oscillatory activity (as in this study) is still unknown [200], [201].

It is worth to note that a pattern already described in other studies from different diseases such as Alzheimer, minimal hepatic encephalopathy, multiple sclerosis and Parkinson was found [202]-[205]. This pattern consists of an increased of functional connectivity in early stages of the disease followed by a failure in connectivity in late stages. Specifically this study pointed out an increased connectivity in $T1DM^-$ (early stage) compared to the healthy controls, followed by a decrease in connectivity in $T1DM^+$ (late stage) for DMN, ECN and MST sub-network. These results revealed that functional alterations are present even before the appearance of microvascular complications. Although the mechanism underlining this pattern of an early increase of functional connectivity followed by a decrease later stage is not yet understood, one hypothesis suggests that a loss of inhibition may be responsible for triggering the initial increase in connectivity and eventually lead to a breakdown of connectivity due to activity dependent degeneration [202].

Results only in lower alpha band are in line with previous studies reporting the role of this rhythm in regulating functional processing, within and between areas, both in healthy subjects and its deviation in pathology [206], [207]. Moreover the relation between the reduction of DMN alpha activity and the diminished cognitive performance in $T1DM^+$ reported in this study are supported by other works reflecting the importance of alpha activity in DMN [208] and the repercussions on cognitive performance due by its dysfunction [103].

Furthermore the impact of DMN alterations on cognition may be explained by the fact that DMN contains the strongest functional hubs [100] and these hubs are the more prone to failure [202].

Strong points of this study are: i) the investigation of functional connectivity within MEG resting-state networks, which is a worthwhile approach as demonstrated by recent studies [209]-[211] and it is also sensitive in detecting functional connectivity alterations related to cognition [137], [196]; ii) the application of an atlas-based beamforming solution to compute MEG RSNs functional connectivity [93], which improved comparability of this study with previous results obtained with different modalities [178]; iii) the MST analysis which allowed also to highlight differences in the 'functional core' of the brain network.

Conversely limitations of this study are: i) the interactions between RSNs were neglected although it is clear that high-order cognitive functions depend on the interactions between RSNs [212] therefore future studies are desirable; ii) this study could be complemented and expanded by a topological assessment of the MST properties [127], thereby providing insight into both local and global properties of the (core of) functional brain networks, and its relation with cognition.

In conclusion, our results confirmed that functional sub-networks (resting-state networks such as DMN, ECN and SMN) are affected by T1DM, and these changes are related to cognitive performance. In addition they showed that the functional core of the network (MST) is also influenced. Taken together these results indicate that functional connectivity and network topology may play a key role in T1DM-related cognitive dysfunction.

3.3 Amyotrophic Lateral Sclerosis (ALS)

3.3.1 Introduction

Amyotrophic Lateral Sclerosis (ALS) represents one of the most severe neurodegenerative diseases, which is known to affect upper and lower motor neurons. The progression of the disease is rapid, several areas of the nervous system can be involved and the survival time is about 3 years from the onset of symptoms. The genesis of ALS is still unknown and no treatment seems to be effective in contrasting the disease [213]. There is increasing agreement in considering ALS a multisystem disorder not only affecting the motor system but also other cognitive domains [214]. Additionally ALS manifest a pathogenically heterogeneous component [215]. Indeed such intrinsic variety is also reflected in clinical settings by a poor diagnostic power in the identification of ALS subtypes [215].

Advanced methods that allow investigating changes in brain organization have introduced exciting new opportunities for the study of multisystem disorder such as ALS [216]. Modern network science represents an important tool for understanding complex systems of interacting units as the human brain [3]. Brain network organization can be described and changes arising from neurological disorders can be elucidated[4].

Studies using Diffusion Tensor Imaging (DTI) and functional magnetic resonance (fMRI), have contributed in elucidating basic mechanisms related to ALS onset and progression. With the introduction of a network perspective, Verstraete et al. [217]have observed (combining DTI and fMRI) both structural degeneration and positive correlation between functional connectedness and disease progression of the motor network.

Recently, it has been reported [218] a disease spread over time along structural connections. In contrast with the classical theory of ALS affecting a fixed set of motor connections, this latter result represents one of the most interesting finding related to ALS mechanisms of action and degeneration.

Only a limited number of studies have investigated possible changes in whole-brain functional organization induced by ALS [219]-[221]. However, Schmidt et al. [222],have reported that the pathogenic process strongly affects both structural and functional network organization.

Since disease-related cortical whole-brain network organization is yet unknown, the present study aims to investigate changes in functional network topology related to time from onset of symptoms on a set of ALS patients. Network modifications were assessed by using the small-world (SW) index [13] and a set of measures extracted from the minimum spanning tree (MST). It has been shown [25], [26] that MST provides similar information as conventional graph measures, but is less sensitive to alterations in connection strength and link density. Therefore, the use of MST, avoiding the introduction of methodological limitations, represents an interesting solution to unbiased network analysis.

3.3.2 Methods

Eight patients, diagnosed with ALS according to the El Escorial criteria, who attended the ALS Centre of the AOU Cagliari (Italy), were included in the study. Informed consent was obtained and the study approved by the local Ethical Committee (NP/2013/438). Patient characteristics are summarized in **Errore. L'origine riferimento non è stata trovata.**.
Electroencephalographic (EEG) signals were recorded using a 64 channels system (Brain QuickSystem, Micromed, Italy) in resting-state condition. The reference electrode was placed in close approximation of the electrode POz. Signals were digitized with a sampling frequency of 256 Hz. For each subject at least four (mean $10{,}50 \pm 4{,}99$) eyes-closed artifac-free epochs of 2048 samples (8 s) were selected and band-pass filtered in the classical frequency bands: delta (0.5–4 Hz), theta (4–8 Hz), alpha (8–13 Hz) and beta (13–30 Hz).
The phase lag index (PLI) [1] was used to estimate functional connectivity (FC) between EEG channels. All pair-wise combinations of channels result in a matrix of 58 x 58 entries (excluding bad channels), each reporting the corresponding PLI value. From each weighted FC matrix, the SW index and measures from the MST were estimated. The SW index represents the ration between the normalized clustering coefficient (a measure of local efficiency) and the normalized path length (a measure of global efficiency). Furthermore, the diameter, the mean eccentricity, the normalized leaf number and the hierarchy were extracted from the MST. To examine the relationship between the network topology and time from onset of symptoms, the computed measures of the individual networks and the were correlated with the time from onset of symptoms.

3.3.3 Results

Significant associations between network organization and time were observed in the alpha band. A significant negative association was found between SW index and time (linear regression, R^2 = 0.62, p =0.019) (Figure 11 a). Significant positive associations were observed between MST diameter and time (linear regression, R^2 = 0.62, p = 0.021) (Figure 11 b) and between MST eccentricity and time (linear regression, R^2 = 0.58, p = 0.029) (Figure 11 c). A trend-level negative association was observed between MST leaf and time (Figure 11 d), while no association was found between MST hierarchy and time (Figure 11 e).

Patient	Age	Sex	Time from onset of symptoms (months)
1	63	F	16
2	50	M	30
3	64	M	23
4	79	F	12
5	64	M	5
6	77	M	22
7	70	F	13
8	73	F	20

Table 6 Patient characteristics

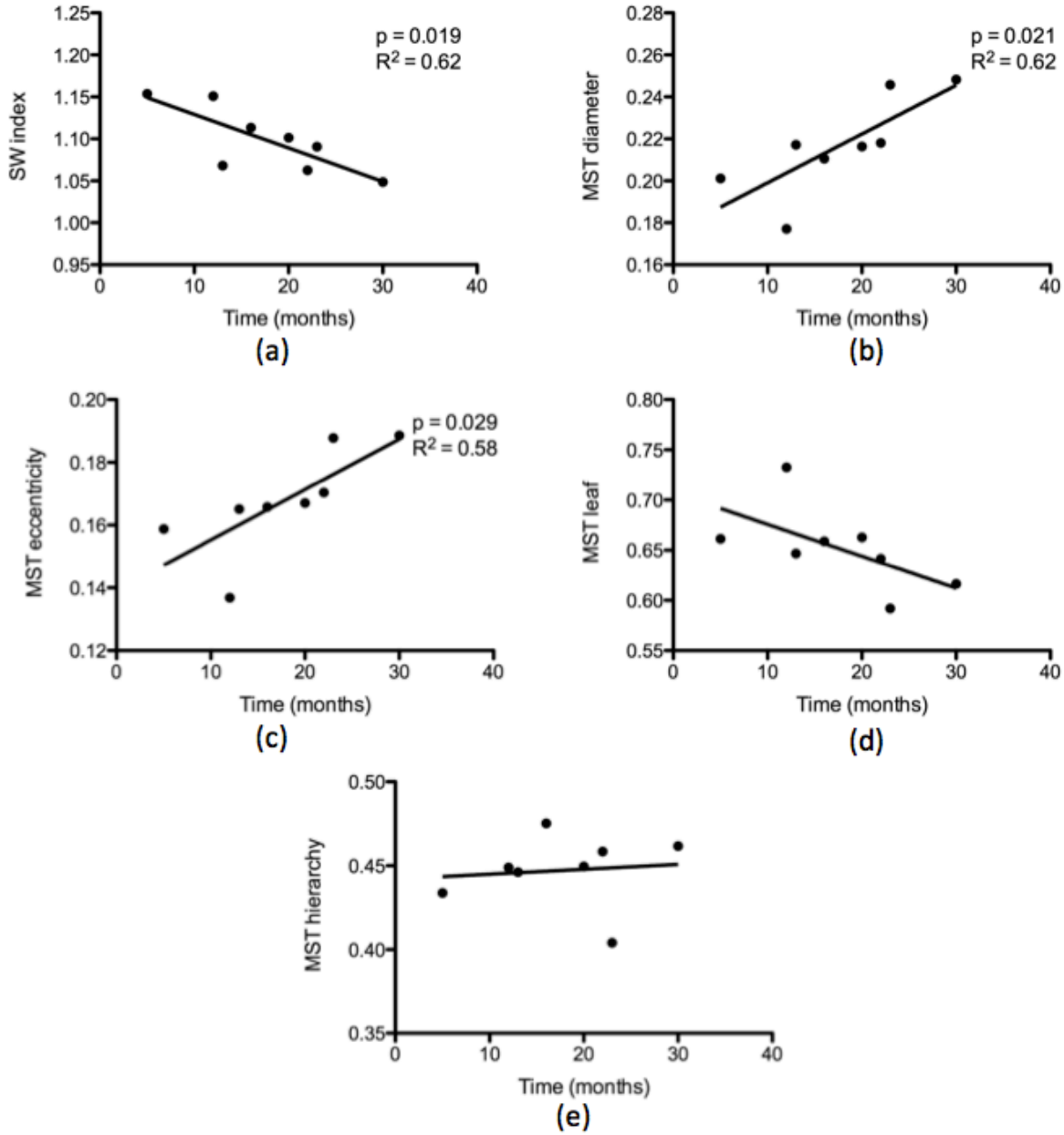

Figure 11 Relationship between disease duration and MST measures: from (a-e) linear regressions between the time from onset of symptoms and MST measures.

3.3.4 Discussion

The reported results suggest the existence of a strong relationship between disease duration and the ongoing disruption (i.e., less efficient and less integrated) of functional whole-brain network.

Other functional imaging studies have observed changes in functional connectivity related to ALS patients compared to healthy subjects [217], [219]-[221] as well as association with disease progression. However these results are often confusing: increased functional connectivity was described as well as decreased functional connectivity. Moreover typically these studies investigate independently functional connectivity in restricted sub-networks (such as Default Mode Network, Sensorymotor Network etc. etc.) and a proper and unbiased whole-brain network analysis focusing on the topology properties is missing. The current study is an attempt to fill this gap and gain an insight on the overall network dysfunction.

EEG alpha rhythm has been already related with ALS [223] and ALS duration [224]. Furthermore, since it has been reported that dynamics of alpha activity are determined by white matter architecture [225], our results support the hypothesis of a relationship between functional and structural brain network disruption in ALS patients.

Despite the interesting results our study suffers from some limitations principally due to the small number of subjects involved in the analysis and the absence of further observations from same patients over time (i.e., need for a longitudinal study). Another limitation is given by the lack of a matched control group of healthy subject in order to compare and assess the reliability of the results.

In conclusion, although this study is preliminary, it shows an important association between ALS disease duration and ongoing disruption of functional whole-brain network as measured by methods (i.e., PLI and MST) robust to both scalp EEG problems and network comparison bias. As for other neurodegenerative disorders, this analysis could be useful in evaluating and monitoring the progression of the disease. Furthermore it can help in the definition of a system-level signature based on network metrics, which can have diagnostic relevance.

4 Summary and General Conclusion

4.1 Summary

The experimental studies of this thesis aim to gain more insight into brain functioning and its impairments induced by the arising of pathology using functional connectivity and brain network analysis. Two neurological diseases, such as epilepsy and amyotrophic lateral sclerosis (ALS), and a third one, type 1 diabetes mellitus (T1DM) were studied. Although T1DM is not a proper neurological disease recently the potential effect of dysglycaemia on the cognitive performance and central nervous system integrity has been investigated [175]-[179].

In Chapter 3.1 it has been discussed how clinical benefit in epileptic patients responding to VNS therapy is related to functional network re-organization in theta band. Results agreed with the formulated hypothesis that VNS therapy affects functional brain network organization toward a more efficient (i.e. more integrated) architecture. The MST was used to characterize the network topology and the observed decrease of MST diameter and eccentricity in VNS responder patients suggested the shift toward a more integrated architecture. These findings are in line with the theory that includes epilepsy in the framework of network disorders: an aberrant topology of structural and functional networks promote seizure occurrence [133], [154], [155].

In chapter 3.3 the existence of a significant correlation (all *p-values*<0.05) between ALS duration and the disruption of the whole functional brain network was reported. Traditional network measures such as *small-world-ness* index, and MST measures were used to assess the topology of ALS function brain network. The *small-word-ness* index, which reflects the efficiency of a network topology, showed a negative correlation with the disease duration. However MST diameter and eccentricity were positively correlated with the disease duration. Together these two results suggested a shift toward a less efficient and less integrated network topology in respect to the time from onset of symptoms.

Integrity of resting-state functional brain networks (RSNs) is important for proper cognitive functioning. In type 1 diabetes mellitus (T1DM) cognitive decrements are commonly observed, possibly due to alterations in RSNs, which may vary according to microvascular complication status. In chapter 3.2 it was tested the hypothesis that functional connectivity in RSNs differs according to clinical status and correlates with cognition in T1DM patients, using an unbiased approach with high spatio-temporal resolution functional network. Patients with microvascular complication ($T1DM^{+}$) showed a reduction of functional connectivity both for MEG resting-state networks (RSNs) and minimum spanning tree analysis when compared to type 1 diabetes patients without microvascular complications (T1DM-), as well as compared to healthy subjects. Significant differences (all *p-values*<0.05) in terms of RSN functional connectivity between the three groups were observed in the lower alpha band, in the default-mode (DMN), executive control (ECN) and sensorimotor (SMN) RSNs, as well as within the MST network. T1DM patients with microvascular complications showed the weakest functional connectivity in these networks relative to the other groups. Furthermore for DMN, functional connectivity was higher in patients without microangiopathy relative to controls (all *p-values*<0.05). General cognitive performance for both patient groups was worse compared with healthy controls. Lower DMN alpha band functional connectivity correlated with poorer general cognitive ability in patients with microvascular complications.
In conclusion altered RSN functional connectivity and MST was found in T1DM patients depending on clinical status. Lower DMN functional connectivity was related to poorer

cognitive functioning. Taken together these results indicate that functional connectivity and network topology may play a key role in T1DM-related cognitive dysfunction.

4.2 General Conclusion

In recent years, it has become clear that the brain can be seen as a complex structural and functional network. Cognitive functioning strongly depends on the organization of functional brain networks [4], [76], [120] [4], [76], [120], [226]. During the last fifteen years EEG/MEG resting-state functional connectivity and functional brain networks studies attempted to characterize normal brain organization [7]as well as deviation from it due to brain diseases[3], [4]. Despite the impact on the understanding of brain functioning that these tools provided there are still methodological hurdles that might have compromised the results [17]-[19].

A key choice in the pipeline of analysis is the selection of a functional connectivity estimator to evaluate functional interactions between brain regions. Different coupling measures can be used [20]. The most important problem to tackle during this choice is the common source problem, which reflect the fact the EEG/MEG scalp recordings pick up signals from the same underlying sources, therefore functional connectivity measures will display spurious results just because both reflect the same activity not because there is a real interaction. In this thesis the phase lag index (PLI) [1] was used as a functional connectivity measure. PLI is relatively insensitive to common source effect because it discards zero-phase lag synchronizations (likely to be affected by common source). A disadvantage of the PLI might be that real interaction between nearby brain areas (at zero-phase lag) could be discarded. However in this thesis the safer approach to avoid zero-phase lag synchronization was preferred at the cost to possibly underestimated synchronization between nearby brain areas.

In functional brain network construction, deciding the edges to include in the network is essential. Van Wijk and others [23] showed how this choice can affect the estimation of network topology and how the comparison between networks can be biased by this choice. Many network studies have already been performed in many diseases and contradictory results [133], [134] were obtained because of the lack of a proper methodology for network comparison. In this thesis the minimum spanning tree (MST) approach was used as a solution to this problem. MST can be considered as the 'core' sub-network consisting of the most important connections. The results reported in this thesis showed how the MST captures relevant changes in network topology and along with previous MST studies [26], [137]-[139] supported the use of MST as a promising approach for network comparison and network characterization.

This thesis confirms that alterations in functional connectivity and functional brain networks in disease may be used as potential biomarkers for more objective diagnosis and for the choice of effective treatment options. Specifically in epileptic patients implanted with VNS these measures can be used as a marker in monitoring the efficacy of the treatment; in amyotrophic lateral sclerosis the relation between disease duration and whole brain network disruption suggests diagnostic relevance of network measures in evaluating and monitoring the disease; and finally in type 1 diabetic mellitus patients functional connectivity measures are complementary to cognitive tests and may help to monitor the effect of T1DM on brain functions.

5 Appendixes

5.1 Appendix A

Table 7 Cognitive domains

Cognitive domain	Neuropsychological test
Memory	Rey auditory verbal learning test WAIS-III-R digit span forward and backward WAIS-III-R symbol substitution incidental learning test
Information processing speed	WAIS-III-R symbol substitution test Stroop color-word test parts 1 and 2 Concept shifting task parts A and B Simple auditory and visual reaction time tests Computerized visual searching task
Executive functions	Stroop color-word test part 3, correct for time on part 1 and 2 Concept shifting task part C, correct for time on part A and B D2-test total errors Wisconsin cart sorting test Category word fluency task
Attention	D2-test range with total correct answers and total span
Motor Speed	Tapping test Concept shifting task part
Psycomotor	Letter Digit Modalities Test

Table 8 Resting-state networks.

Resting-state network	Corresponding AAL atlas ROIs (Rosazza and Minati, 2011)	Corresponding AAL atlas ROIs (1 ROI overlap)
Default mode network	Precuneus, posterior cingulate gyrus, inferior parietal gyrus, medial prefrontal gyrus	Precuneus, posterior cingulate gyrus, anterior cingulate gyrus*, inferior parietal gyrus, medial prefrontal gyrus
Executive control	Medial frontal cortex, superior frontal gyrus, anterior cingulate gyrus	Medial frontal cortex, superior frontal gyrus, anterior cingulate gyrus
Frontoparietal (left/right)	Inferior frontal gyrus pars triangularis, inferior frontal gyrus pars opercularis*, medial frontal gyrus, precuneus*, inferior parietal gyrus, angular gyrus	inferior frontal gyrus pars triangularis, medial frontal gyrus, inferior parietal gyrus, superior parietal gyrus*, angular gyrus

Definitions of the analysed RSNs. Data that were presented as main results in the paper were based on a slight modification of the ROI definition of Rosazza and Minati. This definition was proposed by Tewarie [196] and others, it prevents overlap of connections between RSNs (right column). Our data were analysed using Tewarie's definition. Differences between both definitions were marked with *.

5.2 Appendix B

Papers published during the PhD:

Demuru, M., Fara, F., & Fraschini, M. (2013). Brain network analysis of EEG functional connectivity during imagery hand movements. *Journal of Integrative Neuroscience*, *12*(4), 441–447. doi:10.1142/S021963521350026X

Demuru, M., van Duinkerken, E., Fraschini, M., Marrosu, F., Snoek, F. J., Barkhof, F., et al. (2014). Changes in MEG resting-state networks are related to cognitive decline in type 1 diabetes mellitus patients. *NeuroImage. Clinical*, *5*, 69–76. doi:10.1016/j.nicl.2014.06.001

Fraschini, M., Demuru, M., Puligheddu, M., Floridia, S., Polizzi, L., Maleci, A., et al. (2014). The re-organization of functional brain networks in pharmaco-resistant epileptic patients who respond to VNS. *Neuroscience Letters*, *580*, 153–157. doi:10.1016/j.neulet.2014.08.010

Fraschini, M., Hillebrand, A., Demuru, M., Didaci, L., & Marcialis, G. L. (2015). An EEG-Based Biometric System Using Eigenvector Centrality in Resting State Brain Networks. *Signal Processing Letters, IEEE*, *22*(6), 666–670. doi:10.1109/LSP.2014.2367091

Fraschini, M., Puligheddu, M., Demuru, M., Polizzi, L., Maleci, A., Tamburini, G., et al. (2013). VNS induced desynchronization in gamma bands correlates with positive clinical outcome in temporal lobe pharmacoresistant epilepsy. *Neuroscience Letters*, *536*, 14–18. doi:10.1016/j.neulet.2012.12.044

6 Bibliography

[1] C. J. Stam, G. Nolte, and A. Daffertshofer, “Phase lag index: Assessment of functional connectivity from multi channel EEG and MEG with diminished bias from common sources,” *Hum Brain Mapp*, vol. 28, no. 11, pp. 1178–1193, 2007.
[2] J. B. Kruskal, “On the Shortest Spanning Subtree of a Graph and the Traveling Salesman Problem,” *Proceedings of the American Mathematical Society*, vol. 7, no. 1, pp. 48–58, Feb. 1956.
[3] C. J. Stam, “Modern network science of neurological disorders.,” *Nat. Rev. Neurosci.*, Sep. 2014.
[4] C. J. Stam and E. C. W. van Straaten, “The organization of physiological brain networks.,” *Clin Neurophysiol*, vol. 123, no. 6, pp. 1067–1087, Jun. 2012.
[5] P. Fries, “A mechanism for cognitive dynamics: neuronal communication through neuronal coherence.,” *Trends Cogn. Sci. (Regul. Ed.)*, vol. 9, no. 10, pp. 474–480, Oct. 2005.
[6] K. J. Friston, “Brain function, nonlinear coupling, and neuronal transients.,” *Neuroscientist*, vol. 7, no. 5, pp. 406–418, Oct. 2001.
[7] K. J. Friston, “Functional and effective connectivity: a review.,” *Brain Connect*, vol. 1, no. 1, pp. 13–36, 2011.
[8] N. F. Dronkers, O. Plaisant, M. T. Iba-Zizen, and E. A. Cabanis, “Paul Broca's historic cases: high resolution MR imaging of the brains of Leborgne and Lelong.,” *Brain*, vol. 130, no. 5, pp. 1432–1441, May 2007.
[9] A. Flinker, A. Korzeniewska, A. Y. Shestyuk, P. J. Franaszczuk, N. F. Dronkers, R. T. Knight, and N. E. Crone, “Redefining the role of Broca's area in speech.,” *Proc. Natl. Acad. Sci. U.S.A.*, vol. 112, no. 9, pp. 2871–2875, Mar. 2015.
[10] S. Milgram, “The small world problem,” *Psychology today*, 1967.
[11] N. Biggs, E. K. Lloyd, and R. J. Wilson, *Graph Theory, 1736-1936*. Oxford University Press, 1976.
[12] P. Erdos and A. Renyi, “On random graphs I,” *Publ Math Debrecen*, vol. 6, pp. 290–297, 1959.
[13] D. J. Watts and S. H. Strogatz, “Collective dynamics of ‘small-world’ networks.,” *Nature*, vol. 393, no. 6684, pp. 440–442, Jun. 1998.
[14] A. Barabasi and R. Albert, “Emergence of scaling in random networks,” *Science*, vol. 286, no. 5439, pp. 509–512, Oct. 1999.
[15] M. Girvan and M. E. J. Newman, “Community structure in social and biological networks,” *PNAS*, vol. 99, no. 12, pp. 7821–7826, Jun. 2002.
[16] A. Barrat, M. Barthlemy, and A. Vespignani, *Dynamical Processes on Complex Networks*, 1st ed. New York, NY, USA: Cambridge University Press, 2008.
[17] E. van Diessen, T. Numan, E. Van Dellen, A. W. van der Kooi, M. Boersma, D. Hofman, R. van Lutterveld, B. W. van Dijk, E. C. W. van Straaten, A. Hillebrand, and C. J. Stam, “Opportunities and methodological challenges in EEG and MEG resting state functional brain network research.,” *Clin Neurophysiol*, vol. 0, no. 0, Nov. 2014.
[18] F. De Vico Fallani, J. Richiardi, M. Chavez, and S. Achard, “Graph analysis of functional brain networks: practical issues in translational neuroscience.,” *Philos. Trans. R. Soc. Lond., B, Biol. Sci.*, vol. 369, no. 1653, Oct. 2014.
[19] A. Fornito, A. Zalesky, and M. Breakspear, “Graph analysis of the human connectome: promise, progress, and pitfalls.,” *Neuroimage*, vol. 80, pp. 426–444, Oct. 2013.
[20] E. Pereda, R. Q. Quiroga, and J. Bhattacharya, “Nonlinear multivariate analysis of neurophysiological signals,” *Progress in Neurobiology*, vol. 77, no. 1, pp. 1–37, Sep. 2005.
[21] S. P. van den Broek, F. Reinders, M. Donderwinkel, and M. J. Peters, “Volume conduction effects in EEG and MEG.,” *Electroencephalogr Clin Neurophysiol*, vol. 106,

no. 6, pp. 522–534, Jun. 1998.
[22] J. Sarvas, “Basic mathematical and electromagnetic concepts of the biomagnetic inverse problem.,” *Phys Med Biol*, vol. 32, no. 1, pp. 11–22, Jan. 1987.
[23] B. C. M. van Wijk, C. J. Stam, and A. Daffertshofer, “Comparing brain networks of different size and connectivity density using graph theory.,” *PLoS ONE*, vol. 5, no. 10, p. e13701, 2010.
[24] M. Rubinov and O. Sporns, “Complex network measures of brain connectivity: Uses and interpretations,” *Neuroimage*, vol. 52, no. 3, pp. 1059–1069, Sep. 2010.
[25] P. Tewarie, E. Van Dellen, A. Hillebrand, and C. J. Stam, “The minimum spanning tree: An unbiased method for brain network analysis,” *Neuroimage*, vol. 104, no. C, pp. 1–12, 2014.
[26] C. J. Stam, P. Tewarie, E. Van Dellen, E. C. W. van Straaten, A. Hillebrand, and P. Van Mieghem, “The trees and the forest: Characterization of complex brain networks with minimum spanning trees.,” vol. 92, no. 3, pp. 129–138, Jun. 2014.
[27] D. L. Schomer and F. L. da Silva, *Niedermeyer's Electroencephalography*. Lippincott Williams & Wilkins, 2012.
[28] S. Baillet, J. C. Mosher, and R. M. Leahy, “Electromagnetic brain mapping,” *Signal Processing Magazine, IEEE*, vol. 18, no. 6, pp. 14–30, 2001.
[29] S. Baillet, “Basics of MEG,” *canada-meg-consortium.org*, 2010. [Online]. Available: http://www.canada-meg-consortium.org/EN/MegIntro. [Accessed: 09-Mar-2015].
[30] D. Lehmann and W. Skrandies, “Spatial analysis of evoked potentials in man--a review.,” *Progress in Neurobiology*, vol. 23, no. 3, pp. 227–250, 1984.
[31] G. Pfurtscheller and F. H. Lopes da Silva, “Event-related EEG/MEG synchronization and desynchronization: basic principles,” *Clinical Neurophysiology*, vol. 110, no. 11, pp. 1842–1857, Nov. 1999.
[32] D. Cohen, “Magnetoencephalography: evidence of magnetic fields produced by alpha-rhythm currents.,” *Science*, vol. 161, no. 3843, pp. 784–786, Aug. 1968.
[33] M. Hämäläinen, R. Hari, R. J. Ilmoniemi, and J. Knuutila, “Magnetoencephalography—theory, instrumentation, and applications to noninvasive studies of the working human brain,” *Reviews of modern …*, vol. 65, no. 2, pp. 413–497, 1993.
[34] A. Hillebrand and G. R. Barnes, “A quantitative assessment of the sensitivity of whole-head MEG to activity in the adult human cortex.,” *Neuroimage*, vol. 16, no. 3, pp. 638–650, Jul. 2002.
[35] G. Buzsaki, *Rhythms of the Brain*. Oxford University Press, 2006.
[36] G. Buzsaki and B. O. Watson, “Brain rhythms and neural syntax: implications for efficient coding of cognitive content and neuropsychiatric disease.,” *Dialogues Clin Neurosci*, vol. 14, no. 4, pp. 345–367, Dec. 2012.
[37] E. Başar, C. Başar-Eroglu, S. Karakaş, and M. Schürmann, “Gamma, alpha, delta, and theta oscillations govern cognitive processes.,” *International Journal of Psychophysiology*, vol. 39, no. 2, pp. 241–248, Jan. 2001.
[38] W. Walter, “THE LOCATION OF CEREBRAL TUMOURS BY ELECTRO-ENCEPHALOGRAPHY,” *Lancet*, vol. 228, no. 5893, pp. 305–308, Dec. 1935.
[39] E. N. Brown, R. Lydic, and N. D. Schiff, “General anesthesia, sleep, and coma.,” *N. Engl. J. Med.*, vol. 363, no. 27, pp. 2638–2650, Dec. 2010.
[40] K. Wang, M. L. Steyn-Ross, D. A. Steyn-Ross, M. T. Wilson, and J. W. Sleigh, “EEG slow-wave coherence changes in propofol-induced general anesthesia: experiment and theory.,” *Front Syst Neurosci*, vol. 8, p. 215, 2014.
[41] M. Steriade and I. Timofeev, “Neuronal plasticity in thalamocortical networks during sleep and waking oscillations.,” *Neuron*, vol. 37, no. 4, pp. 563–576, Feb. 2003.
[42] G. Buzsaki, “Theta oscillations in the hippocampus.,” *Neuron*, vol. 33, no. 3, pp. 325–

340, Jan. 2002.
[43] C. H. Vanderwolf, “Hippocampal electrical activity and voluntary movement in the rat.,” *Electroencephalogr Clin Neurophysiol*, vol. 26, no. 4, pp. 407–418, Apr. 1969.
[44] M. E. Hasselmo and C. E. Stern, “Theta rhythm and the encoding and retrieval of space and time.,” *Neuroimage*, vol. 85, pp. 656–666, Jan. 2014.
[45] D. E. Arnolds, F. H. Lopes da Silva, J. W. Aitink, A. Kamp, and P. Boeijinga, “The spectral properties of hippocampal EEG related to behaviour in man.,” *Electroencephalogr Clin Neurophysiol*, vol. 50, no. 3, pp. 324–328, Nov. 1980.
[46] M. J. Kahana, R. Sekuler, J. B. Caplan, M. Kirschen, and J. R. Madsen, “Human theta oscillations exhibit task dependence during virtual maze navigation.,” *Nature*, vol. 399, no. 6738, pp. 781–784, Jun. 1999.
[47] A. D. Ekstrom, J. B. Caplan, E. Ho, K. Shattuck, I. Fried, and M. J. Kahana, “Human hippocampal theta activity during virtual navigation.,” *Hippocampus*, vol. 15, no. 7, pp. 881–889, 2005.
[48] C. D. Tesche and J. Karhu, “Theta oscillations index human hippocampal activation during a working memory task.,” *PNAS*, vol. 97, no. 2, pp. 919–924, Jan. 2000.
[49] R. Kaplan, C. F. Doeller, G. R. Barnes, V. Litvak, E. Düzel, P. A. Bandettini, and N. Burgess, “Movement-related theta rhythm in humans: coordinating self-directed hippocampal learning.,” *PLoS Biol.*, vol. 10, no. 2, p. e1001267, 2012.
[50] J. Snider, M. Plank, G. Lynch, E. Halgren, and H. Poizner, “Human cortical θ during free exploration encodes space and predicts subsequent memory.,” *J. Neurosci.*, vol. 33, no. 38, pp. 15056–15068, Sep. 2013.
[51] G. Pfurtscheller, A. Stancák Jr., and C. Neuper, “Event-related synchronization (ERS) in the alpha band — an electrophysiological correlate of cortical idling: A review,” *International Journal of Psychophysiology*, vol. 24, no. 1, pp. 39–46, Nov. 1996.
[52] W. Klimesch, “α-band oscillations, attention, and controlled access to stored information.,” *Trends Cogn. Sci. (Regul. Ed.)*, vol. 16, no. 12, pp. 606–617, Dec. 2012.
[53] O. Jensen, J. Gelfand, J. Kounios, and J. E. Lisman, “Oscillations in the alpha band (9-12 Hz) increase with memory load during retention in a short-term memory task.,” *Cereb. Cortex*, vol. 12, no. 8, pp. 877–882, Aug. 2002.
[54] G. Thut, A. Nietzel, S. A. Brandt, and A. Pascual-Leone, “α-Band Electroencephalographic Activity over Occipital Cortex Indexes Visuospatial Attention Bias and Predicts Visual Target Detection,” *J. Neurosci.*, vol. 26, no. 37, pp. 9494–9502, Sep. 2006.
[55] E. Başar, “A review of alpha activity in integrative brain function: fundamental physiology, sensory coding, cognition and pathology.,” *Int J Psychophysiol*, vol. 86, no. 1, pp. 1–24, Oct. 2012.
[56] F. H. L. da Silva, A. Hoeks, H. Smits, and L. H. Zetterberg, “Model of brain rhythmic activity,” *Kybernetik*, vol. 15, no. 1, pp. 27–37, 1974.
[57] F. H. Lopes da Silva, J. P. Pijn, D. Velis, and P. C. G. Nijssen, “Alpha rhythms: noise, dynamics and models,” *International Journal of Psychophysiology*, vol. 26, no. 1, pp. 237–249, Jun. 1997.
[58] C. J. Stam, J. P. Pijn, P. Suffczynski, and F. H. Lopes da Silva, “Dynamics of the human alpha rhythm: evidence for non-linearity?,” *Clin Neurophysiol*, vol. 110, no. 10, pp. 1801–1813, Oct. 1999.
[59] O. David and K. J. Friston, “A neural mass model for MEG/EEG: coupling and neuronal dynamics.,” *Neuroimage*, vol. 20, no. 3, pp. 1743–1755, Nov. 2003.
[60] A. K. Engel and P. Fries, “Beta-band oscillations--signalling the status quo?,” *Curr. Opin. Neurobiol.*, vol. 20, no. 2, pp. 156–165, Apr. 2010.
[61] M. Feurra, G. Bianco, E. Santarnecchi, M. Del Testa, A. Rossi, and S. Rossi, “Frequency-

dependent tuning of the human motor system induced by transcranial oscillatory potentials.," *J. Neurosci.*, vol. 31, no. 34, pp. 12165–12170, Aug. 2011.
[62] A. Pogosyan, L. D. Gaynor, A. Eusebio, and P. Brown, "Boosting cortical activity at Beta-band frequencies slows movement in humans.," *Curr. Biol.*, vol. 19, no. 19, pp. 1637–1641, Oct. 2009.
[63] N. J. Davis, S. P. Tomlinson, and H. M. Morgan, "The role of β-frequency neural oscillations in motor control.," *J. Neurosci.*, vol. 32, no. 2, pp. 403–404, Jan. 2012.
[64] A. A. Kühn, F. Kempf, C. Brücke, L. Gaynor Doyle, I. Martinez-Torres, A. Pogosyan, T. Trottenberg, A. Kupsch, G.-H. Schneider, M. I. Hariz, W. Vandenberghe, B. Nuttin, and P. Brown, "High-frequency stimulation of the subthalamic nucleus suppresses oscillatory beta activity in patients with Parkinson's disease in parallel with improvement in motor performance.," *J. Neurosci.*, vol. 28, no. 24, pp. 6165–6173, Jun. 2008.
[65] O. Bai, P. Lin, S. Vorbach, M. K. Floeter, N. Hattori, and M. Hallett, "A high performance sensorimotor beta rhythm-based brain-computer interface associated with human natural motor behavior.," *J Neural Eng*, vol. 5, no. 1, pp. 24–35, Mar. 2008.
[66] S. Waldert, H. Preissl, E. Demandt, C. Braun, N. Birbaumer, A. Aertsen, and C. Mehring, "Hand movement direction decoded from MEG and EEG.," *J. Neurosci.*, vol. 28, no. 4, pp. 1000–1008, Jan. 2008.
[67] O. Bertrand and C. Tallon-Baudry, "Oscillatory gamma activity in humans: a possible role for object representation," *International Journal of Psychophysiology*, vol. 38, no. 3, pp. 211–223, Dec. 2000.
[68] D. Senkowski, D. Talsma, C. S. Herrmann, and M. G. Woldorff, "Multisensory processing and oscillatory gamma responses: effects of spatial selective attention.," *Exp Brain Res*, vol. 166, no. 3, pp. 411–426, Oct. 2005.
[69] O. Jensen, J. Kaiser, and J.-P. Lachaux, "Human gamma-frequency oscillations associated with attention and memory.," *Trends Neurosci.*, vol. 30, no. 7, pp. 317–324, Jul. 2007.
[70] C. S. Herrmann, M. H. J. Munk, and A. K. Engel, "Cognitive functions of gamma-band activity: memory match and utilization.," *Trends Cogn. Sci. (Regul. Ed.)*, vol. 8, no. 8, pp. 347–355, Aug. 2004.
[71] E. Başar, "A review of gamma oscillations in healthy subjects and in cognitive impairment.," vol. 90, no. 2, pp. 99–117, Nov. 2013.
[72] O. David, J. M. Kilner, and K. J. Friston, "Mechanisms of evoked and induced responses in MEG/EEG.," *Neuroimage*, vol. 31, no. 4, pp. 1580–1591, Jul. 2006.
[73] O. Jensen and L. L. Colgin, "Cross-frequency coupling between neuronal oscillations.," *Trends Cogn. Sci. (Regul. Ed.)*, vol. 11, no. 7, pp. 267–269, Jul. 2007.
[74] R. T. Canolty and R. T. Knight, "The functional role of cross-frequency coupling.," *Trends Cogn. Sci. (Regul. Ed.)*, vol. 14, no. 11, pp. 506–515, Nov. 2010.
[75] V. Jirsa and V. Müller, "Cross-frequency coupling in real and virtual brain networks.," *Front. Comput. Neurosci.*, vol. 7, p. 78, 2013.
[76] O. Sporns, "Structure and function of complex brain networks.," *Dialogues Clin Neurosci*, vol. 15, no. 3, pp. 247–262, Sep. 2013.
[77] O. Sporns, "The human connectome: a complex network.," *Ann. N. Y. Acad. Sci.*, vol. 1224, no. 1, pp. 109–125, Apr. 2011.
[78] P. Moses and J. Stiles, "The lesion methodology: contrasting views from adult and child studies.," *Dev Psychobiol*, vol. 40, no. 3, pp. 266–277, Apr. 2002.
[79] P. Broca, "Remarque Sur Le Siege De La Faculté Du Language Articulé, Suivie D'une Observation D'aphémie (Perte De La Parole)," *{Bulletin de la soci\\"{e}t\\"{e}*

anatomique de Paris}, Vol. 36 (1861), pp. 330-356, vol. 36, pp. 330–356, 1861.
[80] C. Wernicke, "THE APHASIC SYMPTOM-COMPLEX: A Psychological Study on an Anatomical Basis*," *Arch Neurol*, vol. 22, no. 3, pp. 280–282, Mar. 1970.
[81] R. W. Sperry and M. S. Gazzaniga, "Interhemispheric relationships: the neocortical commissures; syndromes of hemisphere disconnection," Handbook of clinical …, 1969.
[82] R. Adolphs, D. Tranel, H. Damasio, and A. R. Damasio, "Fear and the human amygdala," *J. Neurosci.*, vol. 15, no. 9, pp. 5879–5891, Sep. 1995.
[83] M. X. Cohen, "It's about Time.," *Front Hum Neurosci*, vol. 5, p. 2, 2011.
[84] M. G. Rosenblum, A. S. PIKOVSKY, and J. Kurths, "Synchronization approach to analysis of biological systems," *Fluct. Noise Lett.*, vol. 4, no. 1, pp. L53–L62, Mar. 2004.
[85] C. J. Stam, "Nonlinear dynamical analysis of EEG and MEG: review of an emerging field.," *Clin Neurophysiol*, vol. 116, no. 10, pp. 2266–2301, Oct. 2005.
[86] N. Rulkov, M. Sushchik, L. Tsimring, and H. Abarbanel, "Generalized synchronization of chaos in directionally coupled chaotic systems.," *Phys Rev E Stat Phys Plasmas Fluids Relat Interdiscip Topics*, vol. 51, no. 2, pp. 980–994, Feb. 1995.
[87] C. J. Stam and B. W. van Dijk, "Synchronization likelihood: an unbiased measure of generalized synchronization in multivariate data sets," *Physica D: Nonlinear Phenomena*, vol. 163, no. 3, pp. 236–251, Mar. 2002.
[88] M. G. Rosenblum, A. Pikovsky, and J. Kurths, "Phase Synchronization of Chaotic Oscillators," *Phys. Rev. Lett.*, vol. 76, no. 11, pp. 1804–1807, Mar. 1996.
[89] A. Tarantola, *Inverse Problem Theory and Methods for Model Parameter Estimation*. SIAM, 2005.
[90] H. von Helmholtz, *Uber einige gesetzeder verbeitung elektrischer strome in koperlichen leitern mit anwendung auf die theorischelektrischen versuche*. Ann. Physik. u Chem, 1853.
[91] M. I. Hadamard, *Hadamard: On problems in partial derivatives, and... - Google Scholar*. Bull. Princeton Univ, 1902.
[92] A. Hillebrand and G. R. Barnes, "Beamformer analysis of MEG data.," *Int. Rev. Neurobiol.*, vol. 68, pp. 149–171, 2005.
[93] A. Hillebrand, G. R. Barnes, J. L. Bosboom, H. W. Berendse, and C. J. Stam, "Frequency-dependent functional connectivity within resting-state networks: an atlas-based MEG beamformer solution.," *Neuroimage*, vol. 59, no. 4, pp. 3909–3921, Feb. 2012.
[94] G. Deco, V. K. Jirsa, and A. R. McIntosh, "Emerging concepts for the dynamical organization of resting-state activity in the brain.," *Nat. Rev. Neurosci.*, vol. 12, no. 1, pp. 43–56, Jan. 2011.
[95] G. Deco, V. K. Jirsa, and A. R. McIntosh, "Resting brains never rest: computational insights into potential cognitive architectures.," *Trends Neurosci.*, vol. 36, no. 5, pp. 268–274, May 2013.
[96] M. D. Greicius, B. Krasnow, A. L. Reiss, and V. Menon, "Functional connectivity in the resting brain: a network analysis of the default mode hypothesis.," *PNAS*, vol. 100, no. 1, pp. 253–258, Jan. 2003.
[97] M. E. Raichle, A. M. MacLeod, A. Z. Snyder, W. J. Powers, D. A. Gusnard, and G. L. Shulman, "A default mode of brain function.," *PNAS*, vol. 98, no. 2, pp. 676–682, Jan. 2001.
[98] B. Biswal, F. Z. Yetkin, V. M. Haughton, and J. S. Hyde, "Functional connectivity in the motor cortex of resting human brain using echo-planar MRI.," *Magn Reson Med*, vol. 34, no. 4, pp. 537–541, Oct. 1995.
[99] M. E. Raichle, "A paradigm shift in functional brain imaging.," *J. Neurosci.*, vol. 29, no.

41, pp. 12729–12734, Oct. 2009.
[100] J. S. Damoiseaux, S. A. R. B. Rombouts, F. Barkhof, P. Scheltens, C. J. Stam, S. M. Smith, and C. F. Beckmann, "Consistent resting-state networks across healthy subjects.," *PNAS*, vol. 103, no. 37, pp. 13848–13853, Sep. 2006.
[101] M. D. Greicius, K. Supekar, V. Menon, and R. F. Dougherty, "Resting-state functional connectivity reflects structural connectivity in the default mode network.," *Cereb. Cortex*, vol. 19, no. 1, pp. 72–78, Jan. 2009.
[102] M. P. van den Heuvel and H. E. Hulshoff Pol, "Exploring the brain network: a review on resting-state fMRI functional connectivity.," *Eur Neuropsychopharmacol*, vol. 20, no. 8, pp. 519–534, Aug. 2010.
[103] S. J. Broyd, C. Demanuele, S. Debener, S. K. Helps, C. J. James, and E. J. S. Sonuga-Barke, "Default-mode brain dysfunction in mental disorders: A systematic review," *Neuroscience & Biobehavioral Reviews*, vol. 33, no. 3, pp. 279–296, Mar. 2009.
[104] E. Van Dellen, P. C. de Witt Hamer, L. Douw, M. Klein, J. J. Heimans, C. J. Stam, J. C. Reijneveld, and A. Hillebrand, "Connectivity in MEG resting-state networks increases after resective surgery for low-grade glioma and correlates with improved cognitive performance," *Neuroimage Clin*, vol. 2, pp. 1–7, Mar. 2010.
[105] C. Rosazza and L. Minati, "Resting-state brain networks: literature review and clinical applications," *Neurol Sci*, vol. 32, no. 5, pp. 773–785, Jun. 2011.
[106] S. Boccaletti, V. Latora, Y. Moreno, M. Chavez, and D. Hwang, "Complex networks: Structure and dynamics," *Physics Reports*, vol. 424, no. 4, pp. 175–308, Feb. 2006.
[107] R. Kötter, "Online retrieval, processing, and visualization of primate connectivity data from the CoCoMac database.," *Neuroinformatics*, vol. 2, no. 2, pp. 127–144, 2004.
[108] P. Hagmann, L. Cammoun, X. Gigandet, S. Gerhard, P. E. Grant, V. Wedeen, R. Meuli, J.-P. Thiran, C. J. Honey, and O. Sporns, "MR connectomics: Principles and challenges.," *J. Neurosci. Methods*, vol. 194, no. 1, pp. 34–45, Dec. 2010.
[109] C. Lewis, C. Bosman, and P. Fries, "Recording of brain activity across spatial scales.," *Curr. Opin. Neurobiol.*, vol. 32, pp. 68–77, Dec. 2014.
[110] E. Bullmore and O. Sporns, "Complex brain networks: graph theoretical analysis of structural and functional systems.," *Nat. Rev. Neurosci.*, vol. 10, no. 3, pp. 186–198, Mar. 2009.
[111] R. C. Craddock, S. Jbabdi, C.-G. Yan, J. T. Vogelstein, F. X. Castellanos, A. Di Martino, C. Kelly, K. Heberlein, S. Colcombe, and M. P. Milham, "Imaging human connectomes at the macroscale," *Nat Meth*, vol. 10, no. 6, pp. 524–539, May 2013.
[112] P. Hagmann, M. Kurant, X. Gigandet, P. Thiran, V. J. Wedeen, R. Meuli, and J.-P. Thiran, "Mapping human whole-brain structural networks with diffusion MRI.," *PLoS ONE*, vol. 2, no. 7, p. e597, 2007.
[113] H. Johansen-Berg and M. F. S. Rushworth, "Using diffusion imaging to study human connectional anatomy.," *Annual review of neuroscience*, vol. 32, no. 1, pp. 75–94, 2009.
[114] Y. He, Z. J. Chen, and A. C. Evans, "Small-world anatomical networks in the human brain revealed by cortical thickness from MRI.," *Cereb. Cortex*, vol. 17, no. 10, pp. 2407–2419, Oct. 2007.
[115] R. Milo, S. Shen-Orr, S. Itzkovitz, N. Kashtan, D. Chklovskii, and U. Alon, "Network motifs: simple building blocks of complex networks.," *Science*, vol. 298, no. 5594, pp. 824–827, Oct. 2002.
[116] M. E. J. Newman, "Modularity and community structure in networks.," *PNAS*, vol. 103, no. 23, pp. 8577–8582, Jun. 2006.
[117] M. D. Humphries and K. Gurney, "Network 'small-world-ness': a quantitative method

for determining canonical network equivalence.," *PLoS ONE*, vol. 3, no. 4, p. e0002051, 2008.
[118] M. Newman, "Mixing patterns in networks," *Phys Rev E Stat Phys Plasmas Fluids Relat Interdiscip Topics*, vol. 67, no. 2, p. 026126, Feb. 2003.
[119] H. Wang, J. M. Hernandez, and P. Van Mieghem, "Betweenness centrality in a weighted network.," *Phys Rev E Stat Nonlin Soft Matter Phys*, vol. 77, no. 4, p. 046105, Apr. 2008.
[120] D. S. Bassett and E. T. Bullmore, "Human brain networks in health and disease.," *Curr. Opin. Neurol.*, vol. 22, no. 4, pp. 340–347, Aug. 2009.
[121] D. S. Bassett and E. Bullmore, "Small-World Brain Networks," *Neuroscientist*, vol. 12, no. 6, pp. 512–523, Dec. 2006.
[122] M. P. van den Heuvel and O. Sporns, "Network hubs in the human brain," *Trends Cogn. Sci. (Regul. Ed.)*, vol. 17, no. 12, pp. 683–696, Jan. 2013.
[123] U. Lee, G. Oh, S. Kim, G. Noh, B. Choi, and G. A. Mashour, "Brain networks maintain a scale-free organization across consciousness, anesthesia, and recovery: evidence for adaptive reconfiguration.," *Anesthesiology*, vol. 113, no. 5, pp. 1081–1091, Nov. 2010.
[124] M. P. van den Heuvel and O. Sporns, "Rich-club organization of the human connectome.," *J. Neurosci.*, vol. 31, no. 44, pp. 15775–15786, Nov. 2011.
[125] D. Meunier, R. Lambiotte, and E. T. Bullmore, "Modular and hierarchically modular organization of brain networks.," *Front Neurosci*, vol. 4, p. 200, 2010.
[126] G. E. A.-J. Hoff, M. P. van den Heuvel, M. J. N. L. Benders, K. J. Kersbergen, and L. S. De Vries, "On development of functional brain connectivity in the young brain.," *Front Hum Neurosci*, vol. 7, p. 650, 2013.
[127] M. Boersma, D. J. A. Smit, D. I. Boomsma, E. J. C. De Geus, H. A. Delemarre-van de Waal, and C. J. Stam, "Growing trees in child brains: graph theoretical analysis of electroencephalography-derived minimum spanning tree in 5- and 7-year-old children reflects brain maturation.," *Brain Connect*, vol. 3, no. 1, pp. 50–60, 2013.
[128] D. J. A. Smit, M. Boersma, H. G. Schnack, S. Micheloyannis, D. I. Boomsma, H. E. Hulshoff Pol, C. J. Stam, and E. J. C. De Geus, "The brain matures with stronger functional connectivity and decreased randomness of its network.," *PLoS ONE*, vol. 7, no. 5, p. e36896, 2012.
[129] F. Vecchio, F. Miraglia, P. Bramanti, and P. M. Rossini, "Human brain networks in physiological aging: a graph theoretical analysis of cortical connectivity from EEG data.," *J. Alzheimers Dis.*, vol. 41, no. 4, pp. 1239–1249, 2014.
[130] Y. Li, Y. Liu, J. Li, W. Qin, K. Li, C. Yu, and T. Jiang, "Brain Anatomical Network and Intelligence," *PLoS Comput Biol*, vol. 5, no. 5, p. e1000395, 2009.
[131] M. P. van den Heuvel, C. J. Stam, R. S. Kahn, and H. E. Hulshoff Pol, "Efficiency of functional brain networks and intellectual performance.," *J. Neurosci.*, vol. 29, no. 23, pp. 7619–7624, Jun. 2009.
[132] S. Maslov and K. Sneppen, "Specificity and Stability in Topology of Protein Networks," *Science*, vol. 296, no. 5569, pp. 910–913, May 2002.
[133] E. van Diessen, S. J. H. Diederen, K. P. J. Braun, F. E. Jansen, and C. J. Stam, "Functional and structural brain networks in epilepsy: what have we learned?," *Epilepsia*, vol. 54, no. 11, pp. 1855–1865, Nov. 2013.
[134] B. M. Tijms, A. M. Wink, W. de Haan, W. M. van der Flier, C. J. Stam, P. Scheltens, and F. Barkhof, "Alzheimer's disease: connecting findings from graph theoretical studies of brain networks.," *Neurobiol. Aging*, vol. 34, no. 8, pp. 2023–2036, Aug. 2013.
[135] E. Estrada, *The Structure of Complex Networks: Theory and Applications*. Oxford University Press, 2011.
[136] C. Li, H. Wang, W. de Haan, C. J. Stam, and P. Van Mieghem, "The correlation of

metrics in complex networks with applications in functional brain networks," *J. Stat. Mech.*, vol. 2011, no. 11, p. P11018, Nov. 2011.
[137] E. van Dellen, L. Douw, A. Hillebrand, P. C. de Witt Hamer, J. C. Baayen, J. J. Heimans, J. C. Reijneveld, and C. J. Stam, "Epilepsy surgery outcome and functional network alterations in longitudinal MEG: A minimum spanning tree analysis," *Neuroimage*, pp. 1–10, Oct. 2013.
[138] P. Tewarie, A. Hillebrand, M. M. Schoonheim, B. W. van Dijk, J. J. G. Geurts, F. Barkhof, C. H. Polman, and C. J. Stam, "Functional brain network analysis using minimum spanning trees in Multiple Sclerosis: An MEG source-space study," *Neuroimage*, pp. 1–11, Oct. 2013.
[139] K. T. E. Olde Dubbelink, A. Hillebrand, D. Stoffers, J. B. Deijen, J. W. R. Twisk, C. J. Stam, and H. W. Berendse, "Disrupted brain network topology in Parkinson's disease: a longitudinal magnetoencephalography study," *Brain*, vol. 137, no. 1, pp. 197–207, Jan. 2014.
[140] P. Van Mieghem and S. van Langen, "Influence of the link weight structure on the shortest path.," *Phys Rev E Stat Nonlin Soft Matter Phys*, vol. 71, no. 5, p. 056113, May 2005.
[141] P. Van Mieghem and S. M. Magdalena, "Phase transition in the link weight structure of networks.," *Phys Rev E Stat Nonlin Soft Matter Phys*, vol. 72, no. 5, p. 056138, Nov. 2005.
[142] R. S. Fisher, C. Acevedo, A. Arzimanoglou, A. Bogacz, J. H. Cross, C. E. Elger, J. Engel Jr, L. Forsgren, J. A. French, M. Glynn, D. C. Hesdorffer, B. I. Lee, G. W. Mathern, S. L. Moshé, E. Perucca, I. E. Scheffer, T. Tomson, M. Watanabe, and S. Wiebe, "ILAE Official Report: A practical clinical definition of epilepsy," *Epilepsia*, vol. 55, no. 4, pp. 475–482, Apr. 2014.
[143] R. S. Fisher, W. van Emde Boas, W. Blume, C. Elger, P. Genton, P. Lee, and J. Engel, "Epileptic seizures and epilepsy: definitions proposed by the International League Against Epilepsy (ILAE) and the International Bureau for Epilepsy (IBE).," *Epilepsia*, vol. 46, no. 4, pp. 470–472, Apr. 2005.
[144] H. Malkki, "Epilepsy—burning questions and emerging therapies," *Nature Publishing Group*, vol. 10, no. 5, pp. 243–243, May 2014.
[145] W. H. Theodore and R. S. Fisher, "Brain stimulation for epilepsy," *Lancet Neurol*, vol. 3, no. 2, pp. 111–118, Feb. 2004.
[146] G. K. Bergey, "Neurostimulation in the treatment of epilepsy.," *Exp. Neurol.*, vol. 244, pp. 87–95, Jun. 2013.
[147] D. J. Englot, "Vagus nerve stimulation versus 'best drug therapy' in epilepsy patients who have failed best drug therapy.," *Seizure*, vol. 22, no. 5, pp. 409–410, Jun. 2013.
[148] E. García-Navarrete, C. V. Torres, I. Gallego, M. Navas, J. Pastor, and R. G. Sola, "Response to "Vagus nerve stimulation: urgent need for the critical reappraisal of clinical effectiveness"," *Seizure*, vol. 22, no. 6, pp. 490–491, Jul. 2013.
[149] C. Hoppe, "Vagus nerve stimulation: Urgent need for the critical reappraisal of clinical effectiveness," *Seizure*, vol. 22, no. 1, pp. 83–84, Jan. 2013.
[150] S. Ogbonnaya and C. Kaliaperumal, "Vagal nerve stimulator: Evolving trends," *J Nat Sc Biol Med*, vol. 4, no. 1, pp. 8–6, 2013.
[151] J. Zabara, "Peripheral control of hypersynchronous discharge in epilepsy," *Electroencephalogr Clin Neurophysiol*, vol. 61, no. 3, pp. S162–, 1985.
[152] S. Krahl, "Vagus nerve stimulation for epilepsy: A review of the peripheral mechanisms," *Surg Neurol Int*, vol. 3, no. 2, pp. 47–6, 2012.
[153] T. R. Henry, R. A. Bakay, J. R. Votaw, P. B. Pennell, C. M. Epstein, T. L. Faber, S. T. Grafton, and J. M. Hoffman, "Brain blood flow alterations induced by therapeutic

vagus nerve stimulation in partial epilepsy: I. Acute effects at high and low levels of stimulation.," *Epilepsia*, vol. 39, no. 9, pp. 983–990, Sep. 1998.
[154] J. Engel, Jr, P. M. Thompson, J. M. Stern, R. J. Staba, A. Bragin, and I. Mody, "Connectomics and epilepsy," *Curr. Opin. Neurol.*, vol. 26, no. 2, pp. 186–194, Apr. 2013.
[155] M. A. Kramer, E. D. Kolaczyk, and H. E. Kirsch, "Emergent network topology at seizure onset in humans.," *Epilepsy Res.*, vol. 79, no. 2, pp. 173–186, May 2008.
[156] B. Clemens, S. Puskás, M. Bessenyei, M. Emri, T. Spisák, M. Koselák, K. Hollódy, A. Fogarasi, I. Kondákor, K. Füle, K. Bense, and I. Fekete, "EEG functional connectivity of the intrahemispheric cortico-cortical network of idiopathic generalized epilepsy.," *Epilepsy Res.*, vol. 96, no. 1, pp. 11–23, Sep. 2011.
[157] F. Pittau, C. Grova, F. Moeller, F. Dubeau, and J. Gotman, "Patterns of altered functional connectivity in mesial temporal lobe epilepsy.," *Epilepsia*, vol. 53, no. 6, pp. 1013–1023, Jun. 2012.
[158] W. M. Otte, R. M. Dijkhuizen, M. P. A. van Meer, W. S. van der Hel, S. A. M. W. Verlinde, O. van Nieuwenhuizen, M. A. Viergever, C. J. Stam, and K. P. J. Braun, "Characterization of functional and structural integrity in experimental focal epilepsy: reduced network efficiency coincides with white matter changes.," *PLoS ONE*, vol. 7, no. 7, p. e39078, 2012.
[159] C. Vollmar, J. O'Muircheartaigh, M. R. Symms, G. J. Barker, P. Thompson, V. Kumari, J. Stretton, J. S. Duncan, M. P. Richardson, and M. J. Koepp, "Altered microstructural connectivity in juvenile myoclonic epilepsy: the missing link.," *Neurology*, vol. 78, no. 20, pp. 1555–1559, May 2012.
[160] M. Chavez, M. Valencia, V. Navarro, V. Latora, and J. Martinerie, "Functional modularity of background activities in normal and epileptic brain networks.," *Phys. Rev. Lett.*, vol. 104, no. 11, p. 118701, Mar. 2010.
[161] L. Douw, E. van Dellen, M. de Groot, J. J. Heimans, M. Klein, C. J. Stam, and J. C. Reijneveld, "Epilepsy is related to theta band brain connectivity and network topology in brain tumor patients.," *BMC Neurosci*, vol. 11, no. 1, p. 103, 2010.
[162] S. C. Ponten, F. Bartolomei, and C. J. Stam, "Small-world networks and epilepsy: graph theoretical analysis of intracerebrally recorded mesial temporal lobe seizures.," *Clin Neurophysiol*, vol. 118, no. 4, pp. 918–927, Apr. 2007.
[163] J. R. Terry, O. Benjamin, and M. P. Richardson, "Seizure generation: the role of nodes and networks.," *Epilepsia*, vol. 53, no. 9, pp. e166–9, Sep. 2012.
[164] L. Douw, M. de Groot, E. van Dellen, J. J. Heimans, H. E. Ronner, C. J. Stam, and J. C. Reijneveld, "'Functional connectivity' is a sensitive predictor of epilepsy diagnosis after the first seizure.," *PLoS ONE*, vol. 5, no. 5, p. e10839, 2010.
[165] M. Fraschini, M. Puligheddu, M. Demuru, L. Polizzi, A. Maleci, G. Tamburini, S. Congia, M. Bortolato, and F. Marrosu, "VNS induced desynchronization in gamma bands correlates with positive clinical outcome in temporal lobe pharmacoresistant epilepsy.," *Neurosci. Lett.*, vol. 536, pp. 14–18, Mar. 2013.
[166] H. Jaseja, "EEG-desynchronization as the major mechanism of anti-epileptic action of vagal nerve stimulation in patients with intractable seizures: clinical neurophysiological evidence.," *Med. Hypotheses*, vol. 74, no. 5, pp. 855–856, May 2010.
[167] F. Bartolomei, G. Bettus, C. J. Stam, and M. Guye, "Interictal network properties in mesial temporal lobe epilepsy: a graph theoretical study from intracerebral recordings.," *Clin Neurophysiol*, vol. 124, no. 12, pp. 2345–2353, Dec. 2013.
[168] B. C. Bernhardt, Z. Chen, Y. He, A. C. Evans, and N. Bernasconi, "Graph-theoretical analysis reveals disrupted small-world organization of cortical thickness correlation

networks in temporal lobe epilepsy.," *Cereb. Cortex*, vol. 21, no. 9, pp. 2147–2157, Sep. 2011.
[169] M.-T. Horstmann, S. Bialonski, N. Noennig, H. Mai, J. Prusseit, J. Wellmer, H. Hinrichs, and K. Lehnertz, "State dependent properties of epileptic brain networks: comparative graph-theoretical analyses of simultaneously recorded EEG and MEG.," *Clin Neurophysiol*, vol. 121, no. 2, pp. 172–185, Feb. 2010.
[170] E. van Dellen, L. Douw, J. C. Baayen, J. J. Heimans, S. C. Ponten, W. P. Vandertop, D. N. Velis, C. J. Stam, and J. C. Reijneveld, "Long-term effects of temporal lobe epilepsy on local neural networks: a graph theoretical analysis of corticography recordings.," *PLoS ONE*, vol. 4, no. 11, p. e8081, 2009.
[171] D. Labar, B. Nikolov, B. Tarver, and R. Fraser, "Vagus nerve stimulation for symptomatic generalized epilepsy: a pilot study.," *Epilepsia*, vol. 39, no. 2, pp. 201–205, Feb. 1998.
[172] M. Koutroumanidis, C. D. Binnie, M. J. Hennessy, G. Alarcon, R. D. C. Elwes, B. K. Toone, C. Chandler, R. Selway, C. E. Polkey, and S. A. O'Connor, "VNS in patients with previous unsuccessful resective epilepsy surgery: antiepileptic and psychotropic effects.," *Acta Neurol. Scand.*, vol. 107, no. 2, pp. 117–121, Feb. 2003.
[173] E. van Dellen, L. Douw, A. Hillebrand, I. H. M. Ris-Hilgersom, M. M. Schoonheim, J. C. Baayen, P. C. de Witt Hamer, D. N. Velis, M. Klein, J. J. Heimans, C. J. Stam, and J. C. Reijneveld, "MEG network differences between low- and high-grade glioma related to epilepsy and cognition.," *PLoS ONE*, vol. 7, no. 11, p. e50122, 2012.
[174] M. Brownlee, "The Pathobiology of Diabetic Complications A Unifying Mechanism," *Diabetes*, vol. 54, no. 6, pp. 1615–1625, Jun. 2005.
[175] I. K. Lyoo, S. Yoon, A. M. Jacobson, J. Hwang, G. Musen, J. E. Kim, D. C. Simonson, S. Bae, N. Bolo, D. J. Kim, K. Weinger, J. H. Lee, C. M. Ryan, and P. F. Renshaw, "Prefrontal Cortical Deficits in Type 1 Diabetes Mellitus," *Arch Gen Psychiatry*, vol. 69, no. 12, pp. 1267–10, Dec. 2012.
[176] E. van Duinkerken, M. M. Schoonheim, R. G. IJzerman, M. Klein, C. M. Ryan, A. C. Moll, F. J. Snoek, F. Barkhof, M. Diamant, and P. J. W. Pouwels, "Diffusion tensor imaging in type 1 diabetes: decreased white matter integrity relates to cognitive functions," *Diabetologia*, vol. 55, no. 4, pp. 1218–1220, Feb. 2012.
[177] E. van Duinkerken, M. Klein, N. S. M. Schoonenboom, R. P. L. M. Hoogma, A. C. Moll, F. J. Snoek, C. J. Stam, and M. Diamant, "Functional Brain Connectivity and Neurocognitive Functioning in Patients With Long-Standing Type 1 Diabetes With and Without Microvascular Complications: A Magnetoencephalography Study," *Diabetes*, vol. 58, no. 10, pp. 2335–2343, Sep. 2009.
[178] E. van Duinkerken and M. M. Schoonheim, "Resting-state brain networks in type 1 diabetic patients with and without microangiopathy and their relation to cognitive functions and disease variables," *Diabetes*, 2012.
[179] A. M. A. Brands, G. J. Biessels, E. H. F. de Haan, L. J. Kappelle, and R. P. C. Kessels, "The effects of type 1 diabetes on cognitive performance: a meta-analysis.," *Diabetes Care*, vol. 28, no. 3, pp. 726–735, Mar. 2005.
[180] A. M. Jacobson DCCT/EDIC Study Research Group, "Long-Term Effect of Diabetes and Its Treatment on Cognitive Function," *N. Engl. J. Med.*, vol. 356, no. 18, pp. 1842–1852, May 2007.
[181] A. M. Wessels, P. Scheltens, F. Barkhof, and R. J. Heine, "Hyperglycaemia as a determinant of cognitive decline in patients with type 1 diabetes," *European Journal of Pharmacology*, vol. 585, no. 1, pp. 88–96, May 2008.
[182] N. Patton, T. Aslam, T. Macgillivray, A. Pattie, I. J. Deary, and B. Dhillon, "Retinal vascular image analysis as a potential screening tool for cerebrovascular disease: a

rationale based on homology between cerebral and retinal microvasculatures.," *J. Anat.*, vol. 206, no. 4, pp. 319–348, Apr. 2005.
[183] A. M. Jacobson, C. M. Ryan, P. A. Cleary, B. H. Waberski, K. Weinger, G. Musen, W. Dahms, DCCT/EDIC Research Group, "Biomedical risk factors for decreased cognitive functioning in type 1 diabetes: an 18 year follow-up of the Diabetes Control and Complications Trial (DCCT) cohort," *Diabetologia*, vol. 54, no. 2, pp. 245–255, Aug. 2010.
[184] G. K. Cooray, L. Hyllienmark, and T. Brismar, "Decreased cortical connectivity and information flow in type 1 diabetes.," *Clin Neurophysiol*, vol. 122, no. 10, pp. 1943–1950, Oct. 2011.
[185] T. Montez, K. Linkenkaer-Hansen, B. W. van Dijk, and C. J. Stam, "Synchronization likelihood with explicit time-frequency priors," *Neuroimage*, vol. 33, no. 4, pp. 1117–1125, Dec. 2006.
[186] J. Vrba, G. Anderson, K. Betts, M. B. Burbank, T. Cheung, D. Cheyne, A. A. Fife, S. Govorkov, F. Haibi, G. Haid, V. V. Haid, T. Hoang, C. Hunter, P. R. Kubik, S. Lee, J. McCubbin, J. McKay, D. McKenzie, D. Nonis, J. Paz, E. Reichl, D. Ressl, S. E. Robinson, C. Schroyen, I. Sekatchev, P. Spear, B. Taylor, M. Tillotson, and W. Sutherling, "151-Channel whole-cortex MEG system for seated or supine positions," *Recent advances in biomagnetism*, pp. 93–96, Jul. 1999.
[187] M. J. Brookes, J. Vrba, S. E. Robinson, C. M. Stevenson, A. M. Peters, G. R. Barnes, A. Hillebrand, and P. G. Morris, "Optimising experimental design for MEG beamformer imaging," *Neuroimage*, vol. 39, no. 4, pp. 1788–1802, Feb. 2008.
[188] J. Ashburner and K. J. Friston, "Unified segmentation," *Neuroimage*, vol. 26, no. 3, pp. 839–851, Jul. 2005.
[189] N. Weiskopf, A. Lutti, G. Helms, M. Novak, J. Ashburner, and C. Hutton, "Unified segmentation based correction of R1 brain maps for RF transmit field inhomogeneities (UNICORT)," *Neuroimage*, vol. 54, no. 3, pp. 2116–2124, Feb. 2011.
[190] G. Gong, Y. He, L. Concha, C. Lebel, D. W. Gross, A. C. Evans, and C. Beaulieu, "Mapping Anatomical Connectivity Patterns of Human Cerebral Cortex Using In Vivo Diffusion Tensor Imaging Tractography," *Cereb. Cortex*, vol. 19, no. 3, pp. 524–536, Feb. 2009.
[191] N. Tzourio-Mazoyer, B. Landeau, D. Papathanassiou, F. Crivello, O. Etard, N. Delcroix, B. Mazoyer, and M. Joliot, "Automated Anatomical Labeling of Activations in SPM Using a Macroscopic Anatomical Parcellation of the MNI MRI Single-Subject Brain," *Neuroimage*, vol. 15, no. 1, pp. 273–289, Jan. 2002.
[192] F. Bartolomei, I. Bosma, M. Klein, J. C. Baayen, J. C. Reijneveld, T. J. Postma, J. J. Heimans, B. W. van Dijk, J. C. de Munck, A. de Jongh, K. S. Cover, and C. J. Stam, "Disturbed functional connectivity in brain tumour patients: Evaluation by graph analysis of synchronization matrices," *Clinical Neurophysiology*, vol. 117, no. 9, pp. 2039–2049, Sep. 2006.
[193] L. Douw, M. de Groot, E. Van Dellen, E. Aronica, J. J. Heimans, M. Klein, C. J. Stam, J. C. Reijneveld, and A. Hillebrand, "Local MEG networks: The missing link between protein expression and epilepsy in glioma patients?," *Neuroimage*, vol. 75, no. C, pp. 195–203, Jul. 2013.
[194] K. T. E. Olde Dubbelink, D. Stoffers, J. B. Deijen, J. W. R. Twisk, C. J. Stam, A. Hillebrand, and H. W. Berendse, "Resting-state functional connectivity as a marker of disease progression in Parkinson's disease: A longitudinal MEG study," *Neuroimage Clin*, vol. 2, no. C, pp. 612–619, 2013.
[195] C. J. Stam, W. de Haan, A. Daffertshofer, B. F. Jones, I. Manshanden, A. M. van Cappellen van Walsum, T. Montez, J. P. A. Verbunt, J. C. de Munck, B. W. van Dijk, H. W. Berendse, and P. Scheltens, "Graph theoretical analysis of

magnetoencephalographic functional connectivity in Alzheimer's disease," *Brain*, vol. 132, no. 1, pp. 213–224, Nov. 2008.
[196] P. Tewarie, M. M. Schoonheim, C. J. Stam, M. L. van der Meer, B. W. van Dijk, F. Barkhof, C. H. Polman, and A. Hillebrand, "Cognitive and Clinical Dysfunction, Altered MEG Resting-State Networks and Thalamic Atrophy in Multiple Sclerosis," *PLoS ONE*, vol. 8, no. 7, pp. e69318–11, Jul. 2013.
[197] "Phase transition in the link weight structure of networks," vol. 72, no. 5, p. 056138, Nov. 2005.
[198] "Betweenness centrality in a weighted network," 2008.
[199] M. Xia, J. Wang, and Y. He, "BrainNet Viewer: a network visualization tool for human brain connectomics.," vol. 8, no. 7, p. e68910, 2013.
[200] N. K. Logothetis, "What we can do and what we cannot do with fMRI," *Nature*, vol. 453, no. 7197, pp. 869–878, Jun. 2008.
[201] K. D. Singh, "Which 'neural activity' do you mean? fMRI, MEG, oscillations and neurotransmitters," *Neuroimage*, vol. 62, no. 2, pp. 1121–1130, Aug. 2012.
[202] W. de Haan, K. Mott, E. C. W. van Straaten, P. Scheltens, and C. J. Stam, "Activity Dependent Degeneration Explains Hub Vulnerability in Alzheimer's Disease," *PLoS Comput Biol*, vol. 8, no. 8, pp. e1002582–14, Aug. 2012.
[203] R. Qi, L. J. Zhang, Q. Xu, J. Zhong, S. Wu, Z. Zhang, W. Liao, L. Ni, Z. Zhang, H. Chen, Y. Zhong, Q. Jiao, X. Wu, X. Fan, Y. Liu, and G. Lu, "Selective impairments of resting-state networks in minimal hepatic encephalopathy.," *PLoS ONE*, vol. 7, no. 5, p. e37400, 2012.
[204] M. M. Schoonheim, J. J. G. Geurts, D. Landi, L. Douw, M. L. van der Meer, H. Vrenken, C. H. Polman, F. Barkhof, and C. J. Stam, "Functional connectivity changes in multiple sclerosis patients: a graph analytical study of MEG resting state data.," *Hum Brain Mapp*, vol. 34, no. 1, pp. 52–61, Jan. 2013.
[205] D. Stoffers, J. L. W. Bosboom, J. B. Deijen, E. C. Wolters, C. J. Stam, and H. W. Berendse, "Increased cortico-cortical functional connectivity in early-stage Parkinson's disease: an MEG study.," *Neuroimage*, vol. 41, no. 2, pp. 212–222, Jun. 2008.
[206] A. A. Fingelkurts and A. A. Fingelkurts, "Alpha rhythm operational architectonics in the continuum of normal and pathological brain states: Current state of research," *International Journal of Psychophysiology*, vol. 76, no. 2, pp. 93–106, May 2010.
[207] S. D. Mayhew, D. Ostwald, C. Porcaro, and A. P. Bagshaw, "Spontaneous EEG alpha oscillation interacts with positive and negative BOLD responses in the visual–auditory cortices and default-mode network," *Neuroimage*, vol. 76, no. C, pp. 362–372, Aug. 2013.
[208] K. Jann, T. Dierks, C. Boesch, M. Kottlow, W. Strik, and T. Koenig, "BOLD correlates of EEG alpha phase-locking and the fMRI default mode network," *Neuroimage*, vol. 45, no. 3, pp. 903–916, Apr. 2009.
[209] M. J. Brookes, M. Woolrich, and H. Luckhoo, "Investigating the electrophysiological basis of resting state networks using magnetoencephalography," presented at the Proceedings of the …, 2011.
[210] F. de Pasquale, S. Della Penna, A. Z. Snyder, C. Lewis, D. Mantini, L. Marzetti, P. Belardinelli, L. Ciancetta, V. Pizzella, G. L. Romani, and M. Corbetta, "Temporal dynamics of spontaneous MEG activity in brain networks," *PNAS*, vol. 107, no. 13, pp. 6040–6045, Mar. 2010.
[211] J. F. Hipp, D. J. Hawellek, M. Corbetta, M. Siegel, and A. K. Engel, "Large-scale cortical correlation structure of spontaneous oscillatory activity," *Nat Neurosci*, vol. 15, no. 6, pp. 884–890, May 2012.
[212] F. de Pasquale, S. Della Penna, A. Z. Snyder, L. Marzetti, V. Pizzella, G. L. Romani, and

M. Corbetta, “A Cortical Core for Dynamic Integration of Functional Networks in the Resting Human Brain,” *Neuron*, vol. 74, no. 4, pp. 753–764, May 2012.
[213] M. C. Kiernan, S. Vucic, B. C. Cheah, M. R. Turner, A. Eisen, O. Hardiman, J. R. Burrell, and M. C. Zoing, “Amyotrophic lateral sclerosis,” *Lancet*, vol. 377, no. 9769, pp. 942–955, Mar. 2011.
[214] J. Phukan, M. Elamin, P. Bede, N. Jordan, L. Gallagher, S. Byrne, C. Lynch, N. Pender, and O. Hardiman, “The syndrome of cognitive impairment in amyotrophic lateral sclerosis: a population-based study.,” *J. Neurol. Neurosurg. Psychiatr.*, vol. 83, no. 1, pp. 102–108, Jan. 2012.
[215] M. R. Turner, O. Hardiman, M. Benatar, B. R. Brooks, A. Chiò, M. de Carvalho, P. G. Ince, C. Lin, R. G. Miller, H. Mitsumoto, G. Nicholson, J. Ravits, P. J. Shaw, M. Swash, K. Talbot, B. J. Traynor, L. H. van den Berg, J. H. Veldink, S. Vucic, and M. C. Kiernan, “Controversies and priorities in amyotrophic lateral sclerosis.,” *Lancet Neurol*, vol. 12, no. 3, pp. 310–322, Mar. 2013.
[216] A. Chiò, M. Pagani, F. Agosta, A. Calvo, A. Cistaro, and M. Filippi, “Neuroimaging in amyotrophic lateral sclerosis: insights into structural and functional changes.,” *Lancet Neurol*, vol. 13, no. 12, pp. 1228–1240, Dec. 2014.
[217] E. Verstraete, M. P. van den Heuvel, J. H. Veldink, N. Blanken, R. C. Mandl, H. E. Hulshoff Pol, and L. H. van den Berg, “Motor network degeneration in amyotrophic lateral sclerosis: a structural and functional connectivity study.,” *PLoS ONE*, vol. 5, no. 10, p. e13664, 2010.
[218] E. Verstraete, J. H. Veldink, L. H. van den Berg, and M. P. van den Heuvel, “Structural brain network imaging shows expanding disconnection of the motor system in amyotrophic lateral sclerosis.,” *Hum Brain Mapp*, vol. 35, no. 4, pp. 1351–1361, Apr. 2014.
[219] B. Mohammadi, K. Kollewe, A. Samii, K. Krampfl, R. Dengler, and T. F. Münte, “Changes of resting state brain networks in amyotrophic lateral sclerosis.,” *Exp. Neurol.*, vol. 217, no. 1, pp. 147–153, May 2009.
[220] C. Luo, Q. Chen, R. Huang, X. Chen, K. Chen, X. Huang, H. Tang, Q. Gong, and H.-F. Shang, “Patterns of spontaneous brain activity in amyotrophic lateral sclerosis: a resting-state FMRI study.,” *PLoS ONE*, vol. 7, no. 9, p. e45470, 2012.
[221] F. Agosta, E. Canu, P. Valsasina, N. Riva, A. Prelle, G. Comi, and M. Filippi, “Divergent brain network connectivity in amyotrophic lateral sclerosis.,” *Neurobiol. Aging*, vol. 34, no. 2, pp. 419–427, Feb. 2013.
[222] R. Schmidt, E. Verstraete, M. A. de Reus, J. H. Veldink, L. H. van den Berg, and M. P. van den Heuvel, “Correlation between structural and functional connectivity impairment in amyotrophic lateral sclerosis.,” *Hum Brain Mapp*, vol. 35, no. 9, pp. 4386–4395, Sep. 2014.
[223] N. Bizovičar, J. Dreo, B. Koritnik, and J. Zidar, “Decreased movement-related beta desynchronization and impaired post-movement beta rebound in amyotrophic lateral sclerosis.,” *Clin Neurophysiol*, vol. 125, no. 8, pp. 1689–1699, Aug. 2014.
[224] T. Kasahara, K. Terasaki, Y. Ogawa, J. Ushiba, H. Aramaki, and Y. Masakado, “The correlation between motor impairments and event-related desynchronization during motor imagery in ALS patients.,” *BMC Neurosci*, vol. 13, no. 1, p. 66, 2012.
[225] P. A. Valdés-Hernández, A. Ojeda-González, E. Martínez-Montes, A. Lage-Castellanos, T. Virués-Alba, L. Valdés-Urrutia, and P. A. Valdes-Sosa, “White matter architecture rather than cortical surface area correlates with the EEG alpha rhythm.,” *Neuroimage*, vol. 49, no. 3, pp. 2328–2339, Feb. 2010.
[226] F. Varela, J.-P. Lachaux, E. Rodriguez, and J. Martinerie, “The brainweb: Phase synchronization and large-scale integration,” *Nat. Rev. Neurosci.*, vol. 2, no. 4, pp.

229–239, Apr. 2001.